

**Laboratory and field evaluation of fiber composite dowel and tie bars for
static and fatigue performances in highway pavement slabs**

by

Kasi P. Viswanath

A Thesis Submitted to the
Graduate Faculty in Partial Fulfillment of the
Requirements for the Degree of
MASTER OF SCIENCE

Department: Civil and Construction Engineering
Major: Civil Engineering (Structural Engineering)

Signatures have been redacted for privacy

Iowa State University
Ames, Iowa
1995

Copyright © Kasi P. Viswanath, 1995. All rights reserved.

TABLE OF CONTENTS

PREFACE	x
CHAPTER 1. INTRODUCTION	1
1.1 General	1
1.2 Research Program	5
1.2.1 Objective	5
1.2.2 Scope	5
1.3 Literature Review	6
CHAPTER 2. FIELD PLACEMENT AND MONITORING OF FC DOWELS AND TIE RODS	8
2.1 Introduction	8
2.2 Preparation and Placement	9
2.3 Evaluation and Monitoring	13
2.4 Discussion of Results	15
CHAPTER 3. THEORETICAL INVESTIGATION	19
3.1 Introduction	19
3.2 Fiber Composite Material Properties	20
3.3 Analysis of Dowels	23
3.4 Fatigue Testing of Full-scale Slabs	32

3.4.1	Introduction	32
3.4.2	Simulation of subgrade	33
3.4.3	Design of test setup	35
CHAPTER 4. EXPERIMENTAL INVESTIGATION		48
4.1	Introduction	48
4.2	Elemental Dowel Static Shear Testing	49
4.2.1	Introduction	49
4.2.2	Materials and specimens	49
4.2.3	Test setup	50
4.2.4	Instrumentation	55
4.2.5	Test procedure	57
4.2.6	Results	58
4.3	Full-Scale Fatigue Slab Testing	61
4.3.1	Introduction	61
4.3.2	Materials and specimens	62
4.3.3	Test setup	64
4.3.4	Instrumentation	69
4.3.5	Test procedure	78
4.3.6	Results	84
4.4	FC Rod Bond Testing	92
4.4.1	Introduction	92
4.4.2	Materials and specimens	92
4.4.3	Test setup	94
4.4.4	Instrumentation	95

4.4.5	Test procedure	95
4.4.6	Results	96
4.5	FC Rod Pullout Tests	97
4.5.1	Introduction	97
4.5.2	Pullout specimen construction	97
4.5.3	Pullout test procedure	103
4.5.4	Pullout test instrumentation	105
4.5.5	Results	106
4.6	FC Rod Tensile Testing	106
4.6.1	Introduction	106
4.6.2	Materials and specimens	107
4.6.3	Test procedure	107
4.6.4	Results	108
CHAPTER 5. ANALYTICAL INVESTIGATION		110
5.1	Introduction	110
5.2	Load Transfer From Supporting Beam Data	110
5.3	Load Transfer From Dowel Strain Gage Data	112
5.4	Load Transfer From Dowel Analysis	118
CHAPTER 6. COMPARISONS AND CONCLUSIONS		121
6.1	Introduction	121
6.2	Comparisons	121
6.3	Conclusions	122
6.4	Recommendations	124
REFERENCES		125

ACKNOWLEDGEMENTS 129

LIST OF FIGURES

Figure 2.1:	Typical rigid highway pavement contraction joint with a dowel	10
Figure 2.2:	Typical jointed concrete highway pavement using dowels at transverse joints	12
Figure 3.1:	Dowels as load transferring devices across the transverse joint of a highway pavement slab	24
Figure 3.2:	Assumed distribution of transferred load (across transverse joint) among the active dowels	27
Figure 3.3:	Dowel as a beam on elastic foundation	30
Figure 3.4:	Actual pavement slab considered for analysis	36
Figure 3.5:	Finite element model of actual pavement slab	39
Figure 3.6:	Laboratory test slab considered for analysis	42
Figure 3.7:	Finite element model of laboratory test setup	44
Figure 3.8:	Comparison of deflection profiles of actual and test slabs . . .	45
Figure 3.9:	Reactions from analysis of test setup applied to supporting beams	46
Figure 4.1:	Schematic of the Iosipescu shear test method (Walrath 1983)	50

Figure 4.2: Elemental dowel shear, or modified Iosipescu testing frame (Lorenz 1993)	52
Figure 4.3: Elemental dowel shear test specimen (Lorenz 1993)	53
Figure 4.4: FC dowel used in elemental shear testing	57
Figure 4.5: Load versus strain relationship for 1.75-inch diameter FC dowels	60
Figure 4.6: Supporting beams for full-scale pavement slab testing	67
Figure 4.7: Laboratory setup for full-scale pavement slab fatigue testing .	70
Figure 4.8: Displacement instrumentation for first full-scale fatigue test slab (with 1.5-inch diameter steel dowels at 12-inch spacing)	72
Figure 4.9: Displacement instrumentation for second full-scale fatigue test slab (with 1.75-inch diameter FC dowels at 8-inch spacing) .	74
Figure 4.10: Displacement instrumentation for third and fourth full-scale fatigue test slab (with 1.5-inch diameter steel dowels at 12- inch spacing)	75
Figure 4.11: Locations of strain gages placed on supporting beams	76
Figure 4.12: FC dowel strain gage locations as placed in fourth full-scale pavement test slabs	79
Figure 4.13: Typical load diagrams for two actuators during cyclic loading	82
Figure 4.14: Load versus strain diagrams for quarter points of supporting beams	85
Figure 4.15: Experimental verification of finite element analysis	87
Figure 4.16: Load versus relative displacement diagrams at the joint of Slab 2	89
Figure 4.17: Load versus relative displacement diagrams at the joint of Slab 3	90
Figure 4.18: Load versus relative displacement diagrams at the joint of Slab 4	91

Figure 4.19: Beam specimen used for the development length tests of FC rod	93
Figure 4.20: Modified beam specimens for development length tests used for Groups 2 and 3	95
Figure 4.21: Load versus displacement for beam specimens tested in Group 1	98
Figure 4.22: Load versus displacement for beam specimens tested in Group 2	99
Figure 4.23: Load versus displacement for beam specimens tested in Group 3	100
Figure 4.24: Pullout test specimen dimensions	101
Figure 4.25: Pullout specimen force schematic	102
Figure 4.26: Pullout test frame	104
Figure 4.27: Dimensions and details of FC rod specimen used in tensile testing	108
Figure 5.1: Percent of load transfer across the joint versus the number of applied load cycles for Slabs 2, 3, and 4.	113

LIST OF TABLES

Table 2.1:	Road Rater TM deflection data for pavement joints on U.S. Highway 30	18
Table 3.1:	Deflections from finite element analyses	40
Table 4.1:	Experimental values for modulus of dowel support for 1.75-inch diameter FC dowels	59
Table 4.2:	Compressive strength and modulus of rupture values of concrete corresponding to full-scale slab specimens	63
Table 4.3:	Determination of area of FC rod	109
Table 4.4:	Tensile Strength of FC rod	109
Table 5.1:	Load transfer across the joint by 1.75-inch diameter FC dowels in the second full-scale test slab	115
Table 5.2:	Load transfer across the joint by 1.5-inch diameter steel dowels in the third full-scale test slab	116
Table 5.3:	Load transfer across the joint by 1.75-inch diameter FC dowels in the fourth full-scale test slab	116
Table 5.4:	Results of analysis of dowel	120

PREFACE

This thesis is based on the work done on a project sponsored by the Iowa Department of Transportation (Iowa DOT) titled, "HR-343 Non-corrosive Tie Reinforcing and Dowel Bars for Highway Pavement Slabs". The investigation was carried out at Iowa State University (ISU) in coordination with Iowa DOT. The laboratory work was conducted at the ISU Structural Engineering laboratory under the auspices of the Engineering Research Institute (ERI) with funds recommended by Iowa Highway Research Board (Iowa HRB) and provided by the Iowa DOT.

The progress report on the project was submitted in January 1993, and the final report in November 1993. The research work along with the presentation of the reports was made possible through the combined effort of two graduate students (one among whom is the author of this thesis), under the supervision and guidance of the principal investigator, Dr. Max Porter, and the research associate, Bruce Barnes.

Certain portions of the research work and the reports have been included by the two graduate students in their theses. While the author made use of the theoretical and analytical investigations of the project for his thesis, the focus of the other graduate student (Bradley W. Hughes) was on the field and experimental investigations. But definitely some topics are common to both the theses since the two students worked on the same project simultaneously and in close association with each other.

CHAPTER 1. INTRODUCTION

1.1 General

The problem of structural deterioration due to corrosion dates back to the early 20th century when actually reinforced concrete construction had revolutionized the field of building construction. Though the cause of corrosion is directly attributed to steel which is used as the reinforcing material, the effect did not prevent the building industry from using steel in reinforced concrete construction, because of the strength, ease of handling and manufacturing, and economy offered by the material (steel). Yet, at the same time, concern for the damage due to corrosion of steel was never ignored. In fact, corrosion was recognized to be the major factor which causes a severe damage to both superstructure and supporting structures, and the resulting cost of rehabilitation, sometimes, exceeds the original cost of construction of the structure itself (Gibson 1987).

One of the attempts to fight the problem of corrosion is to use epoxy coated reinforcement. In fact, the purpose of using epoxy coated steel is to eliminate the problem of corrosion by protecting steel from the corrosive elements. According to the theory of corrosion, the localized exposure of a corrosive material is more damaging than the complete exposure because in the former, the rate of corrosion is predominantly high. The localized damage to the protective coating is always

possible while handling and placing the reinforcement in concrete. The use of epoxy coated steel is sometimes more vulnerable than using ordinary steel because damage to the coating can lead to severe local corrosion. Moreover, the bond strength of reinforcing bars is significantly affected due to the presence of epoxy coating (Cope 1987).

Besides corrosion, electrical and magnetic conduction of steel add to discourage the use of steel in certain applications. In fact, steel cannot be used in hospitals equipped with very sensitive instruments, whose accuracy is affected by the presence of external electric currents (Medical Center Hospital 1985). Such electric currents can be induced in the reinforcement present in the building. To overcome this problem, the heart of Medical Center Hospital, San Antonio, Texas was constructed successfully with fiber composite reinforcement (Richard 1991). Higher electrical resistance was the key demand met by using fiber composites in that construction.

Fiber composite (FC) materials have a potential future as replacement materials for steel in reinforced concrete construction. Since corrosion of steel is so disastrous, fiber composite materials, which are basically corrosion resistant, might not only become an alternative for steel in specialized areas but they may compete with steel in applications where corrosion is a serious problem. Besides being corrosion and electrical resistant, fiber composite materials possess several other advantages which promise a bright future for fiber composites for applications in several fields. FC materials have not been confined to the theoretical and laboratory research, but they have also been practically used in several fields ranging from construction, space and military (Corbo 1990), sports (Brown 1988) , and Orthopaedics. Since material properties and structural advantages of fiber composites have been carefully and

selectively considered with respect to the specific application, the practical use of FC materials has been successful and rather encouraging. The versatility of FC materials can be attributed to the fact that the properties of these materials can be easily tailored to suit the purpose at hand. Fiber composites are ideal materials especially for construction industry because of their light weight, ease of handling, flexibility to be made into many shapes and forms, electrical and corrosion resistance, high tensile strength, good fatigue behavior, architectural appearance, and thermal insulation.

The possibility of incorporating optical sensors in the reinforcement was considered for prestressed concrete construction using Glass Fiber Reinforced Plastic (GFRP) as the primary reinforcing material. The related research not only emphasized the feasibility of GFRP for prestressed concrete construction, but also investigated the possibility of structural monitoring with the help of optical fiber sensors, just like the way a physician monitors the functioning and defects of a human body (Miessler 1991).

Since FC materials need to be researched extensively for establishing the standards and codes of general practice, their applications have not yet been popular. One of the reasons is the higher cost of manufacturing of FC materials. But once FC materials are practically established, demand will increase because of their advantages. The increased demand asks for mass manufacturing which automatically decreases the cost of production. The decreased cost in turn raises the demand, and thence the supply and the consumption of FC materials will be tuned to a demand supply growth cycle. Because of the promising future that they possess, FC materials have been extensively researched both in the areas of science and engineering.

The research is mainly focused on the material properties and structural behavior of fiber composites. Though the early stages of research encompassed a vast variety of FC materials varying in compositions, proportions and shapes, GFRP materials received increased attention recently because of the feasibility of GFRP materials as alternatives for steel in structural applications.

Static and sustained tension tests, and concrete environment tests were conducted on GFRP rods and the results were compared satisfactorily with the results obtained from testing the steel cables (Iyer 1991). Fiber reinforced plastic (FRP) grating was tested against epoxy coated steel bar as reinforcement in concrete slabs, and the feasibility of FRP grating for bridge deck systems was emphasized (Bank 1991). Bending response of FRP reinforced beams was satisfactorily tested (Gan-garao 1991). The application of fiber glass as reinforcement in pretensioned piles in marine environment, and feasibility FRP tendons for post tensioning of concrete structures was successfully evaluated (Rostasy 1991).

The Structural Engineering Division of Civil and Construction Engineering Department at ISU has been actively involved in the research connected with fiber composite materials. The research at ISU included investigation of the application of FC materials for use as connectors in insulated sandwich walls (Wade 1988), and as reinforcing materials in concrete construction (Fish 1992). Several research projects undertaken by ISU resulted in establishment of bond behavior of FC bars (Barnes 1990), tensile strength of GFRP rod (Porter 1991), shear strength of GFRP dowels (Albertson 1990), and effect of aging on performance of fiber composites (Lorenz 1993). The research also resulted in the design of special methods for testing fiber composite materials (Porter 1991).

The research work presented in this thesis was aimed at evaluating the fatigue performances of GFRP and steel dowels, and comparing the dowel efficiencies of both the materials. Also included in this project, was the investigation of feasibility of GFRP rods as tie rods in highway pavement slabs.

1.2 Research Program

1.2.1 Objective

In continued pursuit of advancing the applications of fiber composites as materials for highway pavement dowels and tie bars, and to add to the efforts in establishing fiber composite materials as practical materials for construction, the following objectives were selected for this project:

1. To compare static and fatigue behaviors of FC dowels to those of steel dowels when used as load transferring devices across transverse joints of highway pavement slabs.
2. To study the bond characteristics of FC bars for potential use as tie rods across the longitudinal joints of highway pavement slabs.

1.2.2 Scope

In order to achieve the objectives set, various tests and test methods were considered and developed. In light of the extensive literature search conducted, and past experience gained on fiber composite materials, theoretical and laboratory investigations carried out in this project gave special attention to testing and handling of FC

materials. Accordingly, the scope of this research work included the following tasks in order to facilitate theoretical, field, and experimental investigations:

1. Extensive study of literature in the areas of fiber composite materials, highway pavement joints, and dowel behavior.
2. Development of a theoretical model for evaluation of dowel performance.
3. Design of a comprehensive laboratory experimental program to evaluate the fatigue behavior of doweled concrete slabs.
4. Placement of FC dowels and tie rods in an actual pavement, and monitoring the field performance.
5. Construction, and testing of single dowel specimens, and investigating the dowel behavior in shear.
6. Construction and testing of concrete slabs with FC and steel dowels for direct comparison of fatigue performances of the two types of slabs.
7. Verification of the theoretical model (which is developed under Scopes 1 and 2, and then used under Scope 6 for evaluation of dowel performance).
8. Construction and testing of FC rod bond, pullout and tensile test specimens.

1.3 Literature Review

A thorough literature search was conducted on the topics of fiber composite materials, fatigue and static testing procedures, and analysis and design of concrete pavements, and bond and development of reinforced concrete. Various tests and test

procedures were reviewed for modeling the experimental setup, defining the parameters of investigation, and designing the instrumentation. Information pertaining to the analysis and design of concrete pavement joints and bond and dowel behaviors of reinforced concrete had been gathered for facilitating the analytical investigation. References to the literature can be found in appropriate sections most closely associated with each topic presented.

CHAPTER 2. FIELD PLACEMENT AND MONITORING OF FC DOWELS AND TIE RODS

2.1 Introduction

Included in this research project was the field testing of FC dowels as load transfer devices in a highway pavement. From the field testing, a comparison of performance can be made between FC and steel materials under the same, or very similar, field conditions, such as subgrade, concrete, weather, traffic, and placement. Field placement of the FC dowels was performed in conjunction with the Iowa DOT during the construction of a new section of concrete pavement on U.S. Highway 30 east of Ames, Iowa. Two lanes of pavement were constructed during the project, and two transverse joint locations were selected as test joints. The test joints are located on the westbound lanes of Highway 30 at stations 1527+00 and 1527+20, which are approximately three miles east of Interstate Highway 35. Placed in the two test joints were 1.75-inch diameter FC dowels, replacing 1.5-inch diameter steel dowels. All other transverse joints in the new pavement used steel dowels, which are common for such construction, and will be referred to in this discussion as control joints. The FC dowels were 18 inches in length and were placed at a spacing of eight inches. Steel dowels placed at all other locations were of the same length as that of the FC dowels, but were spaced at 12 inches.

The field test portion of the research must be considered as a long term ongoing program. A comparison of the performance of FC dowels to steel dowels in a highway pavement is best done over the design life of the pavement, which may be in excess of 20 years (Heinrichs 1989). Continuing observation of the performance of the test joints and adjacent joints is necessary in order to fully evaluate the advantages and disadvantages of the materials when compared to each other.

Included in the discussion of the field study will be a description of the procedures used for preparation and placement of the test dowels, including construction techniques. A program for evaluating the performance of the test joints relative to adjacent control joints will also be described. Several methods for monitoring the performance of both types of joints will be included. A brief discussion on results of the test program will be presented by considering the observations made at the test joints (with FC dowels) and the control joints (with steel dowels), which will be followed by a comparison of the performances of the pavement at the two types of joints.

2.2 Preparation and Placement

The standard practice in the construction of new concrete highway pavements in the State of Iowa closely follows the guidelines recommended by AASHTO, including the use of steel dowels placed at the transverse joint locations. In the design of rigid pavements, the dowel diameter is selected to be approximately one-eighth of the thickness of the pavement, and the length is set at 18 inches. After paving is completed, a saw cut is made over the top of the dowels to a depth of one-third of the pavement thickness (AASHTO 1986). Shrinkage of the concrete is assumed to cause

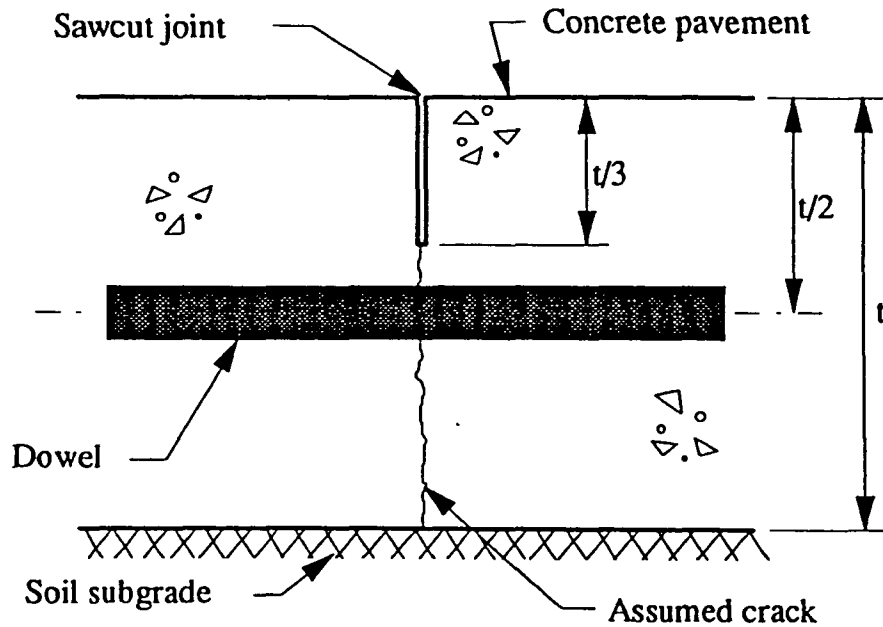


Figure 2.1: Typical rigid highway pavement contraction joint with a dowel

the pavement to crack at these locations, which is shown in Figure 2.1. When using a slip-form type of paving system, the dowels are held in place by steel "baskets" constructed of steel rod stock. The baskets hold the dowels at the correct height and restrain the dowels from movement as the concrete is placed. Steel loops provided on the baskets hold the dowels at the correct locations. One end of the dowel is spot-welded to the basket, with adjacent dowels having opposite ends welded. Welding serves two purposes, one of which is providing a means of holding the dowels in place as the baskets are handled. The second purpose served by welding is that one end of each dowel is tied into the concrete on one side of the joint. The latter purpose allows the pavement slabs on either side of the joint to move independently in the longitudinal direction due to shrinkage or temperature variation.

In the State of Iowa, transverse joints used in concrete pavements are often placed skewed to the center line of the roadway. This skew is at a magnitude of one foot in the longitudinal direction to six feet in the transverse direction. Each dowel, though, is placed so that its longitudinal direction is parallel to the roadway to prevent “binding” of the pavement, while the mid-length of the dowel is located at the joint. Therefore, a line drawn through the mid-point of each dowel coincides with the joint location, and is skewed to the center line of the roadway. The spacing of the dowels is measured in the transverse direction (AASHTO 1986). Figure 2.2 shows a typical highway pavement with dowels placed across joints.

The FC dowels were to be used in place of steel dowels without a supporting “basket” made specifically for them, and so, baskets manufactured for 1.5-inch diameter steel dowels were used to hold the dowels in place during construction. Because the FC dowels to be used in the pavement at the two test contraction joints had a larger diameter than the steel dowels and would be placed at a smaller spacing than their steel counterparts, there was a problem in supporting the dowels properly. The FC dowels were 1.75-inch in diameter and were placed in the pavement at a spacing of eight inches, while the steel dowels that they replaced were 1.5-inch in diameter and spaced at 12 inches. To allow for the placement of the FC dowels, the steel loops holding the dowels in place had to be removed. In order to maintain the dowels in their proper positions, heavy steel wire was used to tie the dowels to the baskets.

Using wire to hold the dowels did not provide as rigid of a support of the dowels as steel loops would have, and slight problems did occur when the concrete was placed over the test dowels. As the concrete flowed over the FC dowels, its weight pushed several of the dowels from their original position so that they were no longer oriented

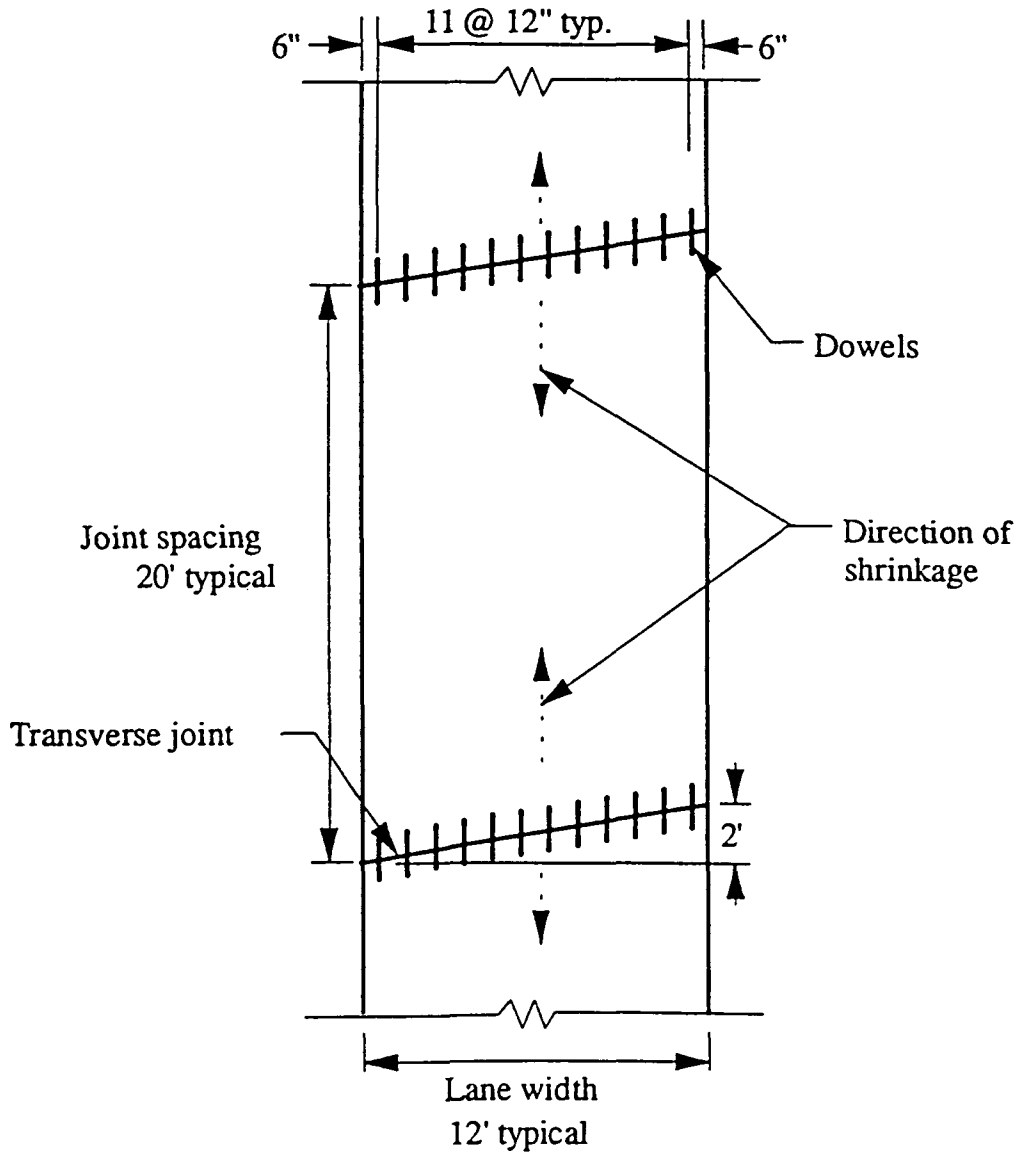


Figure 2.2: Typical jointed concrete highway pavement using dowels at transverse joints

parallel to the center line of the pavement. Where possible, though, construction personnel and observers straightened the dowels before they were completely covered by concrete. Dowels moved during the concrete placement could result in problems if they lie at an angle to the direction of the pavement. When the concrete shrinks or when contraction due to cold weather occurs, the transverse joint will open, and the separate slabs at the joint will move away from one another. Since one side of each dowel is free from the slab, the pavement slides over the dowels. If, though, a dowel is not parallel to the direction that the pavement moves, there is a binding of the pavement. In the extreme case, binding of the joint causes concrete to crack at a point just behind the dowels.

As mentioned earlier, only one end of each dowel is actually tied into the concrete, while the other end is meant to move freely within the concrete. In order for this movement to take place, the dowels must not bond with the concrete. Therefore, besides the epoxy coating that is placed on steel dowels, a bond-breaking material, which is a tar-like substance, is applied to the steel dowels and baskets. In the case of the FC dowels placed in the concrete, another means of freeing one end was used. When the dowels and the baskets were in place on the subgrade, form oil was applied to one half of each dowel. Adjacent dowels had opposite ends oiled to provide a similar condition as for steel dowels with one end tied to the slab.

2.3 Evaluation and Monitoring

In order to make the study of the field performance of FC dowels and tie rods complete, a comprehensive program of evaluation and monitoring was developed. Since the main objective of the field study was to compare the performance of the

test dowels to that of the current standard, the FC materials were evaluated and monitored relative to steel materials. The initial and most basic means of comparison was visual inspection of the test joints. During visual inspection, any cracking of the pavement was noted, either at the joint or away from the joint. Also, the joint opening was checked, which would indicate whether the dowels were allowing movement of the slab in the longitudinal direction. Visual inspection was most effective during cold temperatures when the pavement experienced the most thermal contraction. Another location for inspection was at the pavement edges, where an inspection was made of whether the pavement was cracked through the full depth of the slab by digging away the soil at the edge of the pavement.

A more experimental method of evaluation of the test joint performance was the Road RaterTM which is used by the Iowa DOT to evaluate pavements, subgrades and joints. To evaluate a pavement, a mass was applied to the pavement and oscillated over a range of approximately 2,500 to 4,500 pounds at 30 Hertz. Velocity sensors measure the amplitude of the pavement movement, which was referred to as displacement. A total of four sensors monitored displacements, one located at the load point, and three others spaced at one-foot intervals. To evaluate transverse pavement joints, the load was applied to one side of the joint and the displacements were measured on the opposite side of the joint (Potter 1989). Testing with the Road RaterTM was considered to provide an indication of dowel performance as a function of the soil subgrade, pavement, and any aggregate interlock at the joint. By testing the joints with FC dowels and the nearby joints with steel dowels at the same time, a comparison of performance was made. The comparison was made assuming that the other variables mentioned above were approximately equivalent for all joints tested.

Performance of a pavement joint can also be evaluated by means of conducting a load test at that joint. Such a test included placing displacement measuring devices at the joint and using a loaded truck to apply loads to one side of the joint at a time as displacements were measured. While this was a static test of the pavement, an indication was given of the load transfer abilities of the test joints relative to others nearby. Like the Road RaterTM testing, the performance of the joint during a load test evaluation was a function of many other variables other than the dowels. Again, though, the assumption that these variables were approximately equivalent for adjacent joints was made to allow for a comparison of the performance of FC to steel dowels.

Another means of evaluation of the dowels is coring the pavement exactly at the joint and through a dowel. A core at a dowel location would provide a means of observing whether any fatiguing of the concrete has taken place around the dowel. Fatigue of the concrete might be indicated by the hole around the dowel becoming oval-shaped due to repeated loading of the joint by traffic. This method of evaluation was not included in the field investigation because of the destructive nature associated with coring of the field pavement.

2.4 Discussion of Results

The two test joints where the 1.75-inch diameter FC dowels were placed were visually inspected in the summer and fall following their placement in the roadway. During these inspections, no deviations from the performance of adjacent joints with steel dowels were observed. Further inspection was carried out along with Iowa DOT personnel in January, 1993. The day of this inspection was quite cold, with temper-

atures at approximately 10 degrees F. Such cold temperatures caused significant contraction of the concrete, and, therefore, rather substantial joint openings were observed for the two test joints as well as the adjacent joints with steel dowels. At that time, some slight spalling of the surface concrete was noticed at several locations along the joints. Surface damage was also noticed at adjacent joints and was most likely due to vehicles impacting at the joints, not due to the joint or dowel performance. Because damage was noted at adjacent joints with steel dowels, the damage was not specific to the FC dowels.

Iowa DOT personnel conducted Road RaterTM testing at a total of six joints in the outside traffic lane of the Westbound portion of U.S. Highway 30 during the field test. The joints included the two with FC dowels, along with the two adjacent joints on either side of the test joints which had steel dowels in place. At each of the joints, a test was performed at the locations of the two wheel tracks observed at the joints. The wheel tracks were the locations where a majority of the traffic appeared to pass over the joint. The tracks were located approximately two to three feet inside of each edge of the traffic lane.

During the Road RaterTM testing, load was applied directly adjacent to one side of the joint, and displacements were measured by one sensor at the load point and by another 12 inches away on the opposite side of the joint. The relative vertical displacement movement between the two sensor locations is an indication of the load transfer across the joint.

Data from the tests included the displacement readings, which were expressed in units of mils, or thousandths of an inch, at the two sensor locations. Tests were performed on four joints with steel dowels and two joints with FC dowels. The test

data supplied by the Iowa DOT is included in Table 2.1. The two sensor locations are labeled as the loaded and unloaded sides of the joint. Table 2.1 lists the data at two sensors for the outside (located nearest to the shoulder of the roadway) and inside wheel tracks. From the results in Table 2.1, the deflections measured at the two types of joints due to the dynamic loading conditions applied by the Road RaterTM are very similar.

The variability in both the measured displacement values and the calculated relative displacement values is most likely due to slight variability in the pavement and subgrade construction. The average values of relative deflection at the joints using FC dowels are quite similar to those at the joints using steel dowels. Assuming that the pavement and subgrade characteristics are approximately equivalent for all of the joints tested, the results indicate that the FC dowels are performing as well as the steel dowels at these locations. In addition to testing with the Road RaterTM, inspection of the pavement slab was performed to determine if the concrete was cracked at the joint locations. By digging the shoulder gravel away from one edge of the pavement adjacent to the joint locations, the pavement was observed to be cracked to its full depth at the joints with FC dowels. A crack at the joint location suggests that the FC dowels are permitting movement of the slab over the dowels due to thermal expansion and contraction.

Table 2.1: Road RaterTM deflection data for pavement joints on U.S. Highway 30

Measured and Relative Displacements, mils (1/1000 in.)						
Note: Rel. = relative displacement = (Loaded) - (Unloaded)						
Joints With:	Outside Wheel Track			Inside Wheel Track		
	Loaded	Unloaded	Rel.	Loaded	Unloaded	Rel.
Steel Dowels	0.74	0.70	0.04	0.65	0.58	0.07
	0.72	0.69	0.03	0.67	0.63	0.04
	0.72	0.70	0.02	0.69	0.65	0.04
	0.77	0.75	0.02	0.72	0.69	0.03
	Average relative = 0.03			Average relative = 0.05		
FC Dowels	0.76	0.74	0.02	0.72	0.67	0.05
	0.75	0.70	0.05	0.71	0.66	0.05
	Average relative = 0.035			Average relative = 0.05		

CHAPTER 3. THEORETICAL INVESTIGATION

3.1 Introduction

For the theoretical as well as the analytical methods used throughout this project, the dowel properties are the key variables. The flexural and shear properties of the dowel material are especially vital to the investigations that were carried out. Since the properties of fiber composite materials depend on the proportions of the individual components, and also since the materials are anisotropic, theoretical derivation as well as experimental determination of the material properties of fiber composites were investigated. The next step of theoretical investigation was aimed at understanding the dowel behavior, identification of the parameters for evaluating the efficiency of a dowel, and development of a theoretical model for idealization of a dowel embedded in concrete. The purpose of this part of the investigation was to establish a procedure by which the performance of a dowel can be evaluated. The procedure was necessary for comparison of efficiencies of steel and FC dowels used in the full-scale slab specimens. Finally, a comprehensive laboratory test method was developed for full-scale slab testing. Design of test set up involved simulation of the subgrade support for test slabs, determination of appropriate instrumentation, and selection of dowel spacing to be used in the test slabs.

3.2 Fiber Composite Material Properties

The composite material tested in this study contained E-glass fibers drawn in vinyl ester resin. Since the properties of each of these are different, the combined properties of the material are functions of individual properties of E-glass and vinyl ester. Properties of unidirectional composite materials can be determined by applying simple rule of mixtures (Tsai 1980) which is given by the Equations 3.1 and 3.2.

$$E_x = V_f E_f + V_m E_m \quad (3.1)$$

$$\nu_{xy} = V_f \nu_f + V_m \nu_m \quad (3.2)$$

where,

E_x = modulus of elasticity of FC

ν_{xy} = Poisson's ratio of FC

V_f = Volume fraction of E-glass fibers

V_m = Volume fraction of vinyl ester resin matrix

E_f = modulus of elasticity of E-glass fibers

$$= 10.5 \times 10^6 \text{ psi (Fiber 1991)}$$

E_m = modulus of elasticity of vinyl ester resin

$$= 0.49 \times 10^6 \text{ psi (DERAKANE 1990)}$$

ν_f = Poisson's ratio of E-glass fibers

$$= 0.22 \text{ (Fiber 1991)}$$

ν_m = Poisson's ratio of vinyl ester resin matrix

$$= 0.30 \text{ (DERAKANE 1990)}$$

Volume fractions of the components were derived from the weight fractions and the specific gravities. Weight fractions were determined by means of "burn-down" tests

(Annual 1991) to be 76% and 24% of E-glass and vinyl ester resin, respectively. Specific gravity of the E-glass was taken as 2.57 which is a median value for such materials (Auborg 1986). Specific gravity of the composite material was determined (by simple laboratory method of finding the unit weight of dowel material and dividing with that of water) to be 1.92. The unit weight of the fiber material was determined from the fact that unit weights are in direct proportion of corresponding specific gravities. From the known specific gravities and the known unit weight of composite material, the unit weight of fiber material was determined. Applying the standard relation between volumes, weights, and unit weights, the volume fraction of fiber was found to be 57%, from which the volume fraction of vinyl ester resin was obtained as 43%. By substituting these values in Equations 3.1 and 3.2, the composite material properties were calculated as:

$$E_x = 6.20 \times 10^6 \text{ psi}$$

$$\nu_{xy} = 0.254$$

To determine properties of the fiber composite material in a direction transverse to the direction of the fibers, a model referred to by Tsai and Hahn as the modified rule of mixtures was applied (Tsai 1980). The modified model considers the properties and proportions of each component, while also applying stress partitioning parameters, η_y , and η_G , for transverse modulus of elasticity and transverse shear modulus, respectively. These parameters are a measure of the relative magnitudes of average stresses in the fibers and the matrix of the composite. When using the modified rule of mixtures, the matrix and fiber materials are both assumed to be isotropic, which allows for the calculation of the shear modulus of each using the

relationship involving Young's modulus, E , and Poisson's ratio, ν . Equations 3.3 and 3.4 show these relationships for the resin matrix and for the glass fibers, respectively (Beer 1981).

$$G_m = \frac{E_m}{2(1 + \nu_m)} \quad (3.3)$$

$$G_f = \frac{E_f}{2(1 + \nu_f)} \quad (3.4)$$

Substituting the appropriate values for E and ν into Equations 3.3 and 3.4 resulted in values for the shear moduli of the two components to be:

$$G_m = 0.188 \times 10^6 \text{ psi}$$

$$G_f = 4.300 \times 10^6 \text{ psi}$$

The transverse modulus of elasticity, E_y , and the transverse shear modulus, G_{xy} , of the fiber composite material were determined by applying Equations 3.5 through 3.8 (Tsai 1980) listed below.

$$\frac{1}{E_y} = \frac{1}{V_f + \eta_y V_m} \left(V_f \frac{1}{E_f} + \eta_y V_m \frac{1}{E_m} \right) \quad (3.5)$$

$$\frac{1}{G_{xy}} = \frac{1}{V_f + \eta_G V_m} \left(V_f \frac{1}{E_f} + \eta_y V_m \frac{1}{E_m} \right) \quad (3.6)$$

$$\eta_y = \frac{1}{2} \left(1 + \frac{E_m}{E_f} \right) \quad (3.7)$$

$$\eta_G = \frac{1}{4(1 - V_m)} \left(3 - 4V_m + \frac{G_m}{G_f} \right) \quad (3.8)$$

where,

E_y = transverse modulus of elasticity of the FC material (psi)

G_{xy} = transverse shear modulus of the FC material (psi)

η_y = stress partitioning parameter for transverse modulus of elasticity

η_G = stress partitioning parameter for transverse shear modulus

The known property values for each of the component materials were substituted into Equations 3.7 and 3.8, and the resulting values of η_y and η_G were placed into Equations 3.5 and 3.6, respectively. The values for E_y and G_{xy} were determined to be:

$$E_y = 1.55 \times 10^6 \text{ psi}$$

$$G_{xy} = 0.476 \times 10^6 \text{ psi}$$

The flexural modulus of FC dowel was determined also by experimental methods. Three-point and four-point bending tests were conducted on the dowel specimen. The test procedures involved setting the dowel in pure bending and recording the displacements for corresponding loads. Applying the relationships between the measured load, displacement, dowel section properties, and the beam configurations, the flexural modulus of the dowel was obtained as:

$$E_b = 6.40 \times 10^6 \text{ psi}$$

Since the experimental and theoretical moduli of elasticity were in close agreement with each other, an average of the two was used in the remainder of the study.

3.3 Analysis of Dowels

When a load is applied to one side of a doweled joint (refer to Figure 3.1), some portion of that load is transferred to the subgrade. The remaining part of the load

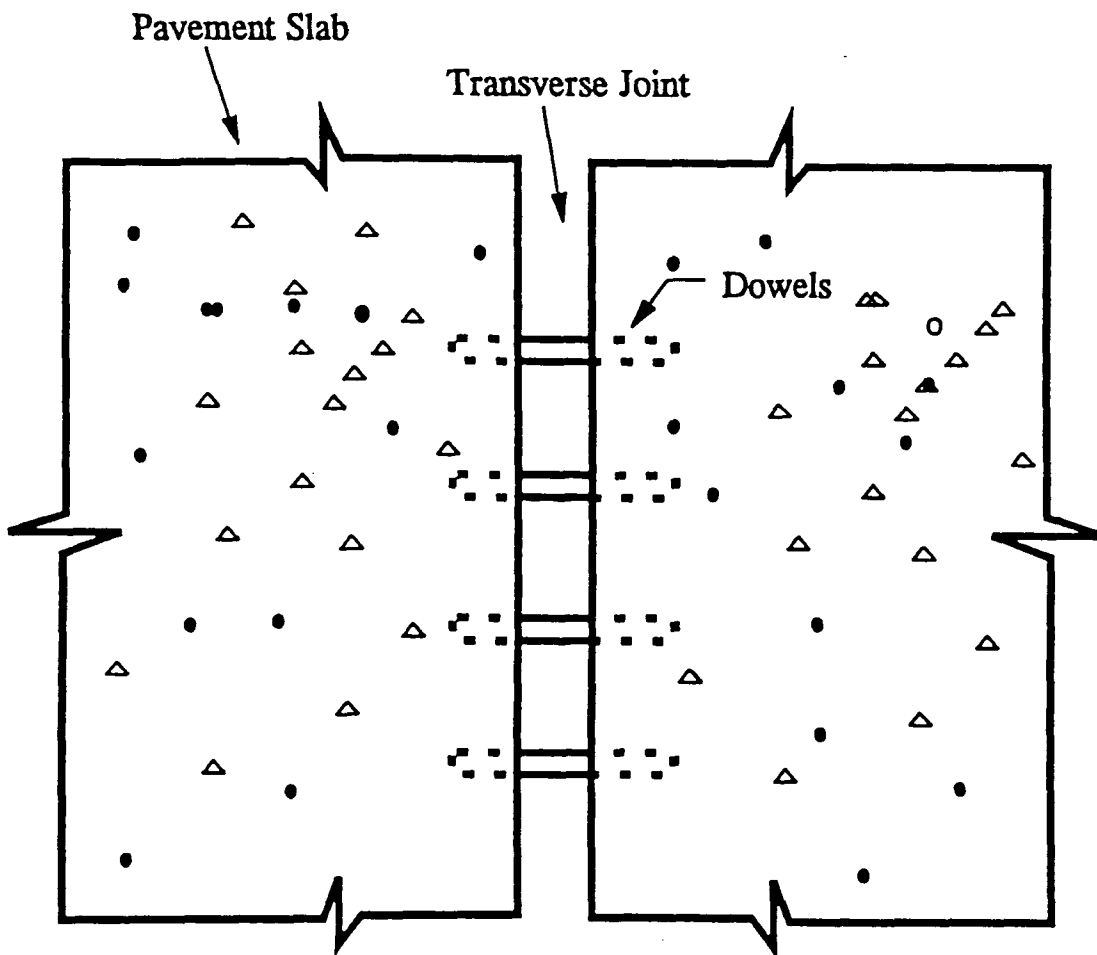


Figure 3.1: Dowels as load transferring devices across the transverse joint of a highway pavement slab

is transferred to the other side of the joint through the dowels spanning across the joint. The portion of the applied load that is transferred through the dowels is a direct measure of the efficiency of the dowels. In an ideal situation where the dowels are fully effective, 50% of the load applied on one side of the joint is transferred to the other side through dowels (Westergaard 1928). Thus, the more the load transfer across the joint, the more efficient are the dowels.

One other measure of dowel efficiency is the relative displacement of the two slab faces at the joint. In case of a 50% load transfer, which is ideal, both the slabs experience the same share of load, and therefore, undergo the same amount of deflection which makes the relative deflection of the two faces, a zero. This is the most effective functioning of dowels because the transition from one slab to the adjoining slab is smooth, and therefore, there is no sudden load applied on the edges of the joint as a vehicle crosses the joint from one side of the joint to the other. However, in real situations 50% load transfer is very rare, and so there is always a relative deflection of slab faces at transverse joints. The less the relative deflection, the more efficient are the dowels.

When a load is applied at a doweled joint, the dowel bar which is directly underneath the point of application of the load, or the dowel bars which are closest to the position of the load assume a larger proportion of the load that is transferred across the joint. The load carried by the dowels decreases as the distance from the load increases. Thus, when a load is applied at a joint, the dowel bar or the bars which are closest to the position of the load are the most highly stressed dowels. The dowels contained within a distance of $1.8 l_r$ from the load are active in transferring the load (Friberg 1938; Yoder 1975) where l_r , the radius of relative stiffness, is defined

as follows (Westergaard 1925):

$$l_r = \sqrt[4]{\frac{Eh^3}{12(1-\mu^2)k}} \quad (3.9)$$

where,

l_r = radius of relative stiffness (in.)

E = modulus of elasticity of the pavement concrete (psi)

h = thickness of pavement (in.)

μ = Poisson's ratio of concrete

k = modulus of subgrade reaction (pci)

The load transfer is assumed to be distributed linearly among the active dowels with the peak value (P_i) located at the position of the applied load, and zero at a distance of $1.8 l_r$ from the load as shown in Figure 3.2. Thus, to find the maximum load transferred (P_i) through a dowel, the distribution of dowel loads as shown in Figure 3.2 has to be carried out for each of the applied loads. The dowel shears calculated individually for each load can then be superimposed to obtain the design load on dowels.

Though the efficiency of a doweled joint is directly related to the total load transferred across the joint, the efficiency is limited by the load transfer capacity of each individual dowel. The load transfer capacity of a dowel is defined as the maximum load that the dowel can transfer from one side to other of the joint bound by the following failure modes: shear of the bar, bending in the bar, bearing or crushing of concrete directly underneath the bar, splitting of the underneath wedge shaped concrete block, or a combination of these modes.

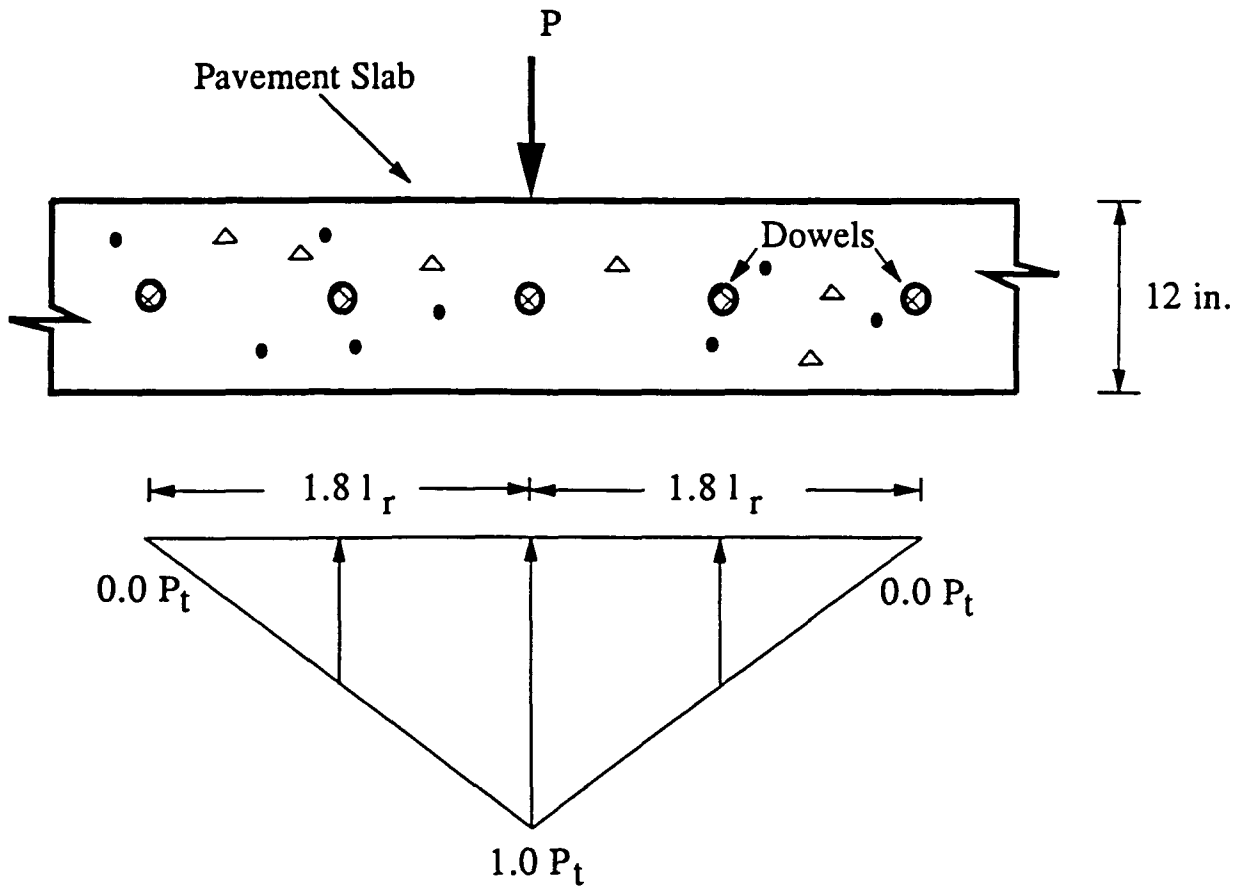


Figure 3.2: Assumed distribution of transferred load (across transverse joint) among the active dowels

Since the design of a doweled joint should consider all the above mentioned failure modes, the bearing stress on concrete, the bending stress in the bar, and the shearing stress in the dowel must be known. Dowel analysis is performed to determine these critical stresses for a given position and magnitude of the load. As explained before, a maximum of 50% can be transferred across a doweled joint. However, a reduction of load transfer always occurs because of the dowel looseness caused by the repetitive loads applied to the joints. This reduction usually varies from 5 to 10 percent but for design purposes a 45% transfer can be assumed (Yoder 1975). Also, this critical transfer is possible only when the position of the load is exactly over one of the faces of the slabs at the transverse joint. Once the total design load transfer is calculated, individual dowel shears can be determined by assuming a distribution similar to the one shown in Figure 3.2. The design shear transferred through a dowel is necessary for investigating the critical stresses that control the load transferring capacity of the dowel. Several methods of idealization of the dowel-concrete system were considered which attempt to analyze the dowel for critical stresses. Analyses based on methods developed by Westergaard (Westergaard 1925), Friberg (Friberg 1938), and Bradbury (Bradbury 1932) were studied. The underlying assumption in all of these methods is that a dowel can be idealized as a beam resting on an elastic foundation. The original problem was solved by Timoshenko, who considered three cases namely infinite, finite, and semi-infinite lengths of a beam resting on an elastic foundation (Timoshenko 1925, 1976). Since the theories developed by Westergaard, Bradbury, and Friberg assume the same idealization of the dowel-concrete system, and since these methods have limitations which restrict them to certain circumstances, the original theory developed by Timoshenko was considered for this research. Timoshenko introduced

a constant K , called the modulus of foundation (or modulus dowel support), which denotes the reaction per unit length when the deflection is unity. This factor assumes that when a beam is deflected, the continuously distributed reaction at every point is directly proportional to the deflection of the beam at that point (refer to Figure 3.3). The differential equation for deflection of the beam can be written as

$$EI_z \frac{d^4 y}{dx^4} = q \quad (3.10)$$

where, q is the intensity of the load acting on the beam which, for the unloaded portion of the beam is equal to $-Ky$, where y is the deflection of the dowel at the point of consideration. Equation 3.10 can be rewritten as

$$EI_z \frac{d^4 y}{dx^4} = -Ky \quad (3.11)$$

The general solution of Equation 3.11 is given by

$$y = e^{\beta x}(A \cos \beta x + \sin \beta x) + e^{-\beta x}(C \cos \beta x + D \sin \beta x) \quad (3.12)$$

where,

K = Modulus of foundation (psi)

EI_z = Flexural rigidity of the beam ($lb - in^2$)

The constants A , B , C and D can be determined by applying the boundary conditions. For the present problem of dowel embedded in concrete, the boundary

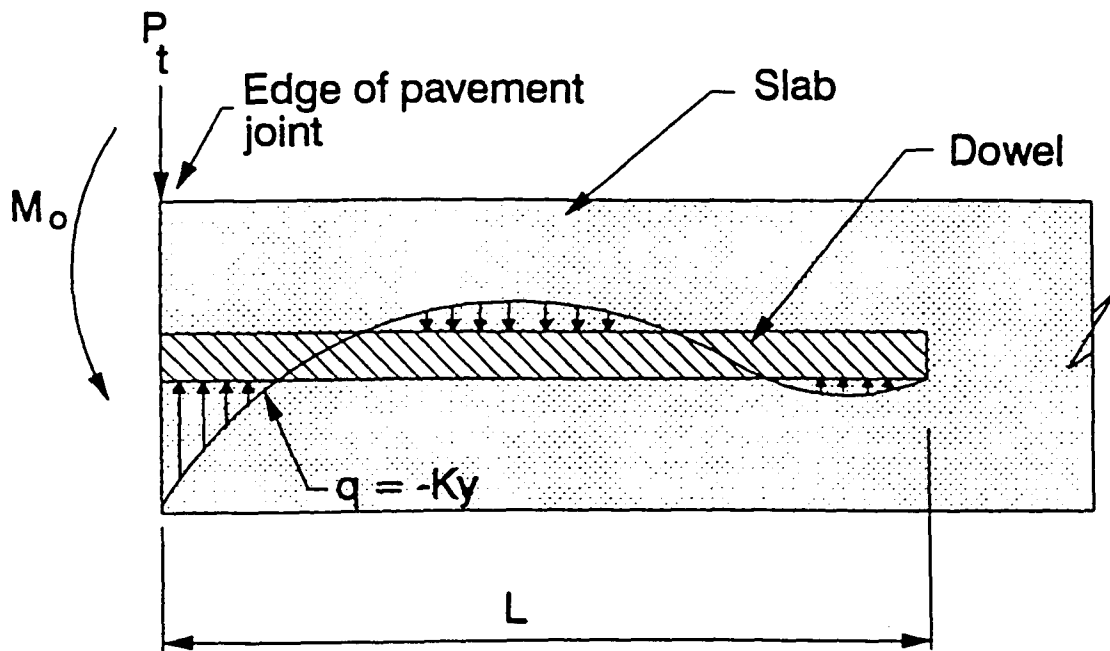


Figure 3.3: Dowel as a beam on elastic foundation

conditions available are

$$\begin{aligned}
 \text{(i)} \quad & \text{at } x = 0, \quad M = EI_Z \frac{d^2 y}{dx^2} = -M_o \\
 \text{(ii)} \quad & \text{at } x = 0, \quad V = -EI_Z \frac{d^3 y}{dx^3} = -P_t \\
 \text{(iii)} \quad & \text{at } x = L, \quad M = EI_Z \frac{d^2 y}{dx^2} = 0 \\
 \text{(iv)} \quad & \text{at } x = L, \quad V = EI_Z \frac{d^3 y}{dx^3} = 0
 \end{aligned}$$

where, P_t is the dowel shear, M_o is the moment in the dowel at the face of the joint, and L is the length of the dowel on one side of the joint. Successive differentiation of Equation 3.12 yields

$$\begin{aligned}
 \frac{d^2 y}{dx^2} &= \beta^2 e^{\beta x} (-2A \sin \beta x + 2B \cos \beta x) + \beta^2 e^{-\beta x} (2C \sin \beta x - 2D \cos \beta x) \quad (3.13) \\
 \frac{d^3 y}{dx^3} &= 2\beta^3 e^{\beta x} [-A(\cos \beta x + \sin \beta x) + B(\cos \beta x - \sin \beta x)] \\
 &\quad + 2\beta^3 e^{-\beta x} [C(\cos \beta x - \sin \beta x) + D(\cos \beta x + \sin \beta x)] \quad (3.14)
 \end{aligned}$$

By applying boundary conditions (i) and (iii) to Equation 3.13 and boundary conditions (ii) and (iv) to Equation 3.14, a set of four simultaneous equations can be formed (Porter 1992). By solving the four simultaneous equations, the unknowns A , B , C , and D can be determined. With the calculated values of A , B , C and D , one can establish the equation for deflection along the dowel. The distribution of bending moment and shear force along the length of the dowel can be derived by differentiating the equation for deflection (or by using Equations 3.13 and 3.14).

The modulus of dowel support, K is a very important term in the analysis of pavement dowels. The value of K can not be easily established theoretically because several factors with respect to the dowel material and sectional properties as well

as those of the surrounding concrete affect the modulus of dowel support. Also since there is no information available as to what value of K is to be used in the analysis of a specific situation, the modulus of dowel support was determined through experimentation. The importance of the single dowel shear tests is to establish the modulus of dowel support using the theory developed for the analysis of dowels.

As elicited by Equation 3.12, the deflection equation is dependent on the value of β , which is in turn a function of K . But the value of K is unknown, and in fact, is the outcome of this part of investigation. And so, a graph relating the modulus of dowel support and the deflection of dowel at the face of the joint was developed by substituting various values of K in Equation 3.12, and evaluating the equation for the location defined by $x=0$. The graph was then consulted to read the particular modulus of dowel support corresponding to the measured dowel deflection at the face of the joint. Accordingly the instrumentation for the single dowel shear tests was designed to measure the relative deflection of the two concrete faces at the joint. The instrumentation also included placement of strain gages along the length of the dowel for gaining more insight into the theoretical model used in dowel analysis, and for establishing a procedure by which the results of the elemental tests can be extrapolated to estimate the behavior of dowels of the full-scale slabs.

3.4 Fatigue Testing of Full-scale Slabs

3.4.1 Introduction

Since the purpose of this part of the investigation was to compare the responses of steel and FC doweled joints, a series of tests on full-scale slabs containing the dowels of the two types of materials were performed. The tests were intended to be

conducted in the laboratory under the conditions close to those of the actual highway pavements. One of the challenges to face in this regard was the laboratory simulation of the soil subgrade support, whereas the other was the selection of spacing of FC dowels which would exhibit the same efficiency as the 12-inch spacing of steel dowels would. The 1.5-inch diameter steel dowels placed at 12-inch spacing is the common practice of Iowa DOT. Since the focus of the investigation is to compare the effect of fatigue on FC and steel dowel efficiencies, both the systems were to be maintained approximately at the same dowel efficiency at the beginning of fatigue loading. That is, the parameters which define dowel efficiency should be similar in both the FC and steel doweled slabs before the fatigue experimentation was initiated, in order to compare the degradation, under repetitive loading of the two types of systems with respect to a common initial stage. After meeting these two challenges, the required instrumentation was designed and a comprehensive test procedure was developed for testing concrete slabs under repetitive loads, which at the end was found out to be quite successful.

3.4.2 Simulation of subgrade

Simulation of soil subgrade is a relatively easy task to perform in laboratory, but the maintenance of the same is not. The soil subgrade can be prepared to simulate the field soil properties, and a modulus subgrade reaction of 100 pci, which is typical for a subgrade supporting an actual highway pavement slab (Pavement 1993). However, proper confinement of the subgrade in order to retain the same behavior and performance is rather difficult. While this is true for a static test, the maintenance of soil subgrade is close to impossible in case of fatigue testing.

Determination of an effective procedure for simulating soil subgrade in laboratory demanded extensive literature search in the area of laboratory testing of concrete slabs in general, and fatigue testing of doweled joints in particular. The previous research performed to evaluate the effect of repetitive loading on load transfer efficiency of dowels is so limited that the author could locate only one reference of such nature which dates back to 1958. However, the contribution of the knowledge of that research (Teller 1958) was so considerable that the same method of subgrade simulation used in that work had been adapted, with some modifications though, for the experimentation conducted in this research project.

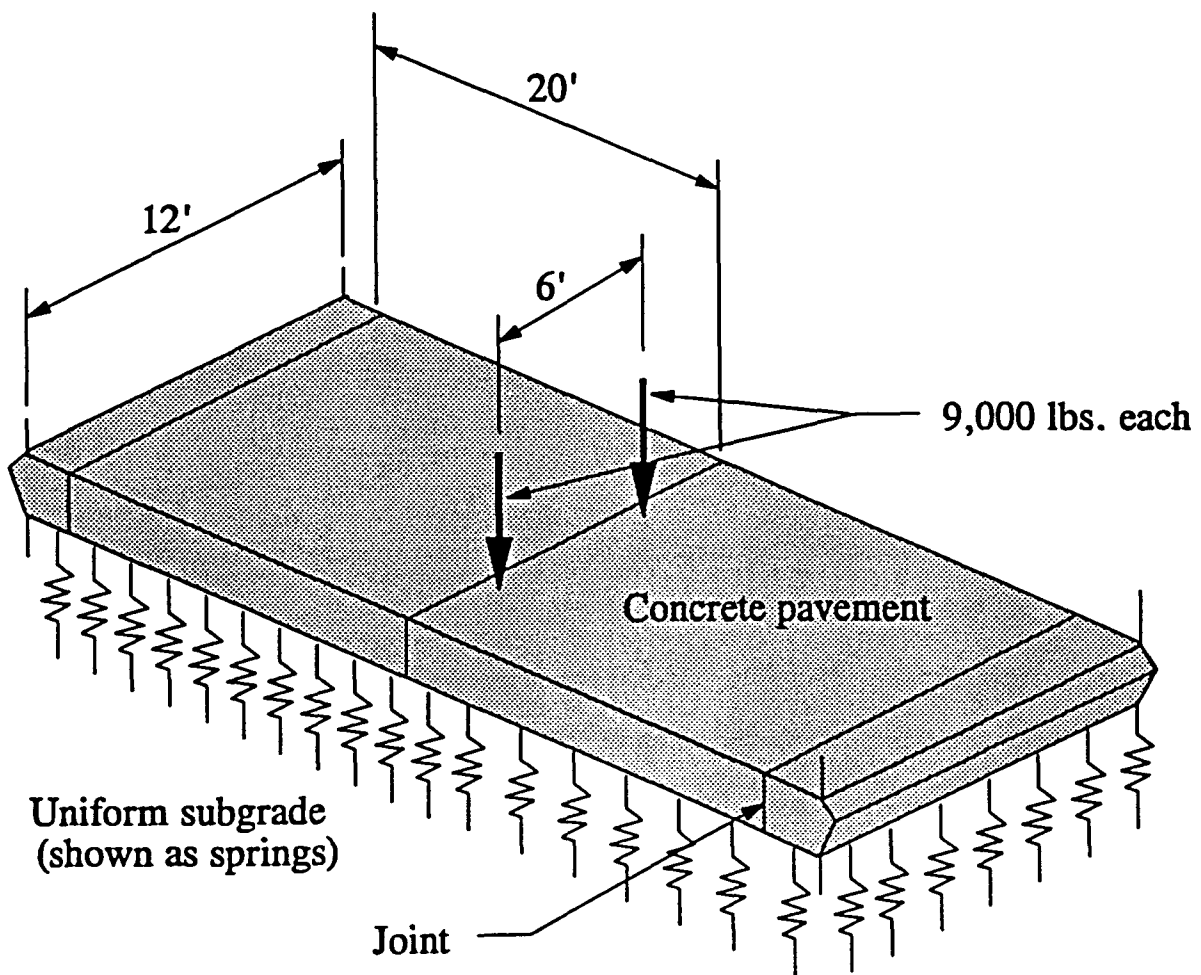
Teller and Cashell studied the effect of fatigue on dowel efficiency by subjecting doweled concrete slabs to repetitive loading. To facilitate the process of experimentation, they supported the test slabs on a series of beams the lengths and sections of which could be tailored to suit the subgrade reaction desired. The design of supporting steel beams was based on achieving a deflection of 0.1 inches, for an applied load of 1000 pounds, which was believed to be similar to how a field soil subgrade would perform. The same concept of supporting the test slabs on a series of steel beams was considered for this work with the view that the simulation would result in the same deflection profile as that of an actual pavement slab under similar loads. This idealization, however arduous it may be, results in a more uniform support of the test slabs throughout the duration of fatigue testing. Also since the lengths and sizes of the supporting beams are variables, the modulus of subgrade can be altered at any time, if desired.

The use of steel beams for simulation of soil subgrade also enabled a very effective method of envisaging the total load transfer across the joint. The beams can be

calibrated to establish the relationship between the applied load and resulting strain. By mounting the strain gages on the supporting beams, and conducting static tests, the above mentioned relationships can be developed. The same strain gages are also useful in measuring the strains experienced by the beams under experimental loads. The beam loads can be calculated from the measured strains using the already established load-strain relationships. These loads when totalled for the supporting beams on the unloaded side of the doweled joint, yield the total load transferred across the joint, which is the direct measure of efficiency of the dowel-concrete system.

3.4.3 Design of test setup

3.4.3.1 Introduction The design of test setup for fatigue testing of full-scale slabs involves selecting the appropriate lengths and sections for the supporting beams which simulate the soil subgrade as explained in Section 3.4.2. Following from the discussion presented in that section is the fact that the supporting beams need to be designed so as to yield the deflections similar to the field deflections. However, knowledge of the deflections an actual concrete pavement undergoes in the field is very limited. Also data corresponding to the field deflections under the conditions used in this research was not found. Therefore, analysis of an actual pavement using finite elements was undertaken. A computer model of the actual pavement resting on an elastic foundation (whose subgrade reaction is set to that of the field) was formulated. Figure 3.4 illustrates a portion of a highway pavement slab considered for computer modeling.



Note: Pavement continues in both directions

Figure 3.4: Actual pavement slab considered for analysis

3.4.3.2 Finite element model of highway pavement slab The overall dimensions of the highway pavement slab considered for finite element analysis were 40 ft x 12 ft x 1 ft which consisted of two 20-foot long strips of the slab separated by a transverse joint. Since the effect of loads applied at a transverse joint was assumed to be local to the two pavement strips meeting at that joint, only those two strips were considered for modeling as opposed to considering a semi-infinite number of strips actually existing on either side of the joint. The assumption was later verified to be quite reasonable by analyzing four and six strips of the slab, and comparing the results with those obtained by analyzing only two strips.

The idealization of the problem consisted of modeling the concrete slab as a mesh of quadrilateral shell elements. The geometry of each shell element was defined by four points which represent the corners of the element. The thicknesses of the shell at the four corners were required to complete the definition of the shell element with respect to geometry. However, since the concrete slab was of uniform thickness, the same value of thickness was repeated for all the four corners. The material properties required for defining the shell element were the moduli of elasticity (E_x , and E_y), Poisson's ratio (μ_{xy}), and shear modulus (G_{xy}). The shell element was capable of accepting elastic foundation stiffness (EFS) as input which simplified the process of idealizing the soil subgrade. Also, since the shell element provided an option for considering the density of the material, explicit idealization of the self weight of the concrete could be omitted.

The width of the joint considered in the analysis was 0.5 inches. Spanning across the joint were the dowels which were modeled as 3D beams. Each beam required two end points to define the geometry. The section properties of the beam element

consisted of the area of cross section (A), and the moments of inertia (I_{XX} , I_{YY} , and I_{ZZ}). The modulus of elasticity (E), and shear modulus (G) formed the material properties required for the beam element.

The vehicle load was idealized as two concentrated loads acting vertically downwards each of which was 9000 pounds (one axle load). The two loads were separated by a distance of 6 feet and were applied on one side of the joint. The boundary conditions consisted of restraining the lateral and longitudinal movements of the two outside edges of the slab.

The finite element mesh used for analyzing the highway pavement is presented in Figure 3.5. As shown in Figure 3.5, the size of the quadrilateral shell element was varied in order to facilitate the connections between the dowels and concrete elements so that such connections occur at the corners of the shell elements. Since certain portions of the dowels were embedded in the concrete slab, the interfacing shell elements located along either side of the joint were assigned combined properties which were derived from the material properties of the concrete and the dowel, by applying the standard rule of mixtures.

The analysis was performed on ANSYS (a finite element analysis program) for the field properties of concrete and subgrade, and the boundary conditions and loading shown in Figure 3.5. The joint consisted of 1.5-inch diameter steel dowels at a spacing of 12 inches. The results of the analysis with respect to deflections were tabulated and presented in Table 3.1 under the column represented by "Large Model". Listed in that column are the deflections obtained along the center line of the slab. Since the maximum values of the slab deflections are along the centerline, the center line deflections were considered for design of the test setup by matching the deflection

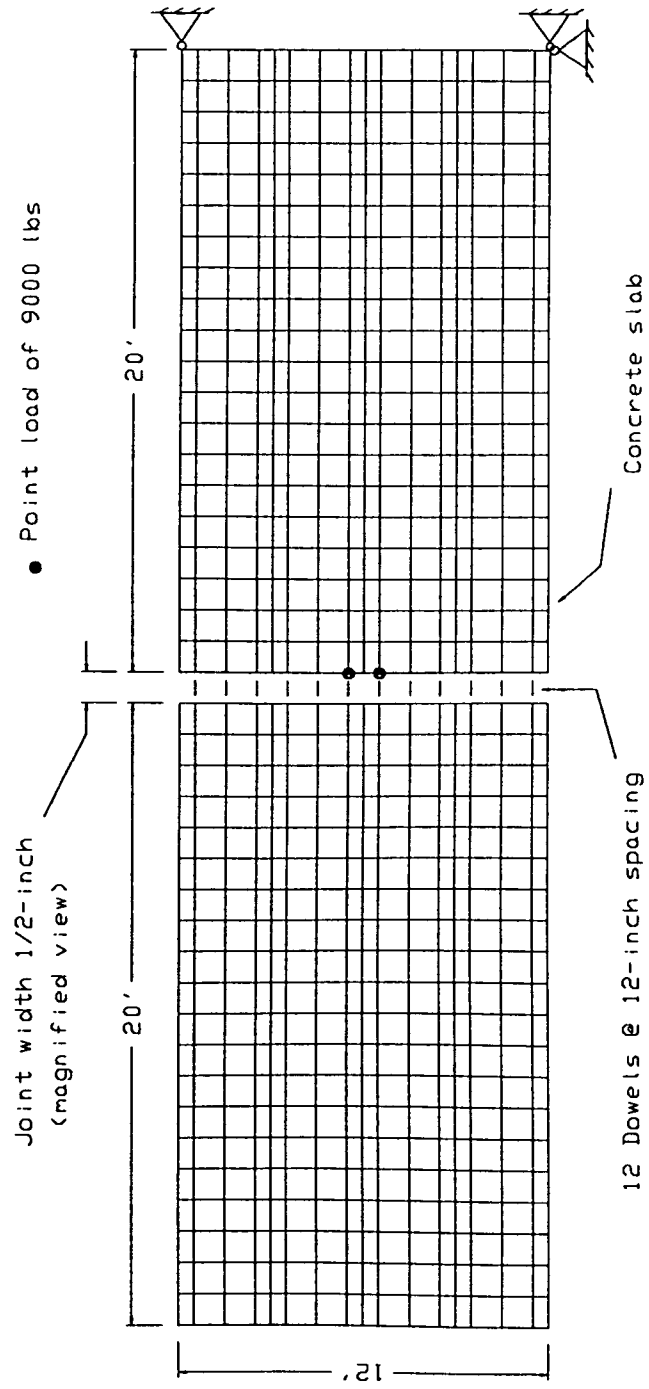


Figure 3.5: Finite element model of actual pavement slab

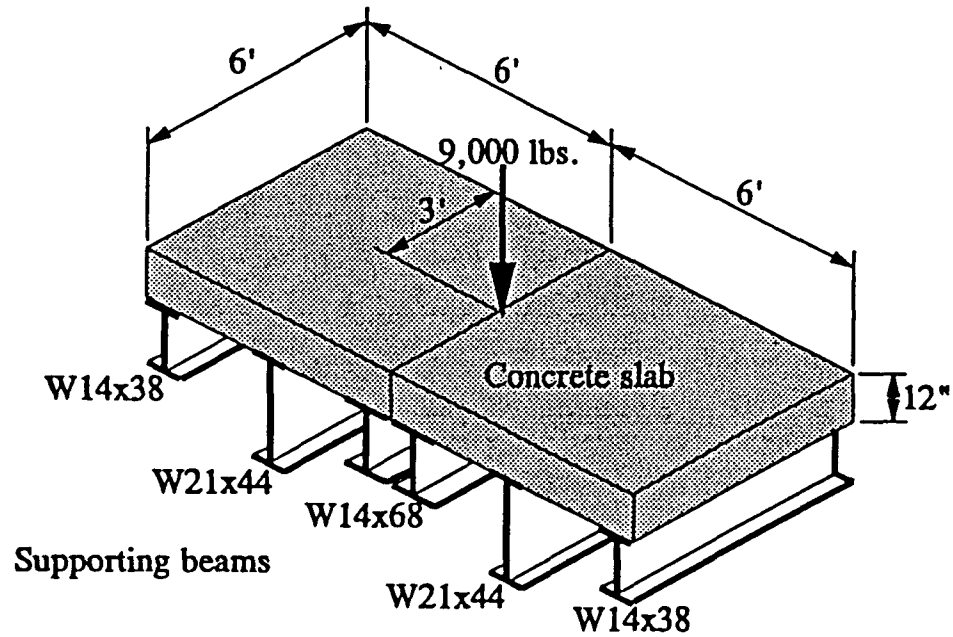
Table 3.1: Deflections from finite element analyses

Distance from joint (ft.)	Large Model (in.)	Distance from joint (ft.)	Laboratory Model (in.)
-7	-0.0059		
-6	-0.0067		
-5	-0.0074	-6	-0.0072
-4.5	-0.008	-4.5	-0.0091
-3	-0.0098	-3	-0.011
-2	-0.0113	-2	-0.0123
-1	-0.013	-1	-0.0137
-0.5	-0.0139	-0.5	-0.0143
0	-0.0148	0	-0.015
0	-0.0147	0	-0.0149
0.5	-0.0138	0.5	-0.0143
1	-0.0129	1	-0.0136
2	-0.0112	2	-0.0122
3	-0.0097	3	-0.0109
4.5	-0.008	4.5	-0.009
5	-0.0074	6	-0.007
6	-0.0066		
7	-0.0059		

profiles of the actual pavement slab (large model) and the laboratory test slab (small model).

3.4.3.3 Finite element model of the laboratory setup As explained in Section 3.4.2, the laboratory test slabs were proposed to be supported on a series of beams. Therefore, simulated subgrade was discrete as opposed to the continuous soil subgrade present in the case of an actual highway pavement. However, the test setup was to be designed so that the behavior of the test slabs with respect to deflections would be as close to that of the actual highway pavement slab as possible. In order to match the deflections of the test slabs to those of the actual pavement, a finite element model of the laboratory setup was essential. However, the configuration of the supporting beams had not yet been determined, and so, a series of spring elements (actually 3D beams oriented in a vertical direction) were used to represent each supporting beam.

The reduced size of the test slabs along with the discrete subgrade formed the differences between the laboratory test slabs and actual pavement slabs which resulted in a slightly different finite element model than the model presented in Section 3.4.3.2. The model for laboratory setup consisted of two concrete slabs meeting at a transverse joint of 0.5 inches wide. The overall dimensions of the model were 12 ft x 6 ft x 1 ft as shown in Figure 3.6. Again, the concrete slab was idealized as a mesh of quadrilateral shell elements, but now, without an EFS input. Instead, a series of spring elements were introduced underneath the slab. The stiffness of each of these elements could be altered by changing either the area, the elastic modulus, or both, of the element. Since the width of the slab was 6 feet, which is the separation of the two axle loads,



Note: Beams only shown to edge of slab. Actually extend 3'-0" beyond each edge of slab.

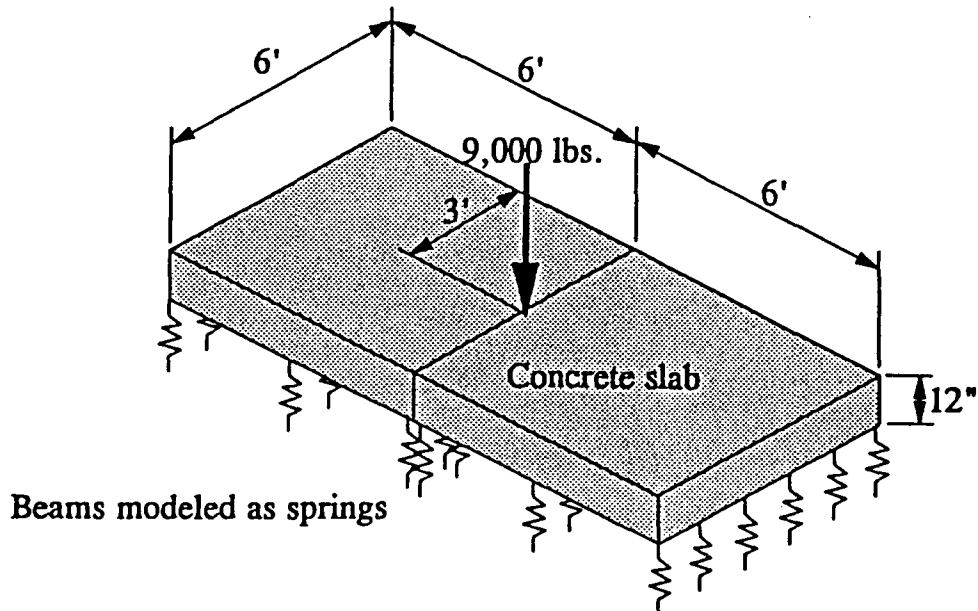


Figure 3.6: Laboratory test slab considered for analysis

only one point load could be applied to the test slabs. The other parameters of the model were the same as those of the model used for the actual pavement slab. The finite element model used for the laboratory setup is illustrated in Figure 3.7.

A trial and error method was required to use the model as a tool in the design of the test setup. The analysis of the laboratory model was performed several times by varying the properties of the spring elements until the displacements approximately matched those of the actual pavement model. The results of the analysis with respect to displacements are reported in Table 3.1 so that a direct comparison of the deflections from the two models can be made. Figure 3.8 shows the comparison of the deflection profiles obtained from the analyses of the two models. As seen from Table 3.1 and Figure 3.8, the deflection profiles obtained for the two models were similar.

3.4.3.4 Selection of supporting beam configurations The reaction values of the spring elements of the laboratory model were used to configure the supporting beams. The reactions experienced by the springs were applied to the supporting beams as an equivalent uniform loading because of the minor differences between the spring reactions at each beam location. With these loads applied, as shown in Figure 3.9, the supporting beam sections were designed to approximately match the displacements desired in the slab. The variables in the investigation included the length, size, and weight of each supporting beam.

3.4.3.5 Equivalent FC dowel system The computer modeling of the concrete slab was not only helpful in designing the test setup, it was also useful in designing the FC dowel system. By performing analysis of the computer model of

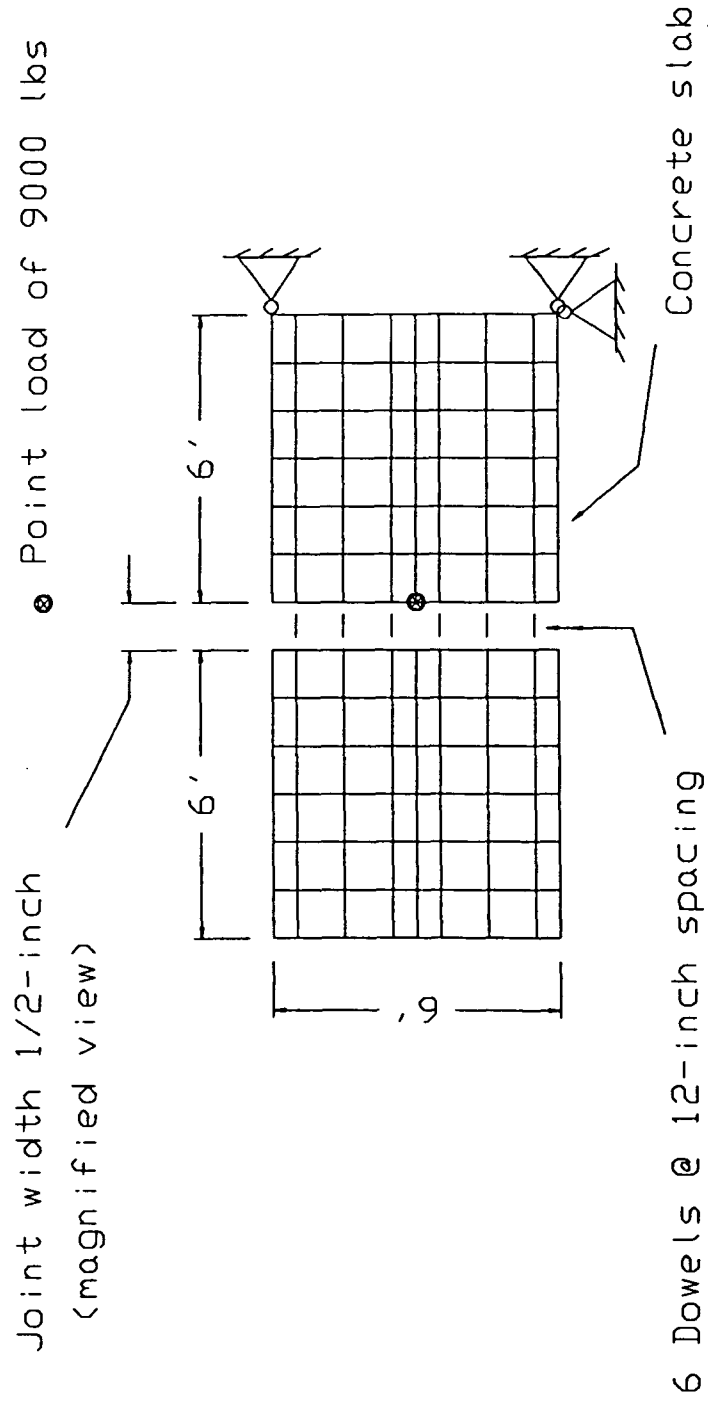


Figure 3.7: Finite element model of laboratory test setup

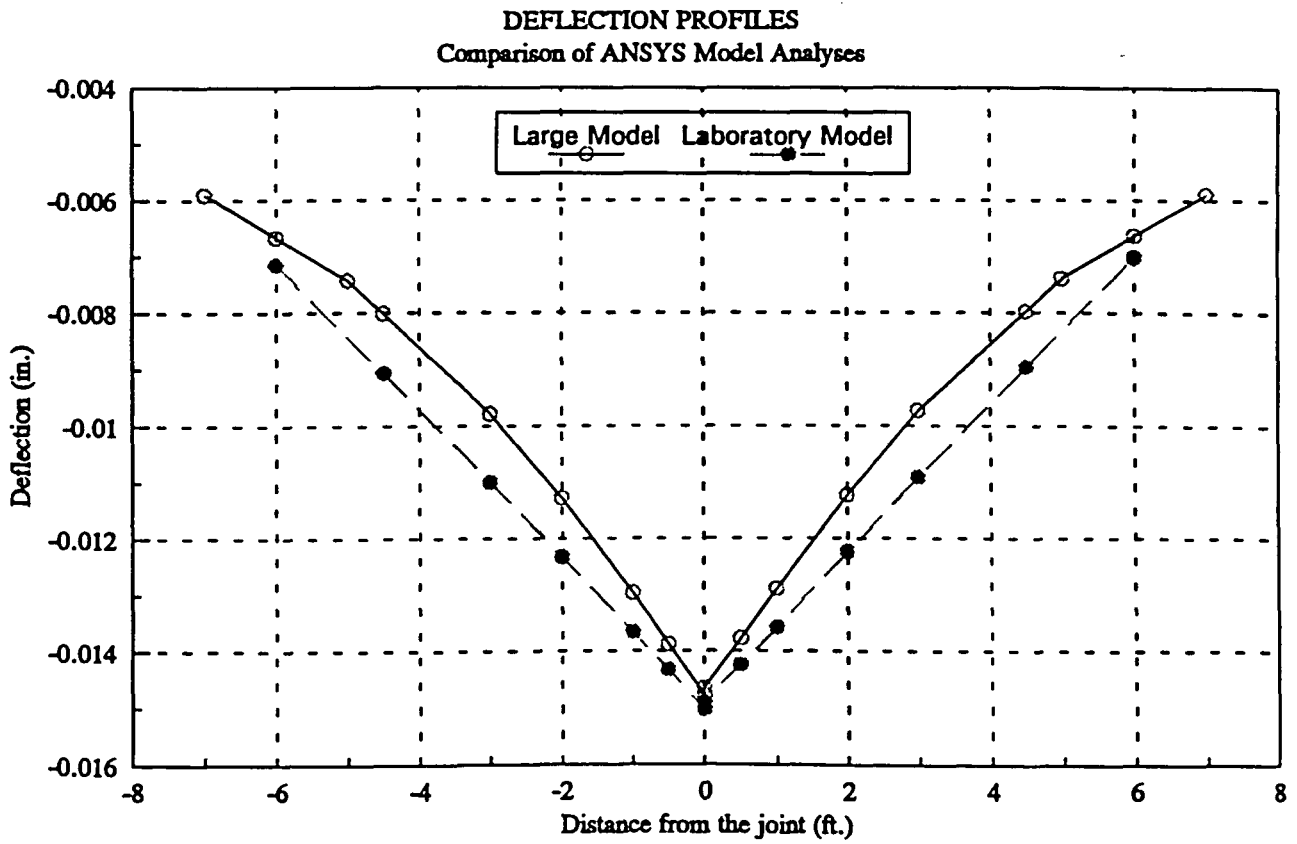


Figure 3.8: Comparison of deflection profiles of actual and test slabs

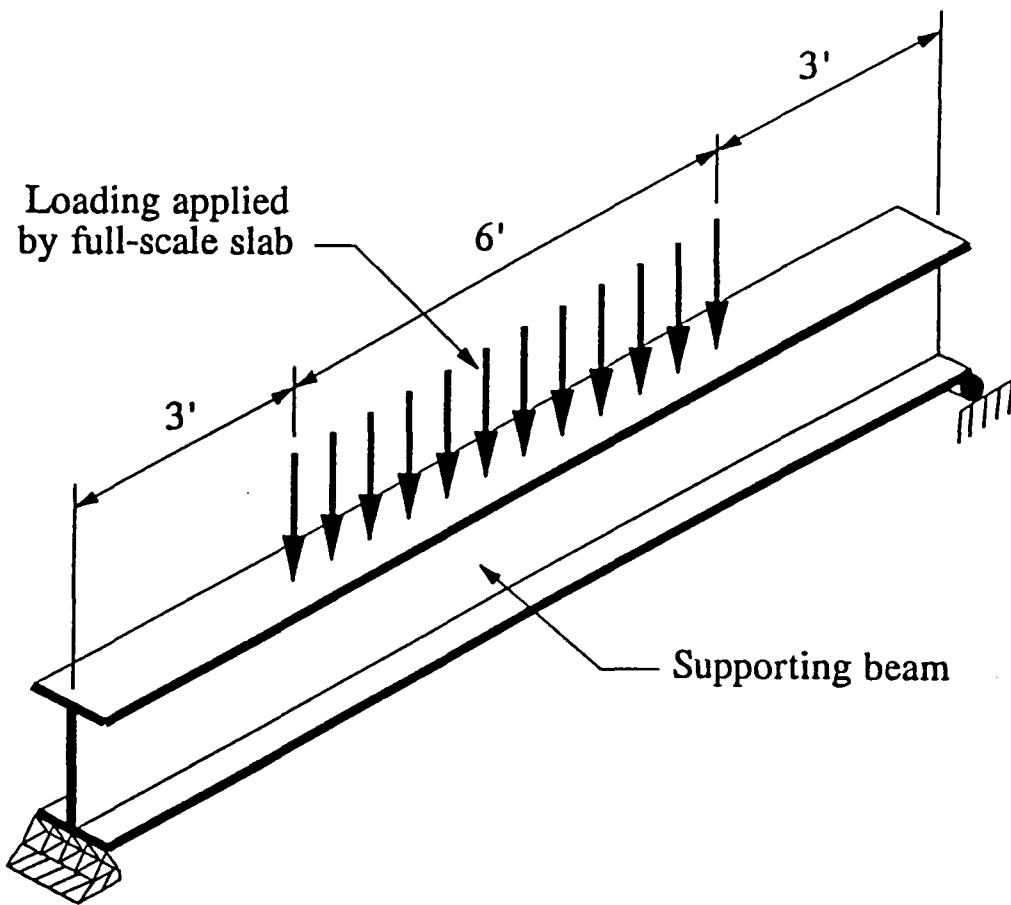


Figure 3.9: Reactions from analysis of test setup applied to supporting beams

actual highway pavement slab for various sizes and spacing of FC dowels, the dowel-concrete system containing 1.75-inch diameter FC dowels at a spacing of 8 inches was found out to be in the close proximity of that of 1.5-inch diameter steel dowels at a spacing of 12 inches. The procedure used for identifying the FC dowel system involved matching the deflection profile of the actual pavement slab with that of the pavement containing FC dowels.

CHAPTER 4. EXPERIMENTAL INVESTIGATION

4.1 Introduction

Various tests and test methods studied and/or developed for facilitating the laboratory experimental investigation are presented in Chapter 3. Since the scope of this research included investigation of the performances of both dowel and tie bars used in highway pavement slabs, two parts of experimentation were programmed. While the tests conducted on dowel bars formed one part of investigation, those performed on tie bars constituted the other.

The single dowel shear tests were conducted for determining of the modulus of dowel support. The purpose of the fatigue tests conducted on full-scale slabs was to compare the efficiencies of steel and FC dowels under the influence of repetitive loads. Bond and pullout tests on FC rods were designed to evaluate the development length requirements of the FC material. Tensile testing of FC rods was performed to evaluate the strength of FC rods to resist the tensile forces caused by lateral movement of two adjacent highway pavement lanes. In addition to conducting the above tests, several auxiliary tests were performed with regard to determining the composite material properties and compressive strength of concrete.

4.2 Elemental Dowel Static Shear Testing

4.2.1 Introduction

The method of evaluating a dowel in concrete, developed through work by Lorenz (1993) and based on work by Timoshenko (1925; 1976), considered a pavement dowel as a finite beam on an elastic foundation, with the bearing pressure between the dowel and the concrete related to the displacement by a constant. The constant, called the modulus of dowel support, K , is fixed for a particular dowel/concrete system. Testing was performed by Lorenz in order to determine K experimentally. During the work by Lorenz, a test method referred to as a modified Iosipescu shear method (Lorenz 1993) was designed and verified for shear testing of a single dowel specimen cast in concrete. Testing by the modified Iosipescu method was previously performed with both 1.5-inch diameter steel and 1.25-inch diameter FC dowels.

The same method of experimental evaluation that was used by Lorenz for testing of FC dowels was applied here. As in the previous work, determination of a value of K was desired for the particular dowel/concrete system studied, which included a 1.75-inch diameter FC dowel.

4.2.2 Materials and specimens

The FC dowels tested in the elemental specimens were the same dowels as those evaluated by the methods described in Section 3.3, and also fatigue tested in the full-scale pavement slabs. The components of the composite material were E-glass fibers in a vinyl ester resin, with properties and proportions as discussed in Section 3.2. Dowel dimensions include a diameter of 1.75 inches and a length of 18 inches.

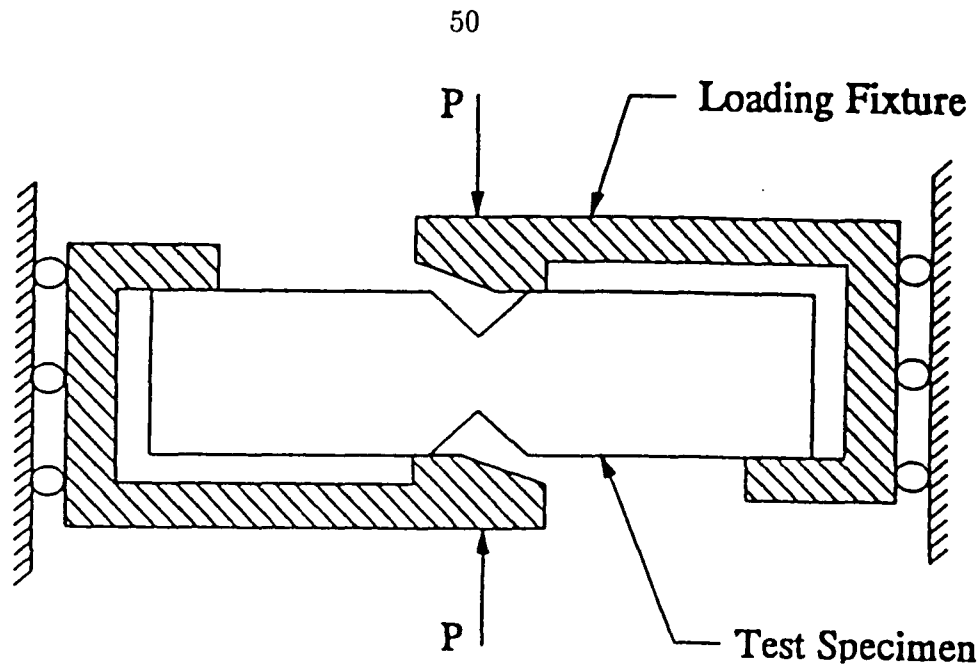


Figure 4.1: Schematic of the Iosipescu shear test method (Walrath 1983)

4.2.3 Test setup

4.2.3.1 General In order to determine the shear resistance properties of the FC dowel and concrete system, the test must apply only shear loading to the test specimen. The shear testing method selected for this research was a modified version of the Iosipescu pure shear test, shown in the schematic of Figure 4.1 (Walrath 1983). By the Iosipescu method, a shear load is applied to a specimen such that there is a maximum shear and no moment at the test section. In order that the test setup used for elemental shear specimens included in this research resemble the Iosipescu test setup, one side of the specimen joint, referred to as the reaction side, was held in a rigid position, while load was applied to the other side of the joint, referred to as the loaded side. In effect, the elemental specimen joint approximated the notch that is present at the test section of the Iosipescu specimens.

4.2.3.2 Testing frame A load frame was previously built for the modified Iosipescu test method using structural steel members and plates. The frame, shown in Figure 4.2, lies horizontally, and uses a single hydraulic cylinder to apply the load to the specimens. The load ram lies between one end of the test frame and a mobile member which applies load to one-half of the specimen. Guide rails direct the mobile portion in a linear movement. Because rotation of the specimen results from the applied load, restraint of the specimen was necessary. Restraint was provided by four threaded rods placed on each half of the specimen, two near the top and two near the bottom. The nuts on the rods bear on steel plates which distribute the restraint to the specimen through thin neoprene rubber pads. A previous study by Lorenz using the same test frame considered the possibility that the restraining rods confine the concrete surrounding the dowel specimen and, therefore, influence the results. Results of the previous testing indicated that the confinement does not influence the results until after the initial failure of the specimen has occurred. Because only the data before failure were of interest in this study, the modified Iosipescu test method was determined to be appropriate (Lorenz 1993).

4.2.3.3 Test specimens Two requirements were to be met by the test specimens used in this study. First, they must provide a good approximation of the conditions experienced by a dowel placed in a highway pavement joint. Second, the specimens must be able to be tested by the modified Iosipescu shear method. Figure 4.3 shows a diagram of the elemental test specimens, which had outside dimensions of 10 in. x 10 in. x 23 in. These dimensions provided a mass of concrete sufficient to approximate field conditions in such a way that the dowel was able to

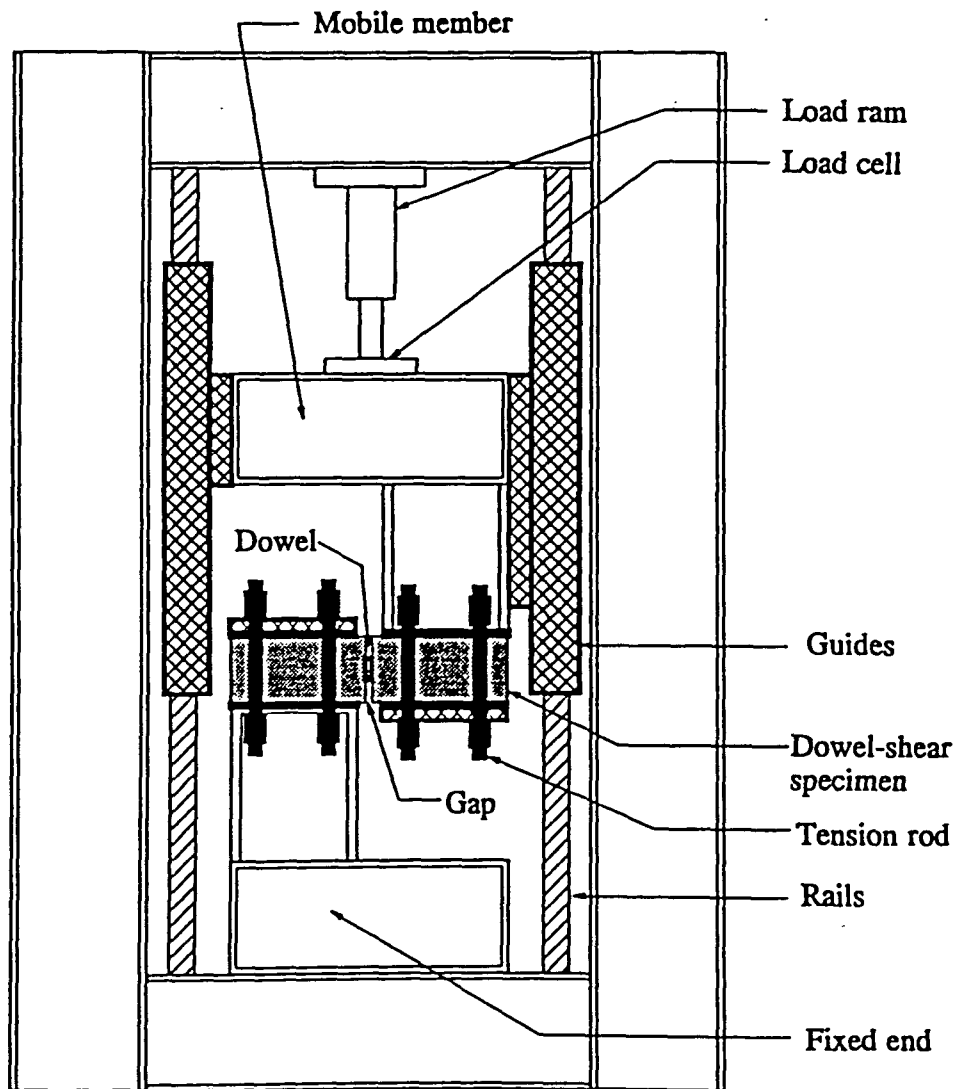
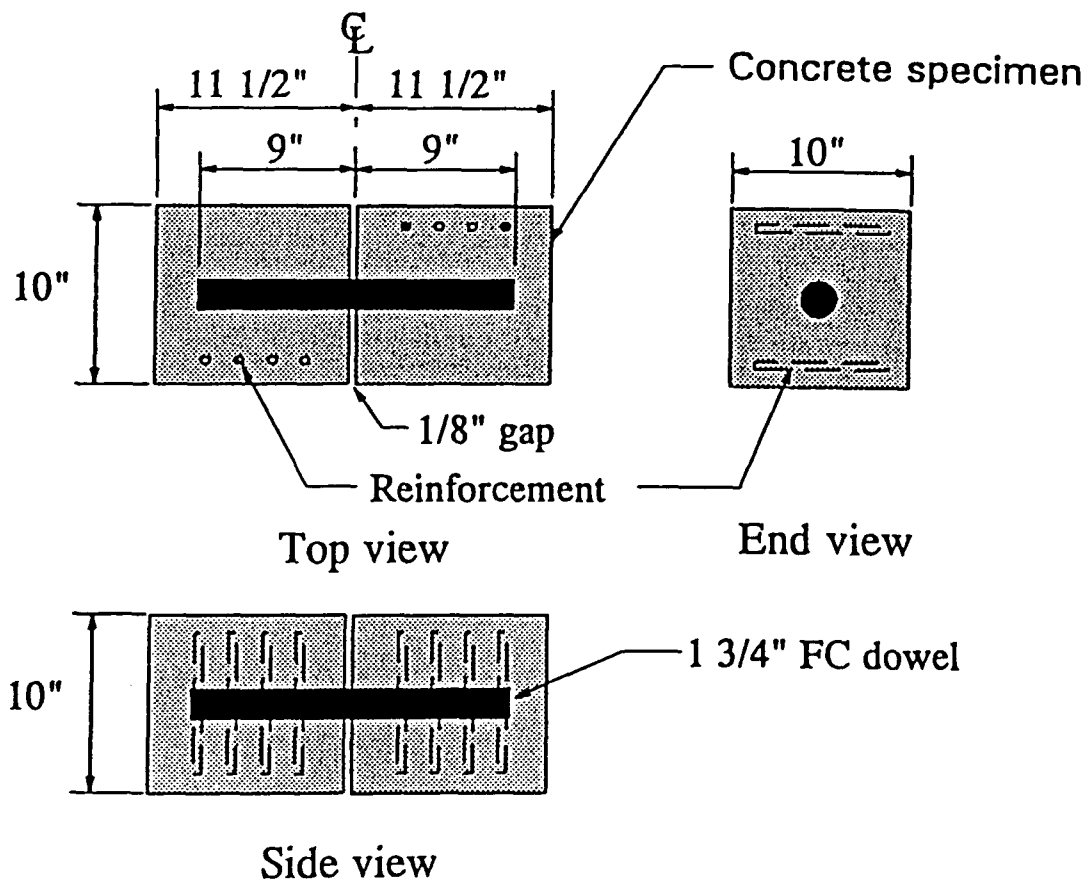


Figure 4.2: Elemental dowel shear, or modified Iosipescu testing frame (Lorenz 1993)



Note: FC dowel is centered in concrete

Figure 4.3: Elemental dowel shear test specimen (Lorenz 1993)

displace within the concrete. Consideration of dowel displacements within the concrete follows from the assumption of an elastic foundation provided by the concrete. Displacements were assumed to be related to the foundation stiffness, and a slight rotation of the end of the dowel was assumed to occur within the concrete. The specimen length provided sufficient cover over the ends of the dowel, while allowing loads to be applied without excessive rotation of the specimen. A joint width of 1/8-inch assured that the shear transfer was limited to the dowel alone, while not introducing significant effects due to bending of the dowel over the joint opening. For the elemental testing portion of the research, a total of nine specimens, in two groups, all using 1.75-inch diameter FC dowels, were constructed and tested. The first group consisted of three, while the second included six elemental shear specimens. Steel form work was used to form the specimens, and 1/8-inch plexiglass was used to form the joint opening. Concrete strengths were determined experimentally by making standard 6-inch by 12-inch concrete cylinders at the time the specimens were cast, and testing the cylinders at the time of the shear tests. A minimum of three cylinders were tested at each time, and the results were averaged to determine the concrete compressive strength, f'_c . Measured strengths for the concrete were quite different for the two groups. The first group of three had a concrete compressive strength of approximately 7,090 psi, while the second group had a concrete compressive strength of approximately 5,090 psi.

From the previous research by Lorenz (1993) on similar specimens, a shear failure mode was noted that could occur during the tests. The failure mode, referred to as vertical shear or concrete splitting, is not common in an actual pavement because of the restraint provided by the large amount of concrete surrounding the dowel, and

because fatigue of the concrete will usually control failure of the concrete surrounding the dowel. During previous testing, steel reinforcing was placed vertically in the specimens on the unloaded side of the dowel for shear strengthening. The initial group of three specimens was reinforced for the splitting failure.

Determination of the modulus of dowel support, K , was performed using the data from the elastic portion of the shear performance of the elemental specimens. The vertical shear failure mode, for which previous research provided reinforcing, occurred outside of the range of the elastic portion. Therefore, the second group of six elemental specimens constructed for this research did not include shear reinforcing.

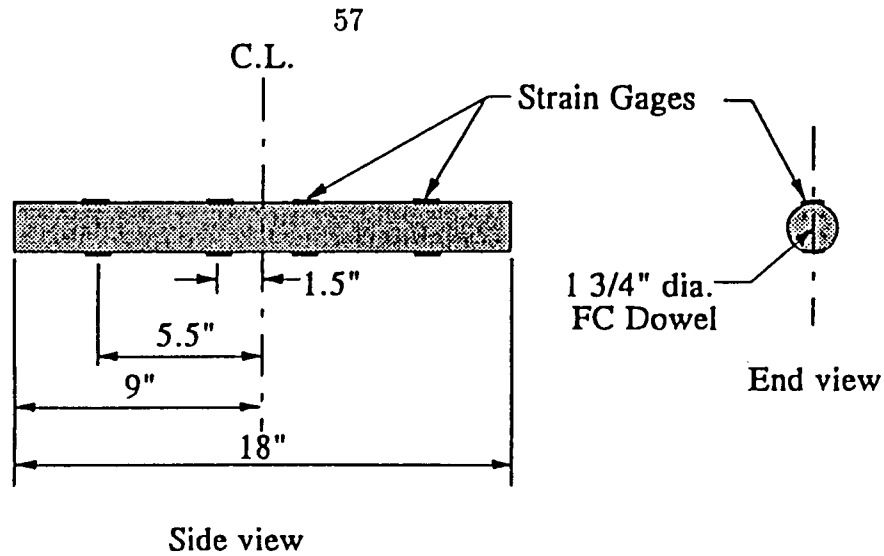
4.2.4 Instrumentation

The data measurements of interest during this testing were the displacements of the loaded side of the specimen relative to the reaction side and the corresponding applied load. A load cell was placed between the hydraulic ram and the mobile portion of the frame to record the applied loads. Displacements were measured with a DCDT, which was anchored to one side of the specimen and measured the relative movement of the two sides of the joint. Though a single DCDT would be sufficient to determine relative displacements between the two sides of the joint, two such instruments were used in order to monitor the rotation experienced by the specimen due to the applied load.

Though the load and displacement data collected as described above can be used to determine a theoretical modulus of dowel support, K , additional instrumentation was applied in an attempt to verify the results. All three of the dowels in the first group of specimens had strain gages placed on them. These were intended, as stated

above, to verify the results from the load and deflection data. Problems with the strain gage instrumentation and data collection, though, prevented strain data from being collected during the testing of these three specimens. On three of the elemental specimens in the second group, strain gages were placed on the FC dowels at two locations on either side of the joint. Locations of the strain gages are shown in Figure 4.4, and, at each location, two strain gages were placed 180 degrees apart, both measuring longitudinal strain. One location was at approximately 1.5 inches from the joint, which was assumed to be near the point of maximum moment in the dowel. The second location was at approximately 5.5 inches from the joint, which was intended to give a general indication of the moment diagram along the dowel. The instrumentation provided a means of determining the flexural performance of the dowel within the concrete while load was transferred across the joint. Results of the strain gage data can then be compared to the theoretical results determined using only the load and displacement data.

Placement of strain gages on steel dowel specimens was found by Lorenz (1993) to influence some of the test results. Steel dowel specimens with gages in place were found to fail at a lower load than those without strain gages. Data collected during the elastic region of the shear testing, though, was found to be unaffected by the placement of strain gages. Because highway pavement dowels experience stresses only in the elastic range during their useful service life, this research was most interested in the dowel performance in the elastic region. For this reason, the use of strain gages on the FC dowels was considered to be acceptable for this research.



Note: Location of strain gages is symmetric about the C.L.

Figure 4.4: FC dowel used in elemental shear testing

4.2.5 Test procedure

Each elemental specimen to be tested was placed in the test frame, and the restraining rods were tightened to hold the specimen in place. Instrumentation was connected to a data acquisition system (DAS) which was interfaced with a personal computer. Before beginning load application to the specimen, the data collection was begun to measure initial conditions. Then, load was applied using a manual hydraulic pump connected to the hydraulic ram. The applied load was constantly monitored by the computer system, and readings of all the instrumentation were automatically taken at a predetermined interval of load set into the controlling program. The test was continued until failure of the specimens. Failure was defined as a severe drop in the measured load while the relative displacement increased. Major cracking of the concrete usually indicated the point of failure of the specimen. The measured load could possibly increase after initial failure, but an increase would be due to restraint

of the specimen due to the steel rods. Behavior after failure would not indicate the performance of the dowels, so data beyond the initial failure was not considered.

4.2.6 Results

Testing was carried out on the two groups of elemental dowel specimens separately, with three specimens tested initially, and followed by testing six others. The differences between the two groups of specimens are explained in Section 4.2.3.3. Also the concrete compressive strengths of the two groups were not the same. Because of these differences, variations in the results were noticed between the two sets.

As discussed in Section 3.3, one of the primary reasons for performing the elemental dowel tests is to determine the modulus of dowel support, K . The theoretical model developed in Section 3.3 involves establishing the four boundary conditions mentioned therein. The establishment of these boundary conditions requires the moment in dowel at the face of the joint (M_o) and the load transferred across the joint (P_t). Whereas the dowel shear is given by the experimental load, the moment, M_o is calculated as

$$M_o = P_t \frac{z}{2}$$

where z is the length of the dowel contained within the joint opening (Bradbury 1932). After setting the required boundary conditions with the experimental load transfer, a relation was established between the relative deflection of the dowel at the face of the joint and the modulus of dowel support according to the procedure explained at the conclusion of Section 3.3. The particular value of modulus of support for the current test configuration was then obtained for the experimental relative deflection.

Table 4.1: Experimental values for modulus of dowel support for 1.75-inch diameter FC dowels

Group	Number of specimens	Concrete compressive strength, f'_c (psi)	Modulus of dowel support, K (pci)
1	3	7090	358000
2	6	5090	247000

The values of K determined from the test results of the two groups of elemental specimens are presented in Table 4.1. These values are specific to the dowel-concrete systems tested in this research which included 1.75-inch diameter FC dowel embedded in concrete of compressive strength listed as in Table 4.1.

From the results of the strain gages mounted on the dowel specimens, a graph relating the measured dowel strain and the experimental load was generated. Though the graph had exhibited non-linearity as the load increases, the initial portion of the graph described rather uniform variation which was approximately the same for all the test specimens considered. Whereas the experimental loads at failure were above 10,000 lbs., only the part of the experimental curve that is contained within 2,000 lbs was considered. The selection of only the lower portion of the experimental load versus dowel strains is further justified by the fact that the range of load transfer for a single dowel that was of most interest in relation to highway pavement dowels is much smaller than the experimental failure loads. From a regression of the measured dowel strain versus experimental load, a relationship was developed as shown in Figure 4.5, and presented in Equation 4.1.

$$P_s = 6.697 S_{1.5} \quad (4.1)$$

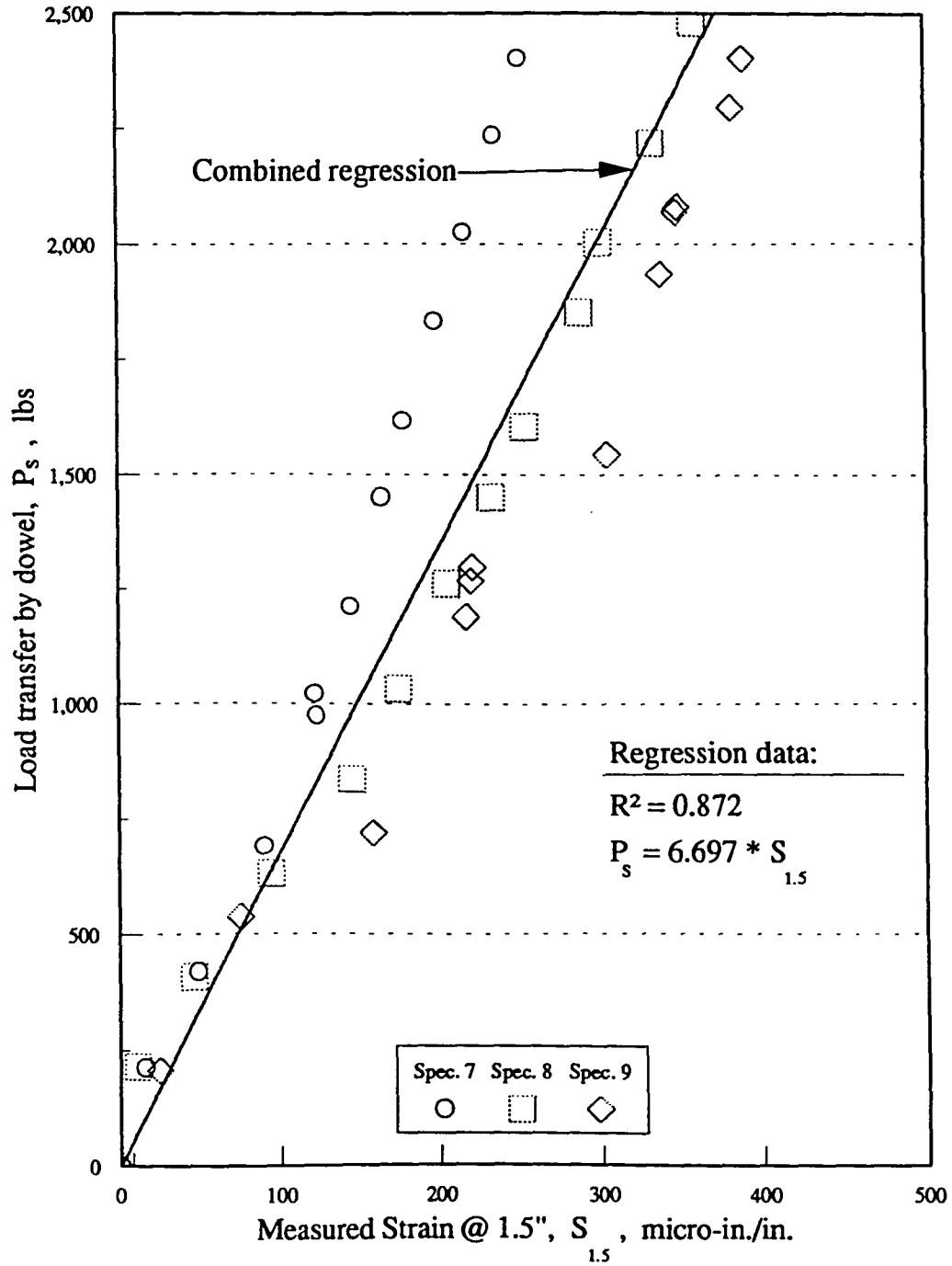


Figure 4.5: Load versus strain relationship for 1.75-inch diameter FC dowels

4.3 Full-Scale Fatigue Slab Testing

4.3.1 Introduction

Efficiency of a highway pavement joint is determined by monitoring two parameters: relative displacement between the two sides of a joint and load transfer across the joint. To compare the performance of steel and FC dowels as load transfer mechanisms in pavement joints, these two parameters must be measured when a joint is loaded. Because an actual pavement joint is repeatedly loaded and unloaded while in service, the fatigue due to cyclic loading must be considered when evaluating the relative displacement and load transfer performance of a joint. The number of repeated load applications may be from 10 to 100 million during a design period of 20 to 40 years for a high volume roadway (Heinrichs 1989). In this research, a method of laboratory testing that monitors the performance of doweled pavement joints while undergoing cyclic loading was developed.

When a doweled pavement joint is in service, the fatigue caused by cyclic loading applied by vehicle traffic is expected to affect the performance of the joint. Fatigue of the joint and dowels will then reduce their efficiency in transferring load (Teller 1958). An indication of reduced efficiency is, first, an increase in the relative displacement of the two sides of the joint, and, second, a decrease in the fraction of load that is transferred across the joint, as the number of load cycles increases. Therefore, testing in this research included monitoring those parameters for a doweled pavement joint under cyclic loading which was modeled by a laboratory setup. Often, when performing a fatigue study, a stress versus cycles, or S-N curve is developed. Such a relationship is determined by testing many specimens to failure at differing stress

levels. Each failed specimen, then, creates a point on the S-N curve. Such a method of study was not followed for the laboratory fatigue testing of full-scale pavement slabs in this research. The purpose of the fatigue portion of this research was to compare the performance of FC and steel dowels under conditions which simulated those of an actual highway pavement joint. As a results of testing the dowels, the feasibility of using FC dowels as load transfer devices was studied. Because failure of an actual dowel/concrete system is difficult to define and rarely occurs, the S-N curve approach was not applied to this study. In addition, the time and cost of such a program for the full-scale study would be quite extreme.

4.3.2 Materials and specimens

Test specimens used in the fatigue testing of pavement dowels were full-scale concrete slabs with dowels placed in the slabs at a joint formed in the specimens. Each slab was cast-in-place in the laboratory on top of steel supporting beams, with a thickness of 12 inches, a width of 6 feet, and a length of 12 feet. Between the steel beams and the slab were 0.25-inch thick neoprene rubber pads which acted to distribute the loading evenly as well as to separate the slab from the beams. Steel forms were used to form the outside of the slab, while wood falsework was used to support the concrete between the beams. Each dowel was placed in the slab at the middle of the thickness with one-half of its length on each side of a formed joint.

Because the laboratory testing was meant to simulate an actual pavement slab, the concrete used was a C-4 mix, which is a mix design commonly used by the Iowa DOT in the construction of new interstate highway pavements (McWaters 1992). Two local concrete companies supplied the concrete, with the same mix requested from

Table 4.2: Compressive strength and modulus of rupture values of concrete corresponding to full-scale slab specimens

Slab #	Compressive Strength f'_c , (psi)		Modulus of rupture f_r , (psi)	
	North	South	North	South
1	5370	5370	—	—
2	6819	7051	553	585
3	5476	5517	485	462
4	7031	6373	647	518

each. A minimum of 21 days of curing was allowed before beginning cyclic loading of the slab specimens. The reason for this length of time was that the concrete strength needed to have stabilized before beginning the load cycling. The cyclic loading was applied over a period of up to four weeks, and, if the strength was not stabilized before beginning, the concrete strength would be changing during the cycling, which would influence the results.

Concrete strength was determined using the standard 6- by 12-inch test cylinders for compressive strength, f'_c , and standard 6- by 6-inch beams for modulus of rupture, f_r . Compressive strength testing was performed at 7, 14, 21, and 28 days in order to determine when the concrete strength had stabilized. Beam testing to determine the modulus of rupture was performed only at 28 days of curing. The strengths determined at 28 days curing for the test specimens are shown in Table 4.2.

In Table 4.2, notation is used to differentiate between the two halves of the slabs (North and South sides), and this notation will be used when necessary throughout the discussion of results of the full-scale testing. Labeling the two sides was necessary in order to maintain consistency when referencing the performance of the test slabs. Further discussion of the labeling of the two sides will be included in later sections.

4.3.3 Test setup

4.3.3.1 Test slabs The first slab specimen was cast using 1.5-inch diameter steel dowels spaced at 12 inches center-to-center along the joint. In order to create the equivalent of a crack at the location of the joint, a piece of heavy plastic sheeting was placed vertically at the location of the joint. The dowels passed through the sheeting, and directly above the center of the dowels, a 0.375-inch wide joint was formed into the slab. The joint was formed to a depth of one-third of the thickness of the slab, which is the joint size in current practice for such pavements (McWaters 1992). A formed joint was used in place of the sawed joint that would be found in an actual pavement and was chosen because of the difficulty in sawing such a joint in the laboratory.

Because of problems resulting from the method of forming the crack used in the first specimen, a different method was applied in subsequent specimens. During the casting of the first slab the plastic sheeting placed at the joint did not remain vertical as the concrete was placed against it. As unequal amounts of concrete were placed on each side, the plastic was pushed slightly to one side. The result was a curved “crack”, with approximately one-half-inch of deviation from a vertical plane. Since the interest during the testing was to isolate the dowels for transfer of the load across the joint, a crack located at the joint that was not vertical was not desirable. In effect, the curvature created a mechanical method of load transfer by the concrete.

A second slab specimen was again formed and cast-in-place in the laboratory, but using 1.75-inch diameter fiber-composite dowels in place of steel dowels. A dowel spacing of eight inches center-to-center along the joint was used, which was determined by the computer model to be equivalent to using 1.5-inch diameter steel dowels

at 12 inches. A 12-inch spacing was also used in the field placement of FC dowels, as discussed in Section 2.2. Because of the problems experienced with creating the crack in the first specimen, a different method of forming the crack was developed. The solution was to cast the slab in two halves on consecutive days. One half of the length of each dowel was embedded in the first pouring, with a cold joint created at the location of the desired crack. The cold joint takes the place of the crack that is assumed to be created at the location of the dowels and the sawcut in an actual pavement. At the cold joint very little interlock between the two halves was desired, but a formed gap was also not desirable. Therefore, the face of the joint was greased when the formwork (with a formed saw cut) was removed from the first half, and when the second half was poured against the face, there was no bonding of the concrete at the joint.

The third slab was formed in the same manner as the first two, using 1.5-inch diameter steel dowels with 12-inch spacing. For Slab 3, the method of forming the crack at the joint that was developed for the second slab was applied. The fourth slab specimen was prepared exactly like the third slab, but using 1.75-inch diameter FC dowels.

Concrete strengths for the specimens after the first slab were determined at 7, 14, 21, and 28 days from the time that the second half of the slab was cast. Because the two halves were poured only one day apart, final strengths of the two halves differed by very little as seen in Table 4.2.

4.3.3.2 Simulated subgrade In the design of the testing setup, several options were considered for the type of subgrade to use in the laboratory testing. The

options included using an actual soil subgrade or using a simulated subgrade with steel supporting beams. A simulated subgrade was chosen because of advantages in the ease of construction and the reduced laboratory space that was required. A test method including a simulated subgrade was previously applied in testing by Teller and Cashell (Teller 1958) on pavement dowels in a concrete pavement.

The discussion of the computer modeling of the laboratory test setup in Section 3.4.3 covers the procedure used to determine the loads for designing the supporting beams. As mentioned earlier in Section 3.4.3.4, the reactions in the springs from the computer analysis were used as applied loads in the design of the beams. Several configurations for the beams were considered with the length of the span between simple supports and the number of beams varied. The criteria used for the beam designs were the displacements at the center of the span and at three feet on either side of center, which would be the locations of the edges of the slab. Displacements at these locations were to be as close as possible to those determined from the computer modeling of a full-size highway pavement. Other considerations in the selection of the beams were the depth of the steel beam sections and their weight. Also, the span length of the beams was to be selected to fit into limited lab space while minimizing the beam curvature when loaded. The final beam design resulted in a span of 12 feet with standard steel sections selected to be W14x38, W21x44, and W14x68. The layout of each of the beam sizes and the names by which the beams will be referred can be seen in Figure 4.6.

By using steel beams to simulate a soil subgrade, several differences between the two were considered. The simulated subgrade was a non-uniform and non-continuous support system, unlike a soil subgrade, which is normally considered to be uniform

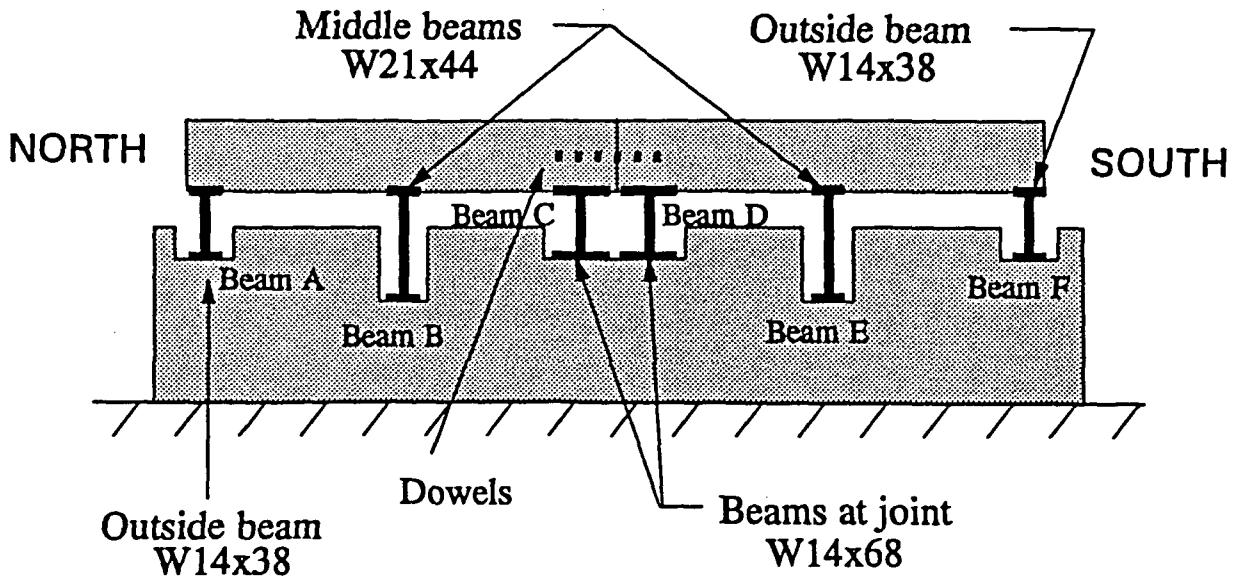


Figure 4.6: Supporting beams for full-scale pavement slab testing

and continuous. Another difference mentioned earlier is that the simulated subgrade was constant over time, despite being subjected to cyclic loading during the testing. Properties of an actual subgrade change over time due to climatic conditions, settling and compaction. For example, a subgrade may fail in a small region under the pavement, which greatly influences the performance of the pavement as well as the stresses exerted on the pavement dowels.

4.3.3.3 Loading system This research consisted of observing the behavior of dowel bars in a full-scale pavement slab as they were loaded repeatedly to a very large number of cycles. Though the simulation of the repetitive loading experienced

by a highway pavement is important, the laboratory specimen must be subjected to these cycles in a reasonable amount of time. To limit the time required, a loading system that can provide the desired loads at a reasonable frequency of 3 to 5 hertz in a laboratory setting was needed.

In the ISU Structural Engineering Laboratory, a MTS Service Corporation servo-controlled dynamic loading system was used. The system used two hydraulic actuators and a dynamic controlling system which was capable of loading as described above. Several load diagram shapes were available through the system, including: sinusoidal, square, and linear. For this research, the sinusoidal load diagram was selected because of the assumption that the sinusoidal shape most closely simulated the loading of a truck tire upon a joint. The actuators may be controlled by several variables, including stroke or load control. Since this research called for a maximum load of 9,000 pounds to be applied to the specimen throughout the test, load control was selected.

Load cells were integral with the actuators, located between the piston and the base. The load cells were constantly monitored by the controlling system in order to provide the same desired load with each stroke. The load magnitude as well as the frequency of the loading was set at the controller. Between the actuators and the test specimen were placed three-inch thick neoprene pads, which are shown in Figure 4.7. The pads served to "soften" the load applied to the slab, much like the suspension of a truck.

The actuators were mounted to a large steel load frame which was tied down to the floor of the laboratory. A mobile member transferred the load from the actuators to the structural frame and could be moved on wheels resting on the flanges of the

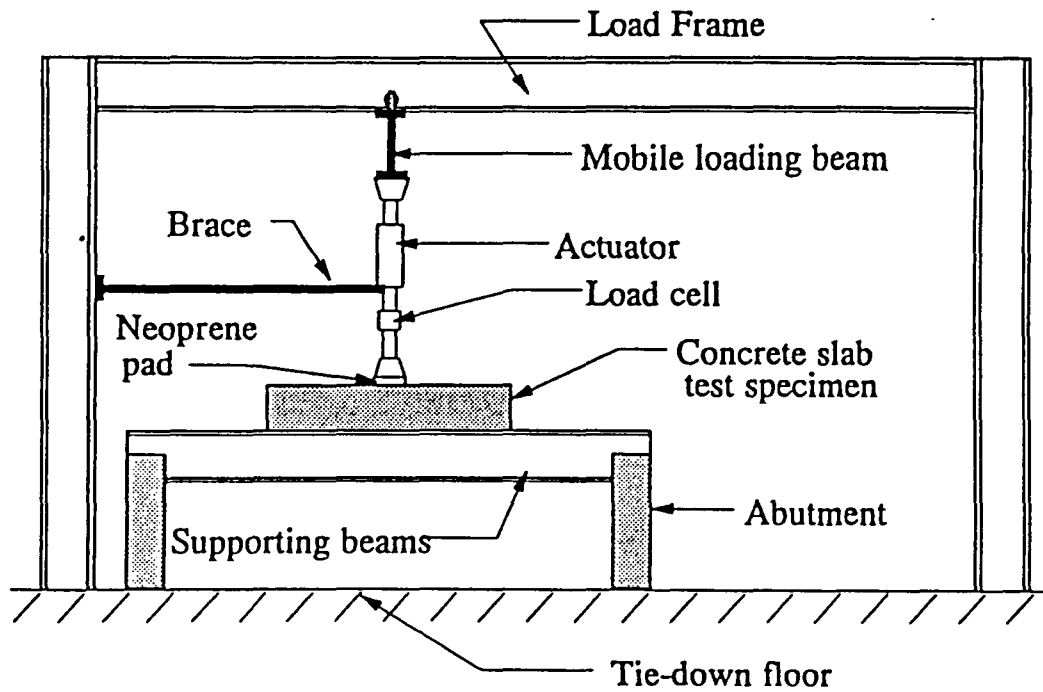
frame. The actuators could be moved from their location while testing the slabs to a location to the side while the slabs were being constructed. Because of the vibration of the actuators while cycling, a bracing frame was constructed to brace the actuators horizontally to the frame as shown in Figure 4.7.

4.3.4 Instrumentation

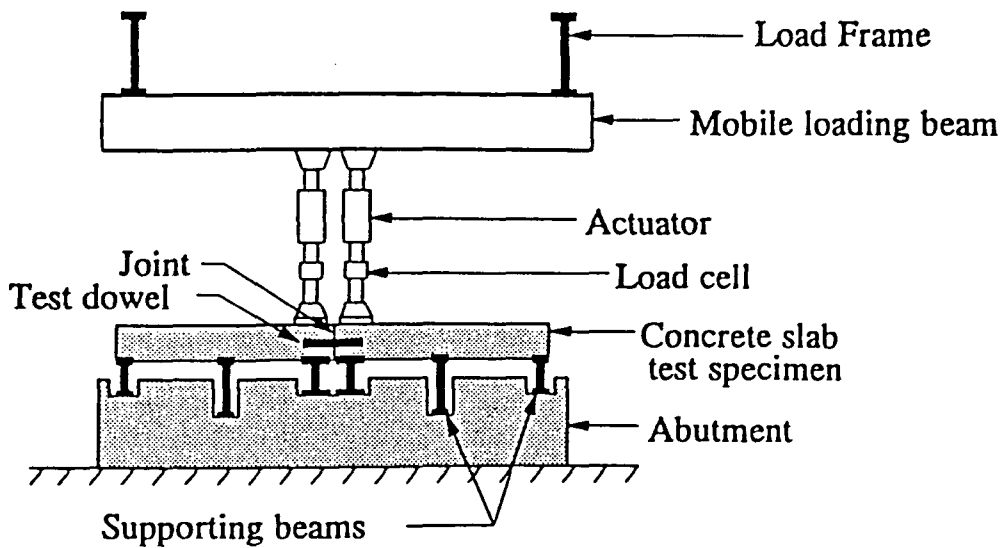
4.3.4.1 Displacement measurement Relative displacements at the joint could be determined by two methods. One method included using a single DC DT at the location of displacement desired with the instrument fixed to one side of the joint and the measuring stem resting on the other side. With a single instrument, only relative displacements could be measured. A second method would require displacements to be measured on both sides of the joint with respect to a datum outside of the slab. Then, the relative displacements at a particular point would be the difference between the two measured values.

In this research, the latter alternative was chosen because of the need to verify that the actual displacements during the testing were comparable to the values that were used in the design of the test setup. To measure displacements relative to an external datum, a reference frame was built to which all of the displacement instrumentation on top of the slab could be attached during the test.

Because of differences in the spacing used for FC and steel dowel bars, the displacement instrumentation locations were different for each slab. For each of the slabs, DC DT's placed at the joint for monitoring the relative displacements were located on top of the test slabs, directly above each dowel bar location. The instruments were placed as close to the joint as possible, with the DC DT stem resting



End elevation view



Side elevation view

Figure 4.7: Laboratory setup for full-scale pavement slab fatigue testing

on small plastic or glass plates glued to the concrete to guarantee a flat surface. In addition to the instruments on either side of the joint, DCDT's were placed above the locations of the middle beams on both sides of the joint.

For the first full-scale test specimen, a total of 22 DCDTs were in place on top of the slab, with 20 measuring vertical displacements and two placed horizontally to measure the change in joint opening. A diagram showing the DCDT layout is given in Figure 4.8. With six dowels placed at the joint in this specimen, a total of 12 DCDTs were placed to determine absolute and relative displacements at the joint. At each of the middle supporting beam locations, three DCDTs were placed in a line corresponding with the centerline of the beam. The final two instruments on top of the slab were located directly above the centerline of the outside supporting beams at midspan. In addition to those on top of the slab, two DCDTs were placed at midspan and underneath the two supporting beams at the joint. These were meant to determine whether the thin neoprene placed between the slab and the beams had an influence on the displacements.

Because the FC dowels used in the second slab were placed at a spacing of eight inches, a total of nine dowels were placed at the joint. Therefore, the placement of displacement instrumentation differed from the first slab. Also, because of a limited amount of instruments available, measurements from the first test slab that proved to be insignificant were eliminated. Measurements taken at the outside supporting beams were found to be small enough to be considered insignificant. Monitoring of the horizontal displacement at the joint was also found to be unimportant because of the small movements and little importance to analysis. These changes then allowed for DCDTs to be placed at all dowel locations as well as over the middle beams on

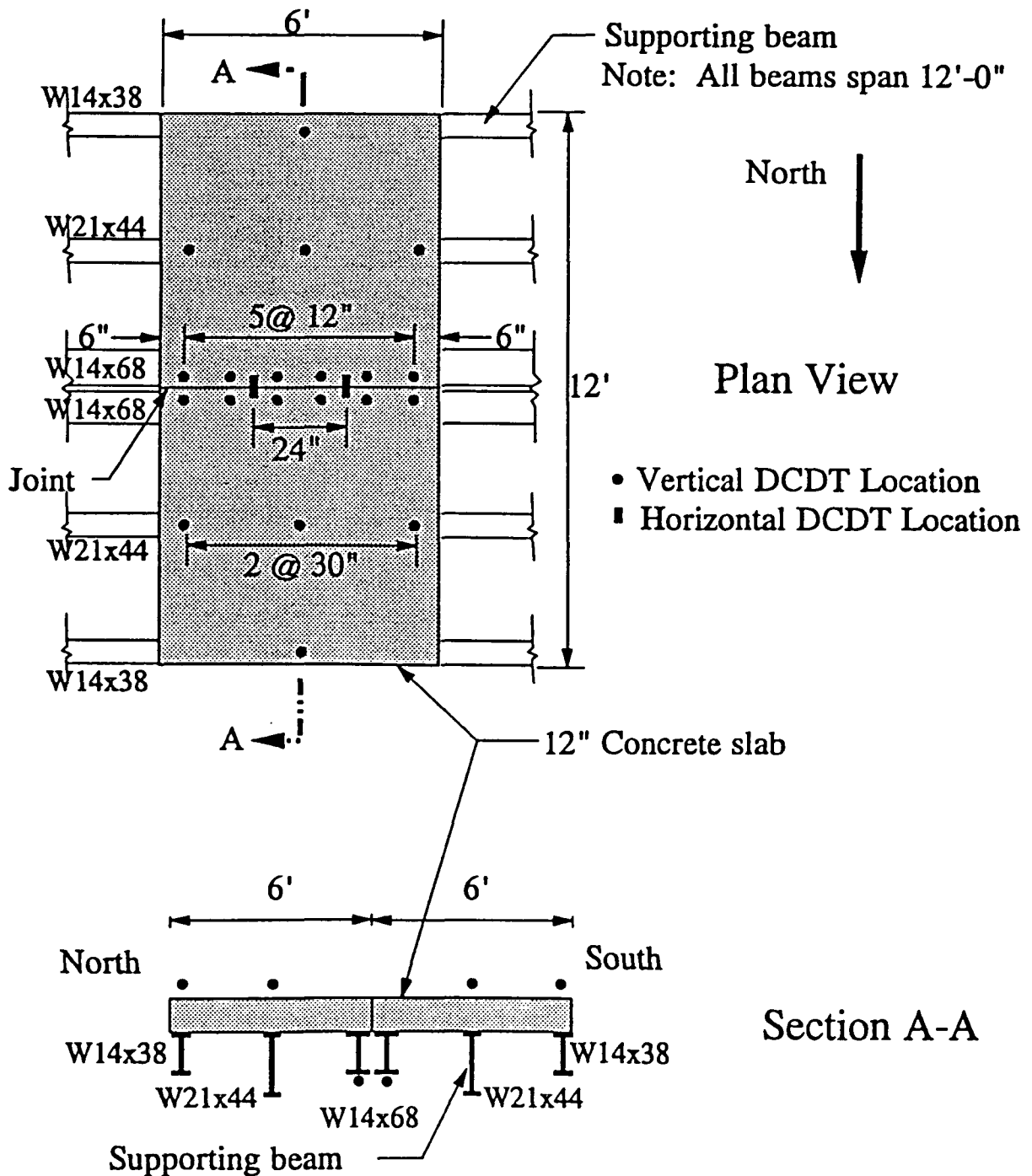


Figure 4.8: Displacement instrumentation for first full-scale fatigue test slab (with 1.5-inch diameter steel dowels at 12-inch spacing)

both sides. The layout of the instruments for the second slab is shown in Figure 4.9. Because one dowel was located directly below the point of load application, DCDTs were again placed underneath and at midspan of the beams at the joint. Since the third and fourth slab specimens again used a dowel spacing of 12 inches along the joint, the displacement instrumentation used in these slabs was very similar to that used in the first slab. The only difference being that DCDTs were not placed above the locations of the outside supporting beams and were not placed to measure horizontal displacements at the joint. A diagram of the DCDT locations for the third and fourth slabs is shown in Figure 4.10.

4.3.4.2 Load transfer The second variable requiring monitoring and measurement during the static load testing was the load transferred across the joint by the dowels. Determination of the load transfer had to be accomplished in a less direct manner than for displacements. Strain gages were mounted on the steel supporting beams underneath the test specimens, from which the strains were measured and the moment and the load applied to each of the beams could be calculated.

Loads were applied to the supporting beams through the concrete slab which was six feet wide and rested in the middle of the 12-foot span of the supporting beams. Strain gages were placed at three locations along the span, which are shown in Figure 4.11. One location was at the middle of the span, and the other two were below both edges of the slab, three feet on either sides of the midspan. At each location, four strain gages were placed on the beam, as is shown in Figure 4.11 for each of the three beam sections used. The method used to determine the load transferred to each beam involved the development of calibrations between a known applied load

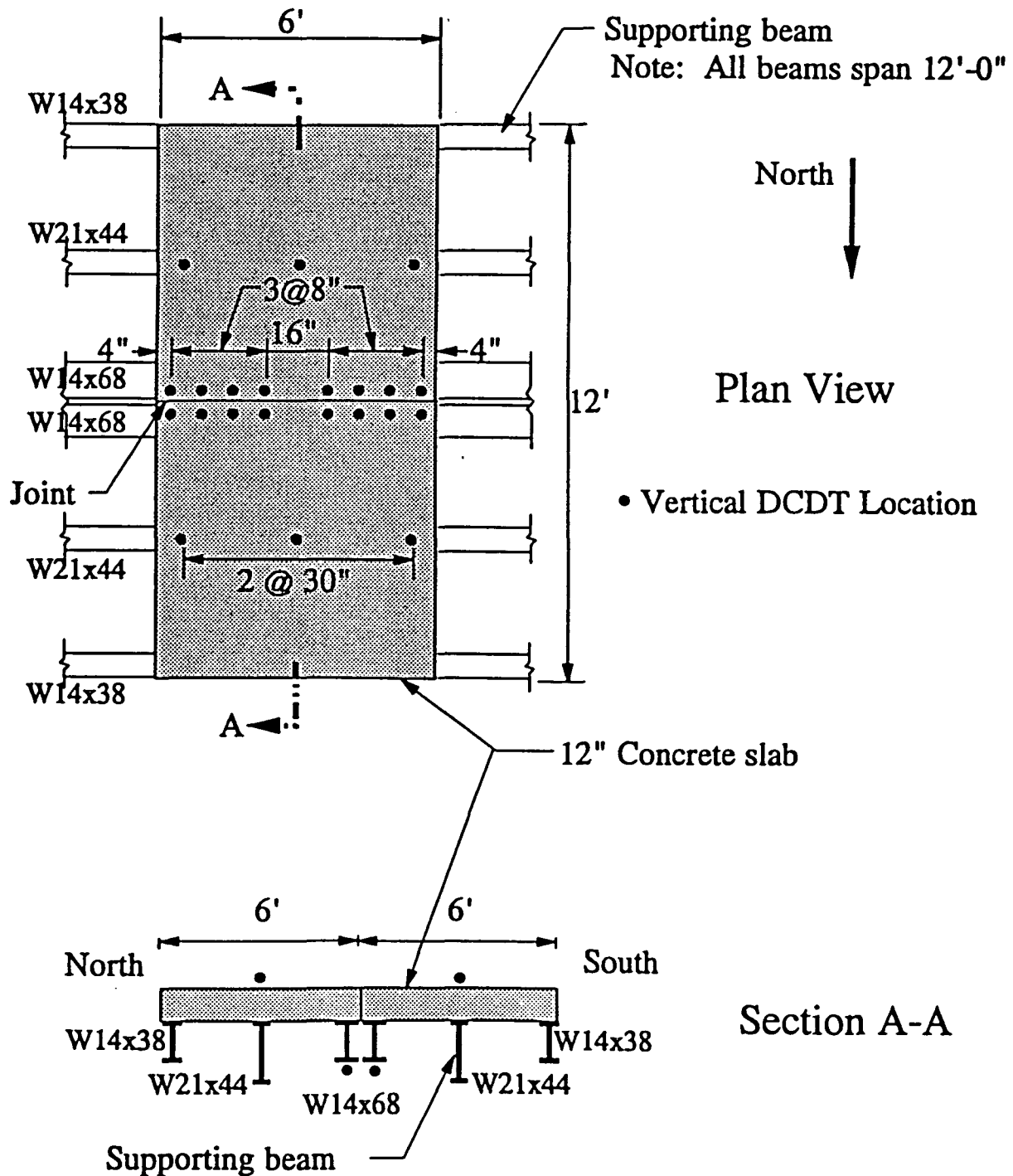


Figure 4.9: Displacement instrumentation for second full-scale fatigue test slab (with 1.75-inch diameter FC dowels at 8-inch spacing)

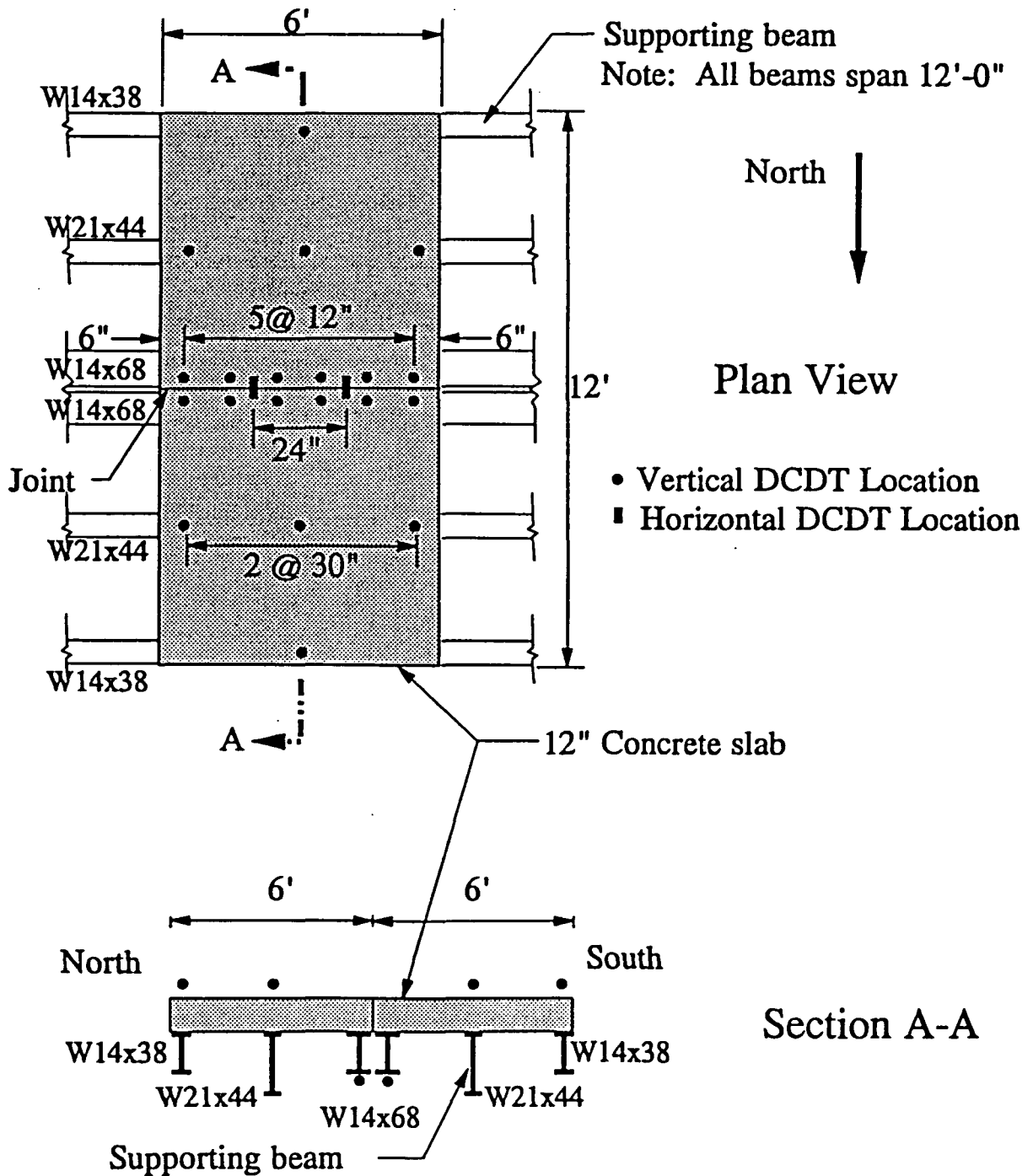
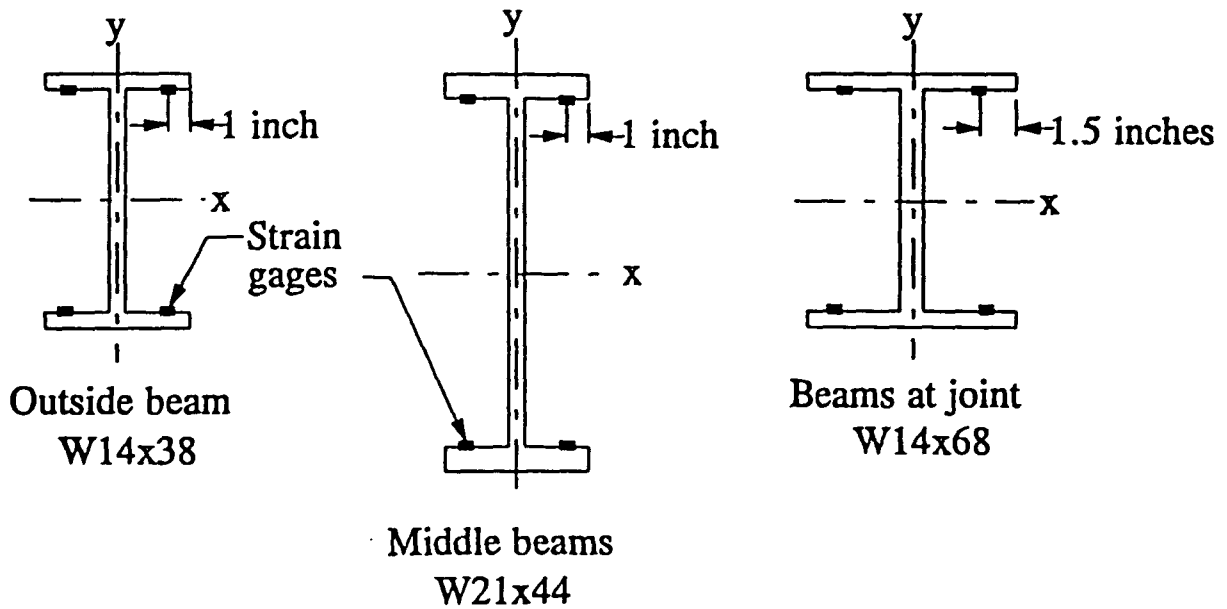
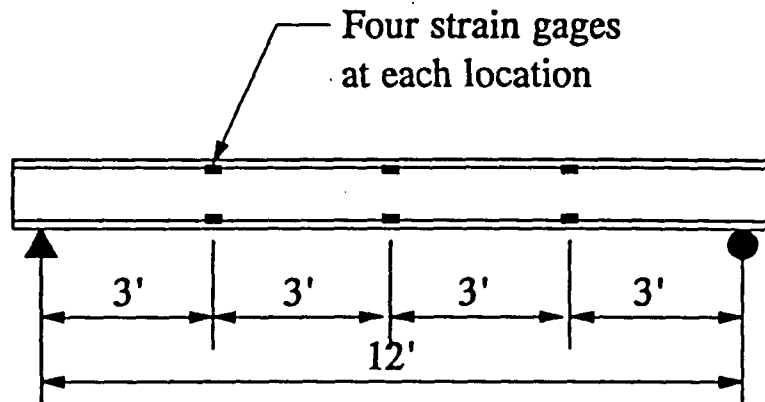


Figure 4.10: Displacement instrumentation for third and fourth full-scale fatigue test slab (with 1.5-inch diameter steel dowels at 12-inch spacing)



Note: All strain gages are placed symmetrically about the x- and y-axes

Figure 4.11: Locations of strain gages placed on supporting beams

and the resulting measured strains in the beams. After conducting load tests of each beam individually, linear relationships were developed from the data. Then, during static load testing of the slabs, the load applied to each beam was determined by applying the calibration to the strains measured in the beams. Load testing of the supporting beams is discussed further in Sections 4.3.5.2 and 4.3.6.1.

As an additional means of monitoring the load transfer through the dowels, strain gages were mounted directly on the dowels. In the second slab, strain gages were mounted on the three center dowels, which were 1.75-inch diameter FC rods placed at an 8-inch spacing. These three dowels were selected because the majority of the load was transferred through the dowels which were located near the point of load application (Heinrichs 1989). On each half of each dowel, the gages were placed at two locations, the first at 1.5 inches, and the second at 5.5 inches from the center of the dowel. The strain gage locations on the dowels were essentially the same as those used in the elemental dowel specimens as shown in Figure 4.4. At each of the locations, two gages were mounted, each diametrically opposite the other. The bending of the dowel was determined by averaging the two values of strain. When placed in the slab, care was taken to guarantee that the dowels were oriented so that all of the gages were positioned in a vertical plane.

Again, for the third slab, strain gages were placed on the dowels closest to the load application, which included the middle two 1.5-inch diameter steel dowels. The gages were placed at the same locations along the length of the dowels as were used in the elemental dowel specimens (1.5 and 5.5 inches from center), and therefore Figure 4.4 can be referred for the locations of the dowel strain gages used in the third slab specimen. Strain gages were also placed on the 1.75-inch diameter FC dowels of the

fourth slab. As with the third slab, the middle two dowels closest to the application of load were selected for mounting the strain gages. These dowels were placed on either side of the center line of the test slab at a distance of 6 inches from the center line. Accordingly the locations of the instrumented dowels will be referred in this report as 6 inches east or 6 inches west of the center line.

The number of strain gages on the dowels of the fourth slab was increased in order to get three data points on each side of the dowel for observing the distribution of moment along the length of the dowel. Strain gages were placed at three locations (1.5, 4.0, and 6.0 inches) on the dowels of the fourth slab. Figure 4.12 shows the details of the instrumentation on the dowels of the fourth slab specimen.

4.3.5 Test procedure

4.3.5.1 Introduction The initial step in the test procedure was to perform load tests of the supporting beams, which was then followed by testing of the full-scale slab specimens under static and cyclic loading. In general, the full-scale slab testing procedure involved subjecting the specimen to cyclic loading, and, at times during the cycling, stopping to test the slab under static loads equivalent to those during cycling. Data was collected only during the static load tests performed on the slabs. For example, during the testing of the first specimen, which used 1.5-inch diameter steel dowels, static tests were performed at the completion of the following numbers of load cycles, in thousands: 0; 50; 100; 200; 300; 400; 500; 750; 1,000; 1,500; and 2,000.

Before the full-scale concrete slabs were cast, the supporting beams were tested with strain gages in place. Using beam test results, calibrations were determined

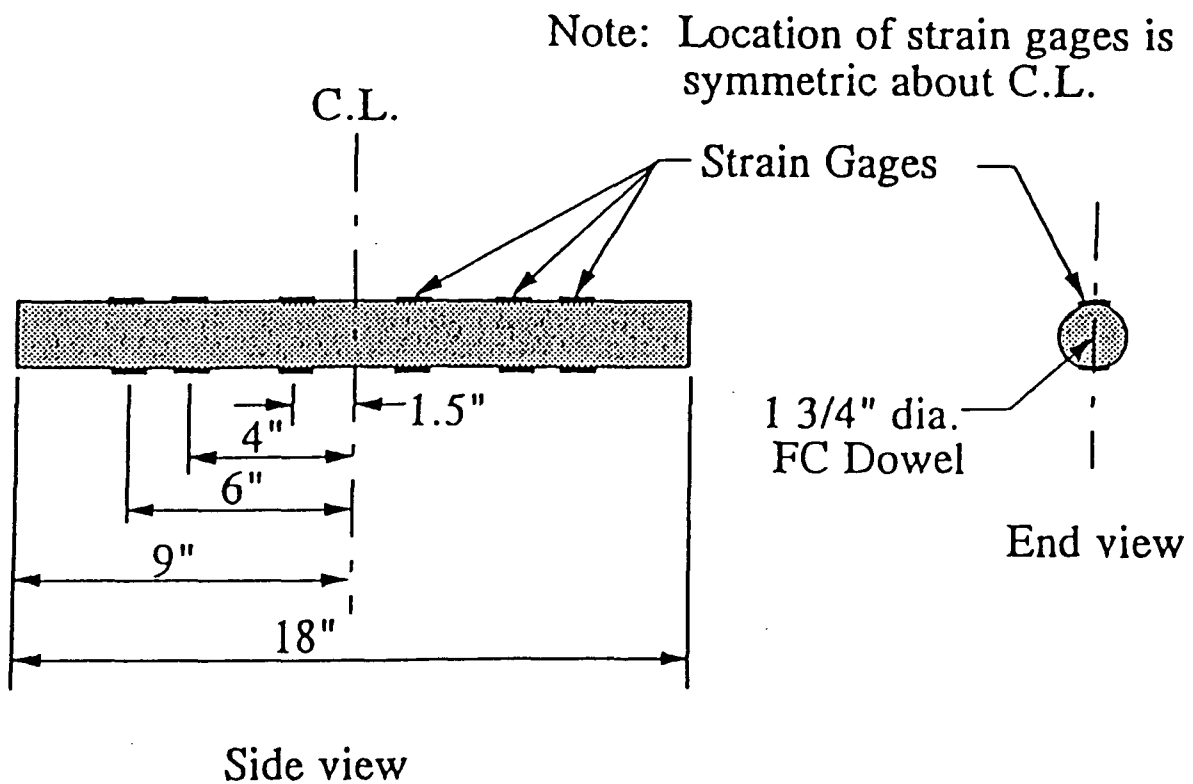


Figure 4.12: FC dowel strain gage locations as placed in fourth full-scale pavement test slabs

between the applied load and the measured strains in the beams. The calibrations were used in the analysis of the load transfer across the joint, and will be discussed in more detail in Section 5.2.

4.3.5.2 Supporting beam load tests As discussed in Section 4.3.4.2, strain gages were placed on the supporting beams in order to monitor load transfer across the joint as load was applied to the slabs during static load tests. Using the strains measured as load was applied during a static test, the magnitude of the load distributed to each supporting beam could be determined by applying the section properties of the beams. The beam properties, though, were assumed to not match exactly those specified for the particular section designation, such as W14x38. Therefore, load tests were conducted on each of the supporting beams with the strain gages in place in order to determine calibrations between load and strain values.

The procedure for the tests involved applying a load at the middle of the span while the beams were simply supported in the same manner as when in place under the slab. Then, as load was applied at intervals, the measured strains were collected using the same data acquisition system used during the static load testing.

4.3.5.3 Cyclic loading During the cyclic loading of the specimens, load was applied to both sides of the joint in order to simulate truck traffic passing over the joint. The two electronically controlled hydraulic actuators, which were discussed in Section 4.3.3.3, applied the loads. The load was applied by each actuator in a sinusoidal-shaped function, with the two functions 180 degrees out of phase. Therefore, when one of the actuators was at the maximum load on one side of the joint, the second was at the minimum load on the other side. For each actuator, a maximum of

9,000 pounds, and a minimum of 200 pounds were applied during the cyclic loading. Load diagrams for the two actuators are shown in Figure 4.13. The minimum load was required only during the cyclic loading so that the actuators stayed in contact with the slab at all times. Therefore, summing the load applied by both actuators, the specimen was loaded with a net load of approximately 9,200 pounds at all times during the load cycling.

While the joint was never unloaded during the cycling, the action that the dowel underwent was of the most interest. The dowel experienced a full range of load transfer reversal during the repeated loading. Relative displacement across the joint cycled between the maximum when one side was loaded, to the same maximum when the other side was loaded. Movement such as this subjected the dowel/concrete system to the most extreme fatigue loading conditions that an actual system would be subjected to with the same magnitude of load. In fact, the relative movement of the two sides of the slab while cycling was visually observed at the edges of the slab specimens.

The loading frequency used during the cycling was approximately five Hertz. Adjustments were made to the frequency at the beginning of the cyclic loading program of the first slab so that there was not excessive vibration of the loading frame. At the beginning of the cycling program for each of the following test specimens the frequency was set at five Hertz, and the system was examined for vibrations of the loading frame. If necessary, adjustments were made to the frequency, though, the frequency remained very near five Hertz for all tests.

A maximum of two million load cycles were applied to the first two slab specimens. The first using 1.5-inch diameter steel dowels at a 12-inch spacing and the

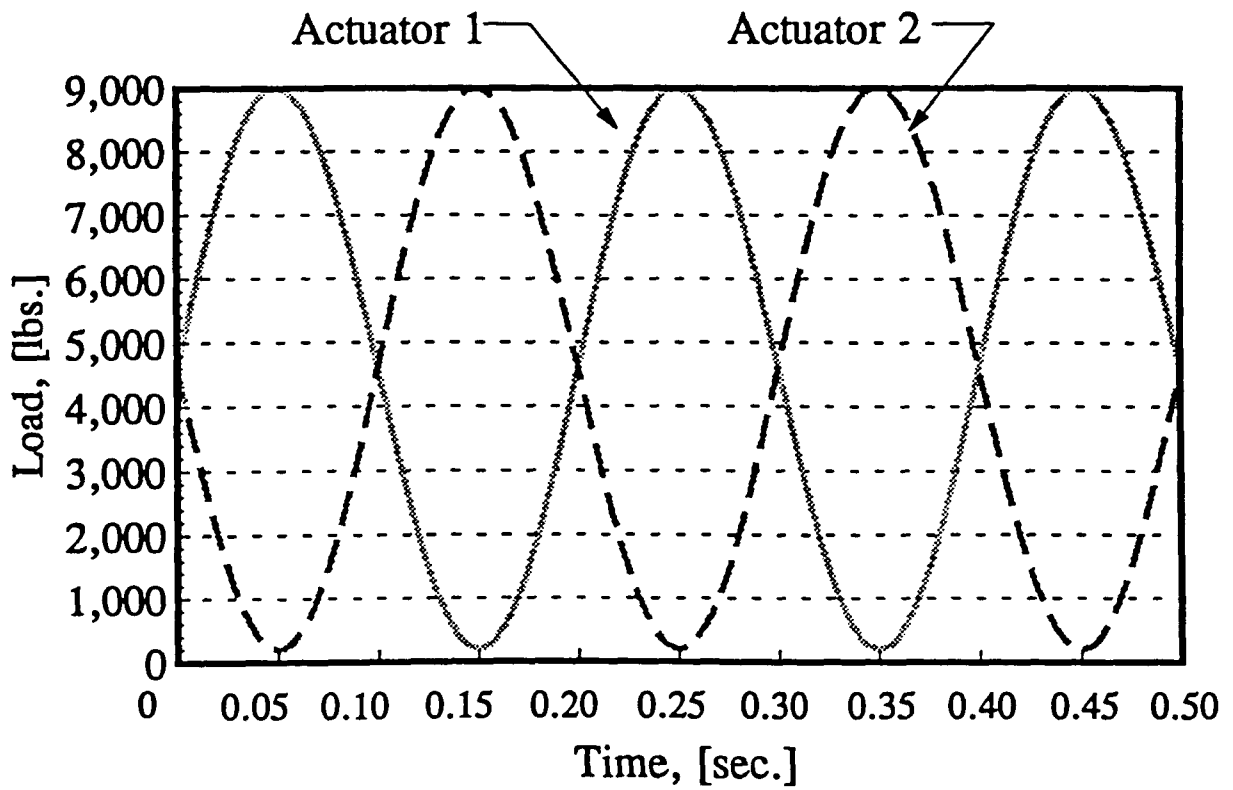


Figure 4.13: Typical load diagrams for two actuators during cyclic loading

second using 1.75-inch diameter FC dowels at an eight-inch spacing. Ten million cycles were applied to the third and fourth slabs having 1.5-inch diameter steel and 1.75-inch diameter FC dowels respectively, spaced at 12 inches.

4.3.5.4 Static load testing Static load tests were performed using the same hydraulic actuators as were used in the cyclic loading. During the static tests, though, the load was applied using the manual controls instead of the electronically controlled system. The static tests were performed so that instrumentation could be read while applying the loads that were applied during the fatigue or cyclic loading. At the beginning of each test, readings of the instrumentation were taken with no load applied, giving the baseline for readings to follow. Then, the static load was applied to one side of the joint at a time in many load step intervals. At each load step the instrumentation data was collected as the load was increased to a maximum of 9,000 pounds and decreased, again at intervals, until no load was applied. The same procedure was then followed as the other side of the joint was loaded.

During the tests conducted on the first specimen, a load interval of 500 pounds was followed while loading to the maximum load and while unloading. Reading the instrumentation at the 500-pound interval resulted in an excessive amount of load points, since the behavior of the specimen was quite constant over the range of load. Therefore, for the testing of the second slab, the number of load steps was reduced by adjusting the load intervals used. While loading the slab, an interval of 500 pounds was used up to 4,000 pounds. Then, from 4,000 to 9,000 pounds, a 1,000-pound interval was applied. When unloading, the load was decreased at steps of 1,000 pounds throughout. These changes reduced the amount of data collected for each

test, still providing 14 data points as the load increased. An additional change was made to the procedure between the testing of the first two specimens. From the first slab tests, the results indicated that a large part of the degradation of the dowels in the slab occurred during the first 200,000 load cycles. Therefore, collection of more data during that time was desired so any possible critical time during the degradation was not overlooked. A total of 14 static load tests were conducted, compared to 11 for the first test.

4.3.6 Results

As discussed in Section 3.4, load tests were conducted on the supporting beams in order to determine calibrations between the strain values measured on the beam flanges during static load testing of the slabs and the amount of load applied to each beam. The objective was to determine the load transfer across the test joint by measuring the amount of load applied to the supporting beams.

Tests were performed on the two middle supporting beams, referred to as Beams B and E, and the two beams at the joint, or Beams C and D (refer to Figure 4.6). No tests were performed on the two outside beams, referred to as Beams A and F because the measured strains in those beams during static load testing were considered to be too small for consistent results. Results of the beam tests are shown in Figure 4.14 for the four beams tested. The resulting regression equations relating strain and applied load are included in the figures. As expected, all of the relationships are quite linear, and were applied effectively to determine load transfer during the static load tests.

While the data collected from the testing of the initial full-scale slab specimen was not valuable in the analysis of the performance of the pavement dowels, several

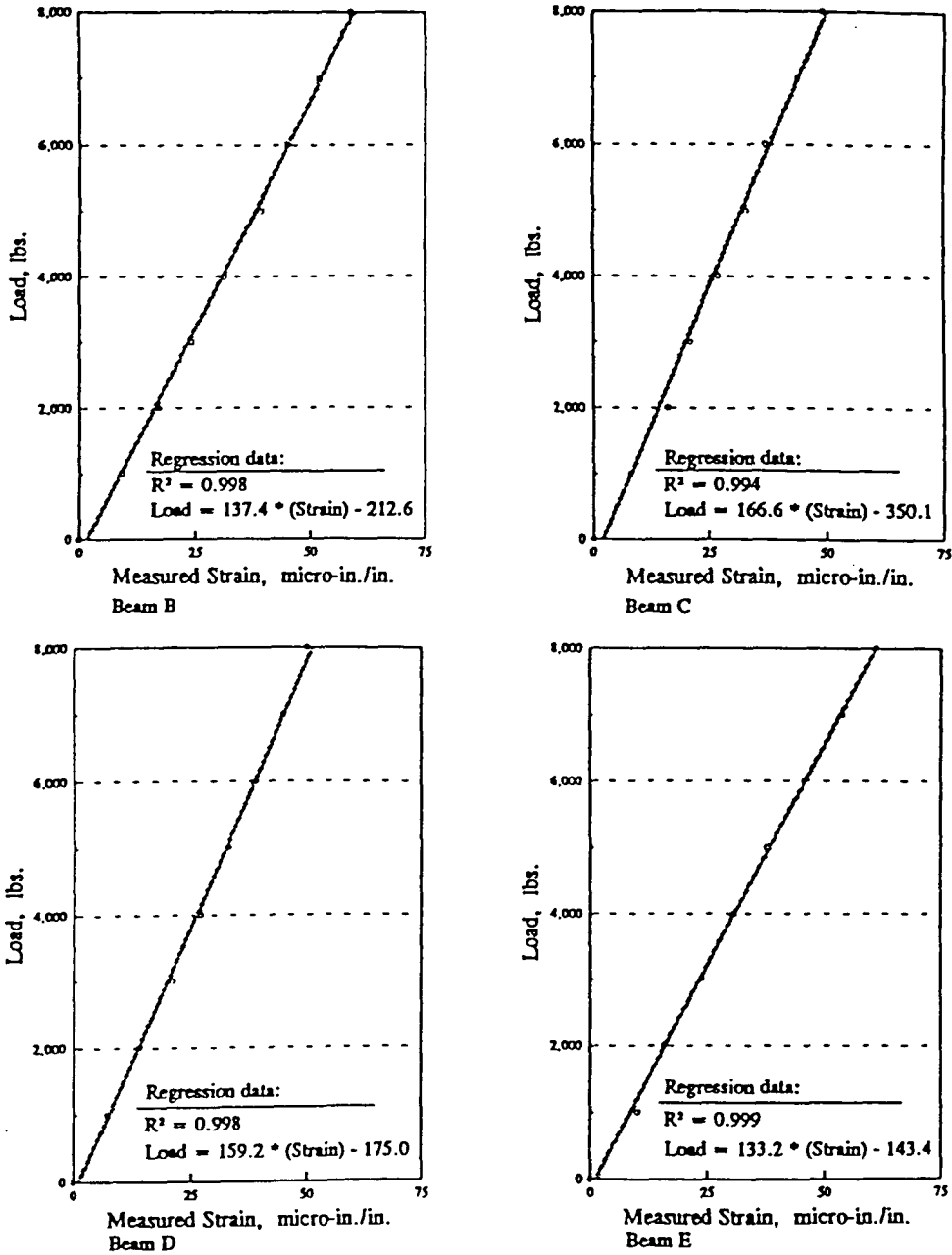


Figure 4.14: Load versus strain diagrams for quarter points of supporting beams

concepts were studied during the test. Because of the problems experienced with the formed joint, the results from the tests on Slab 1 were not considered in the analysis, but by performing the first complete test, the procedure for subsequent testing was fully developed. Also, the first test provided a check of the laboratory setup design, including the performance of the supporting beams as a means of providing a simulated subgrade. The finite element analysis performed for designing the test setup could be verified successfully by comparing of the experimental deflections with those obtained from the computer model analysis as presented in Figure 4.15.

The fatigue testing of the second slab was much the same as for the first slab, with some adjustments made to the static load testing procedure, as discussed in Section 4.3.5.4. Both the first and the second slabs were subjected to a maximum of two million cycles. The changes between the two slabs included decreasing the number of readings of the instrumentation during each static test, and, also, performing additional static load tests during the first 200,000 load cycles. As discussed in Section 4.3.3.1, the method of forming the pavement joint in the test specimens was changed after completing the original slab. Casting the specimen in two halves on consecutive days isolated the dowel for the transfer of load by eliminating aggregate interlock across the joint. The difference in concrete strengths between the two sides was found to be minimal when the fatigue testing was begun.

In general, the measured displacements of the slab were expected to be linear with respect to the applied load. The linearity was anticipated because the displacements were a function of the support provided by the supporting beams, which were simply supported members. Displacements are proportional to the applied load in such a case, and this was found to be the case for measured displacements.

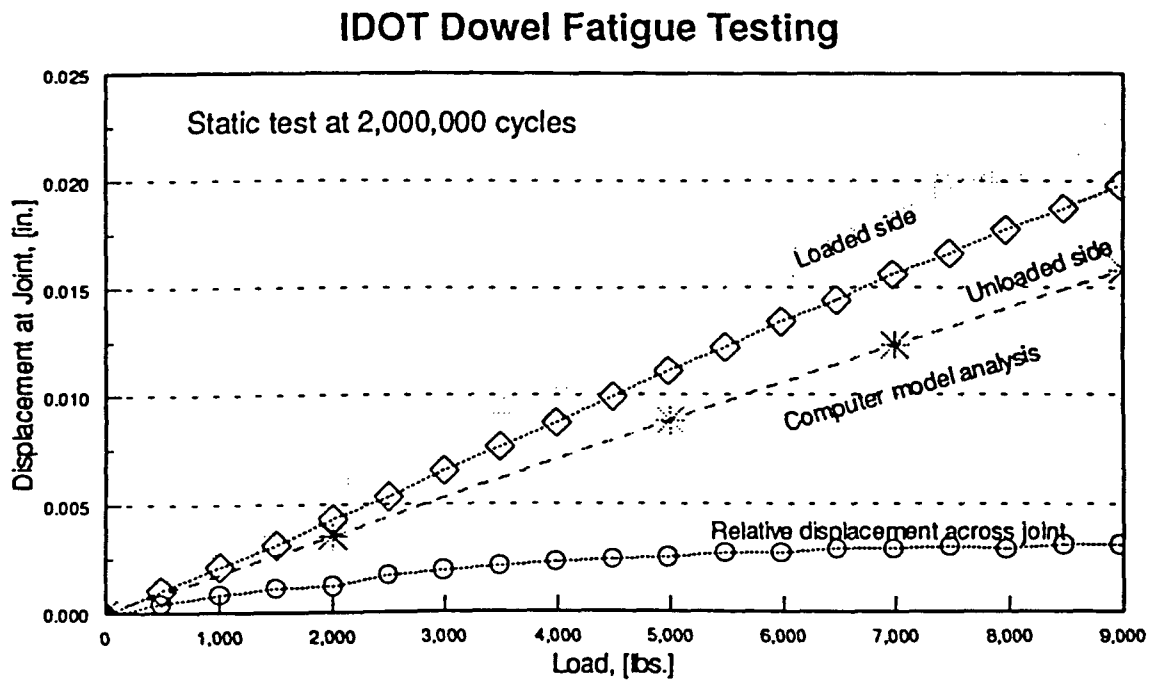


Figure 4.15: Experimental verification of finite element analysis

The influence of the load cycles on the relative displacements at the joint is observed by comparing plots of load versus relative displacements at the joint for individual static load tests. Results from testing of the three slabs showed that, as the number of applied cycles increased, the plots of load versus relative displacements changed. At the beginning of the test program for each slab, or zero fatigue cycles applied, the load versus relative displacement plot was rather linear at all displacement locations. As the number of load cycles increased toward two million, the shape of the load versus relative displacement plots changed, having increased curvature which indicate the fatigue degradation of the dowel performance. The changing load versus relative displacement relationship is shown in Figure 4.16 by the plots of data at four times during the cyclic loading program of the Slab 2. Similar plots for Slabs 3 and 4, which were subjected to ten million cycles, are displayed in Figures 4.17 and 4 .18, respectively.

The changes in the plots for Slab 3 were more significant than those for Slabs 2 and 4, which indicated a greater modification of the composite action of the steel dowel with concrete than for the FC dowel and concrete. An apparent increase in the slope of the data as the load increased indicated somewhat of a "seating" behavior of the specimen, meaning that any looseness of the dowel within the concrete was taken out as the load approached 9,000 pounds. From the results of the third slab, the seating behavior appeared to be more significant, which demonstrated greater looseness of the steel dowel compared to that of the FC dowel. An additional observation made from Figures 4.16 thru 4.18, was that of significant change in the load versus relative displacement curves from 0 to 200,000 cycles, and less significant change beyond 200,000 cycles.

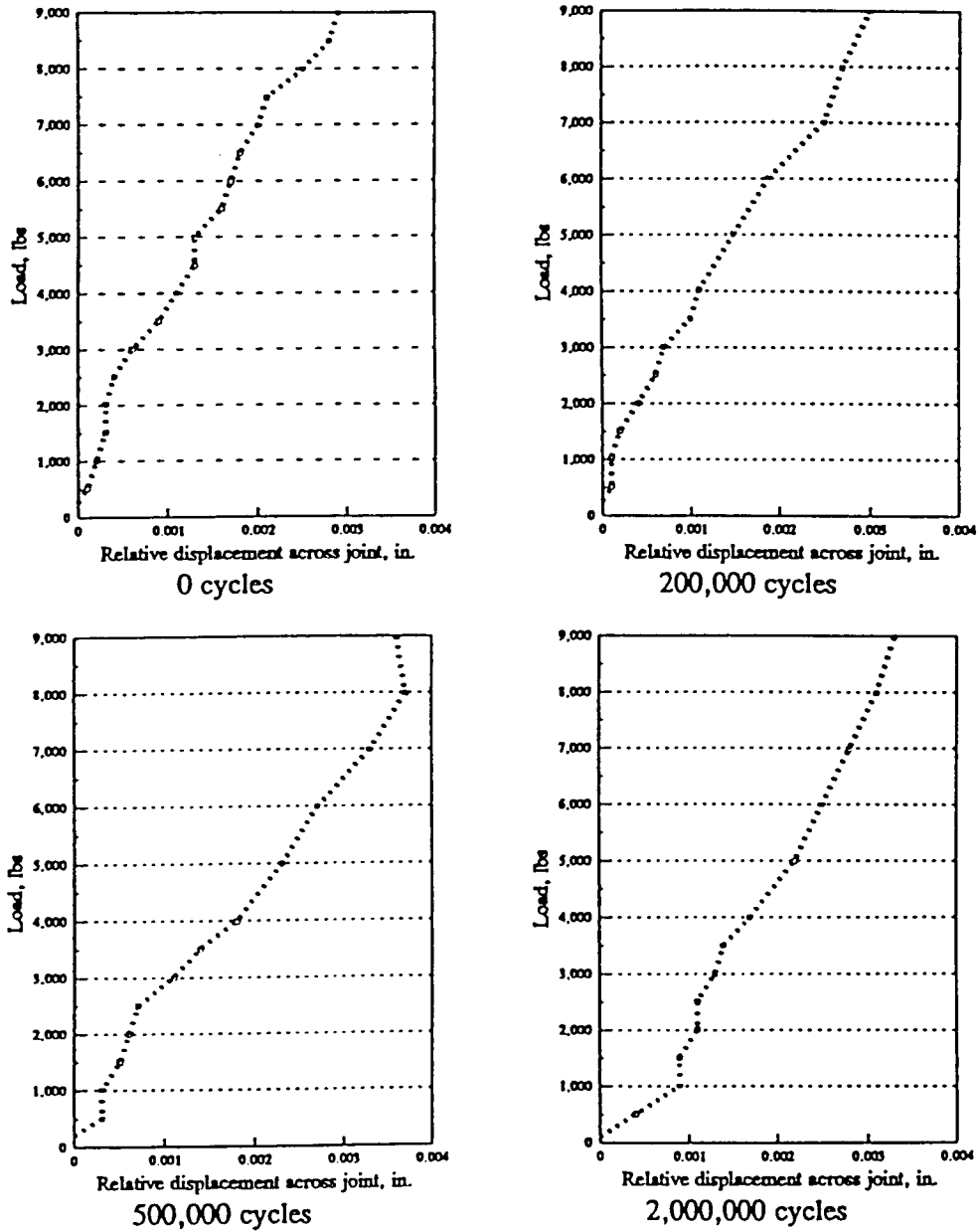


Figure 4.16: Load versus relative displacement diagrams at the joint of Slab 2

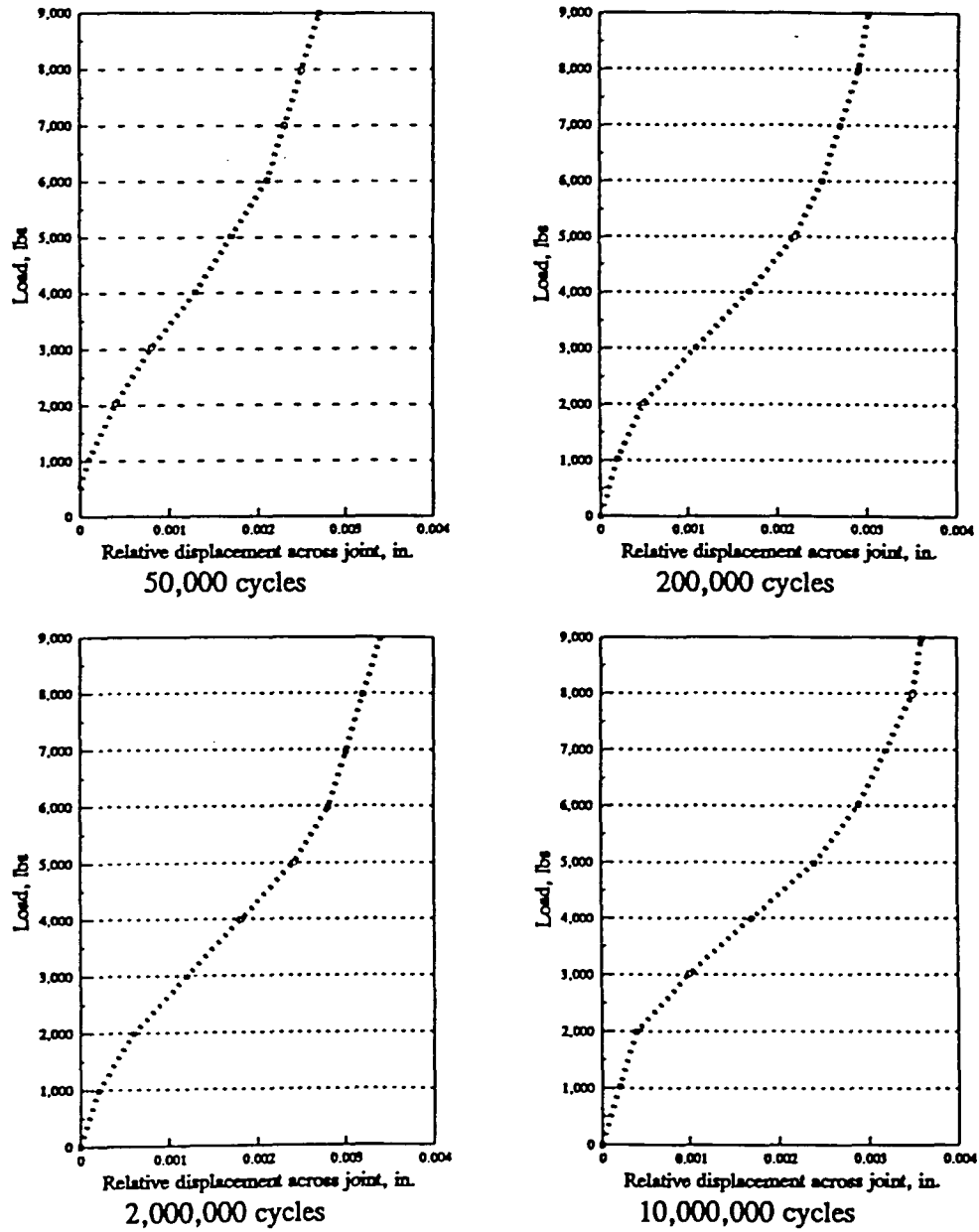


Figure 4.17: Load versus relative displacement diagrams at the joint of Slab 3

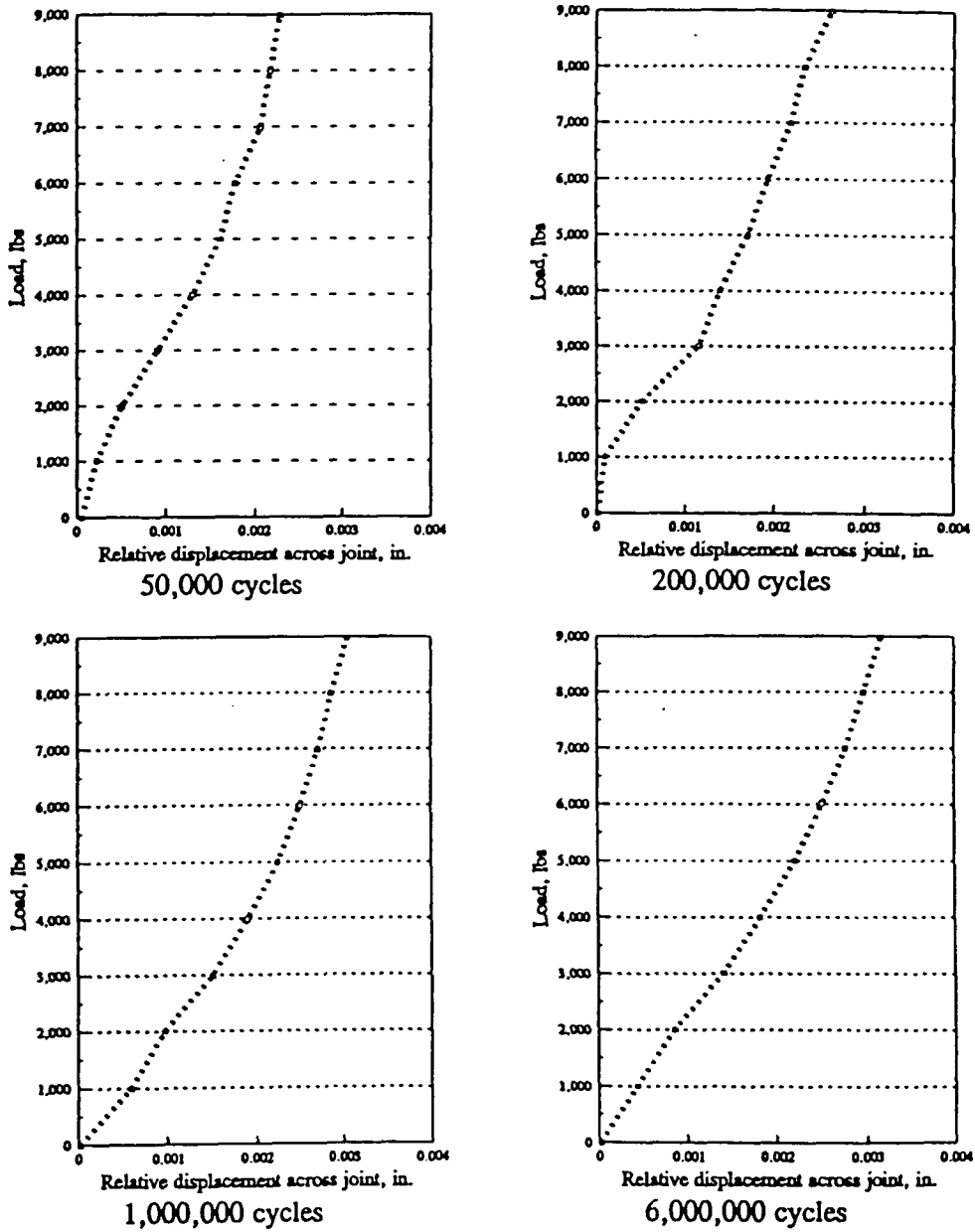


Figure 4.18: Load versus relative displacement diagrams at the joint of Slab 4

4.4 FC Rod Bond Testing

4.4.1 Introduction

The use of FC rods in place of steel products as tie rods between two adjacent lanes of concrete pavement requires that the rod be fully developed on both sides of the longitudinal joint between the two lanes. Previous testing performed at ISU resulted in the development of a test method for determination of the development length of FC rods (Fish 1992). Several advantages over other methods for determination of development length are present in the new method. The embedment length that is evaluated in each beam is in a section of changing shear and moment as well as curvature because of the load applied to the overhang. The same test method was applied in this project to analyze the development length of the FC rods studied.

4.4.2 Materials and specimens

The FC rod that was studied in this research was constructed with a helical wrap. This helical wrapping of the rod provided for a mechanical anchoring system when embedded in concrete. Three groups of ISU beams each consisting of six beam specimens, as well as six pullout specimens were constructed and tested in order to study the bond development of the FC rod. The first group of beams were constructed in exactly the same manner as in the previous research. A beam depth of 12 inches and width of six inches were used, with outcroppings (dogbones) as shown in Figure 4.19. Embedment lengths that were studied ranged from 15 inches to 25 inches at increments of two inches. A concrete compressive strength of approximately 5,100 psi was used in the construction of the first group.

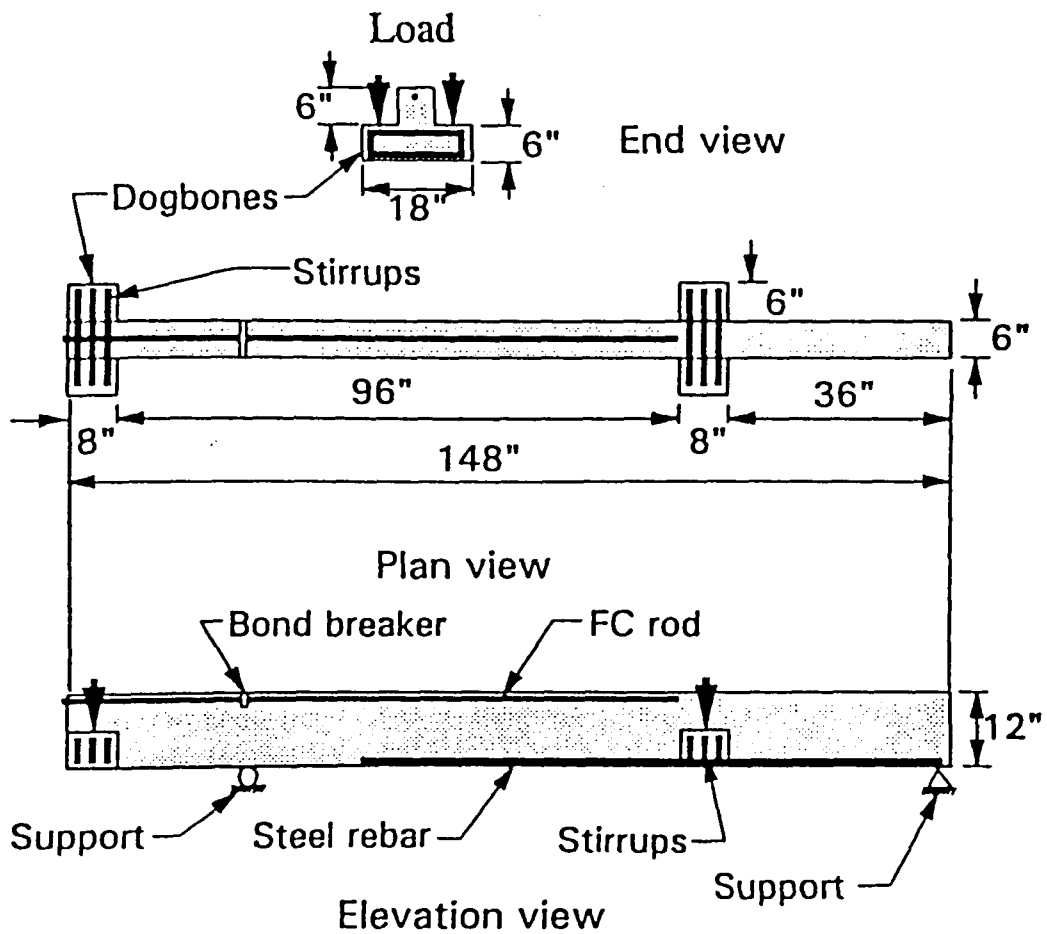


Figure 4.19: Beam specimen used for the development length tests of FC rod

Modifications were made to the beam configuration for the second group of test beams. In order to provide embedment lengths shorter than were used in the first group, while maintaining a sufficient lever arm for the cantilever load, the beams were notched at the top to expose the test rod as shown in Figure 4.20. The beams in the second group were setup to provide approximate embedment lengths ranging from 11 to 21 inches. Actual embedment lengths were measured at the time of testing. Another change made in the test setup from the first group involved changing the position of the FC rod. The rod was lowered in the section from 1.5 inches to 2.25 inches from the top of the beam. In effect, this resulted in a less efficient reinforcing system, so that smaller applied loads would be required to fully stress the rod. The concrete used in the second group of ISU beams was a C-4 mix, which is a typical highway pavement mix, with a compressive strength of approximately 6,500 psi.

The six test specimens of the final group were constructed to have approximately the same embedment lengths of the previous group, with the difference between the second and final groups being the concrete strengths. The concrete compressive strength for the third group was approximately 2,200 psi.

4.4.3 Test setup

Loads were applied to the beams at the dogbone locations using U-shaped steel load members constructed to slide over the beams. Hydraulic rams were mounted to a heavy steel frame to apply loads to the U-shaped members. The frame was free-standing with the beams simply supported on steel members crossing under the beams. A roller supported the beam underneath the bondbreaker, while a “pin” provided support at the other end which was actually a steel roller welded to a plate.

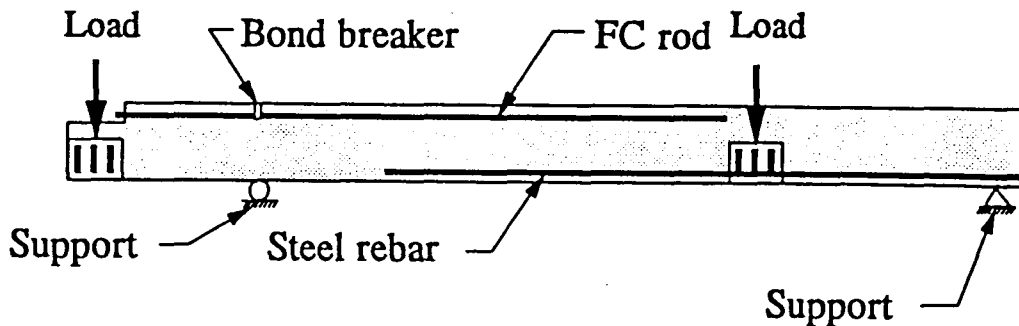


Figure 4.20: Modified beam specimens for development length tests used for Groups 2 and 3

4.4.4 Instrumentation

Measurements of interest during the testing of the beams included vertical displacements at the cantilever end and near the load point between the supports. Also, the slip of the FC rod was measured at the end of the rod extending out of the embedment length. All of the displacements were measured using DCDT instruments. Vertical displacements were referenced to the load frame, while the DCDT for slip measurement was mounted to measure the slip between the concrete and the FC reinforcing bar at the exposed unloaded end. Applied loads were measured using load cells placed between the two loading rams and the two loading members. Instrumentation was read using a data acquisition system interfaced with a personal computer using a controlling program.

4.4.5 Test procedure

Testing of the beams consisted of applying loads at the dogbone locations while reading the instrumentation at an interval entered into the computer controlling

program. Application of load at intervals of 200 pounds was continued till the failure of the specimen which gave sufficient data.

The result of greatest interest from the testing was the ultimate load applied to the cantilever at bond failure. Throughout the test, the displacement data was collected, which provides for load versus displacement plots to indicate the behavior of the beam as the load increased. Slip of the FC rod within the concrete over the embedment length indicated the load at which the bond of the rod to the concrete was broken.

4.4.6 Results

The three groups of test specimens were tested at three different times, allowing for adjustments to be made to the next group of specimens after each group was tested. From the testing of the first group of beams, the results indicated that the embedment lengths that were used were longer than the length required to develop the rod. No slipping of the rods was noted for any of the beams. Therefore, the range of embedment lengths for investigation was reduced in the second group of test beams. Also to reduce the load required to fully develop the rod, the position of the rod in the beam was lowered. However, no slipping of the rod could be observed in the second series of tests. Also there was little change in the load at failure. The reason for the similar loads can be attributed to the higher concrete strength of the second group of beam tests (6500 psi) compared to that of the first group (5100 psi). With the intention of developing slippage in the rod, the concrete strength for the third group of specimens was reduced to an experimental value of 2200 psi. In this group, slippage of the FC bar in the specimens could be observed at small

development lengths of 11 to 19 inches. Figures 4.21, 4.22, and 4.23 present the load versus cantilever deflection curves for the beams tested in groups one, two, and three, respectively, for the designated embedment lengths shown in the legend boxes.

4.5 FC Rod Pullout Tests

4.5.1 Introduction

The pullout specimens used in this study were designed to minimize the effects of the loading apparatus. Reaction forces, a result of the pullout forces, can serve to confine a specimen and thus produce false strength characteristics by increasing forces normal to the pullout specimen. These normal forces will serve to confine the concrete surrounding the specimen and thereby possibly increasing the required pullout force. In order to avoid these reactions, the concrete surrounding the FC specimens was sized to minimize these effects. In addition to the physical dimensions of the concrete, the reaction forces were distributed at four locations and along the length of embedded threaded rods. The specimen configuration and force schematic are shown in Figures 4.24 and 4.25. The FC specimen was embedded in the center of the specimen. A two-inch slice of insulation was placed between the concrete blocks to provide for set embedment dimensions.

4.5.2 Pullout specimen construction

Construction of the pullout specimens addressed several important variables. These variables had a direct impact upon the pullout resistance of the specimen and concrete strength. The geometric shape of the specimens and rigidity during lifting operations could adversely affect the pullout resistance of the specimen by

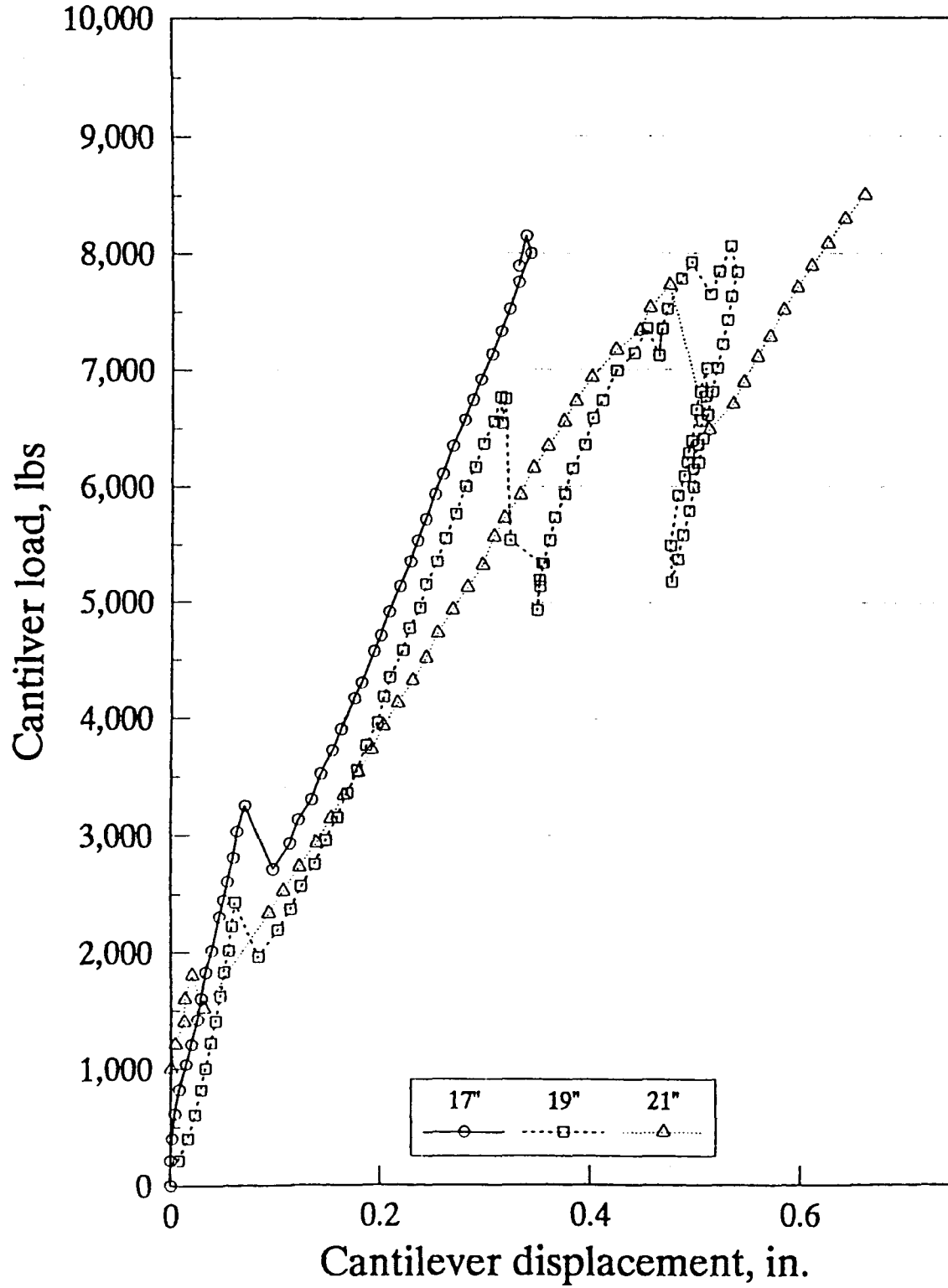


Figure 4.21: Load versus displacement for beam specimens tested in Group 1

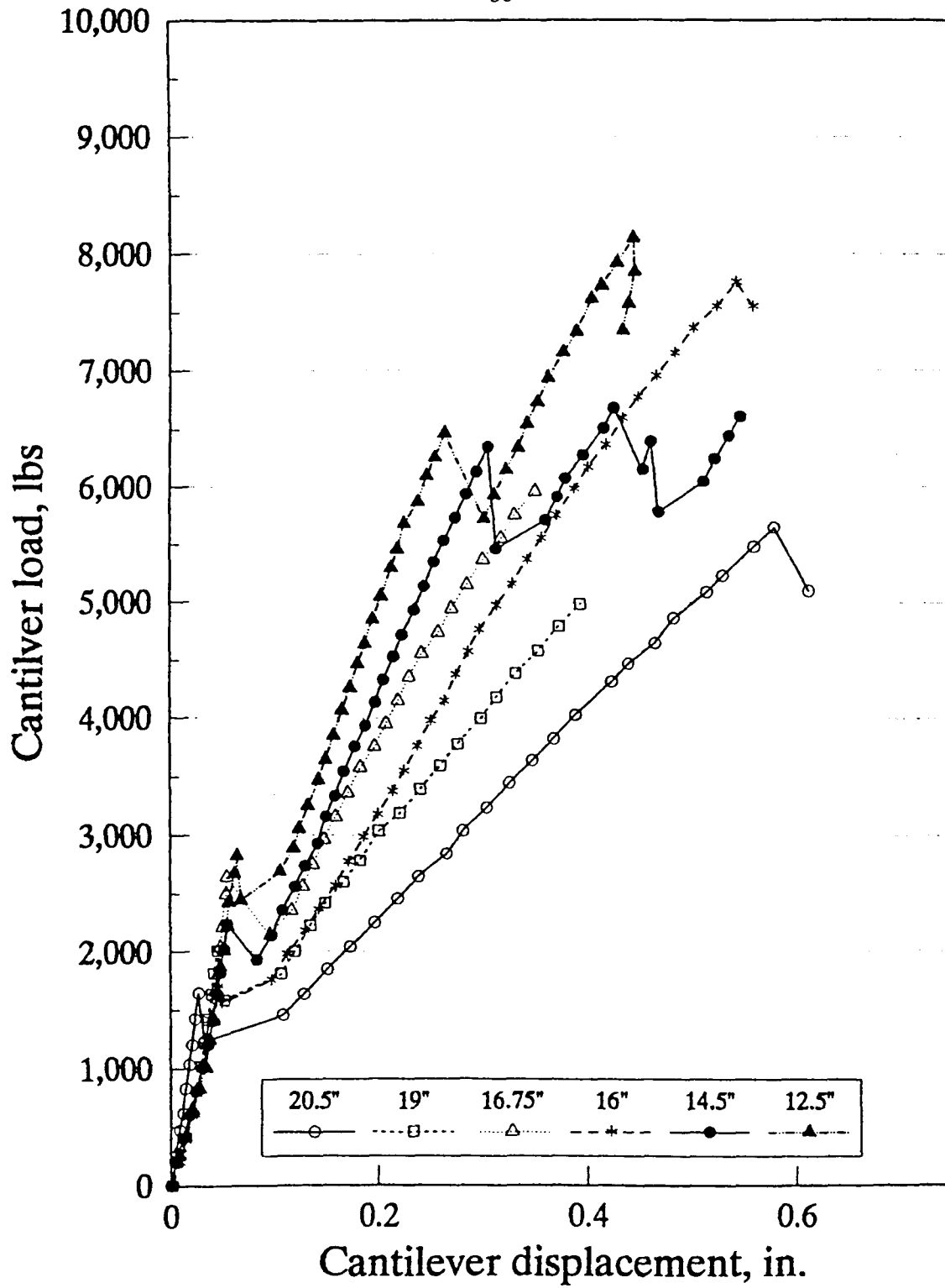


Figure 4.22: Load versus displacement for beam specimens tested in Group 2

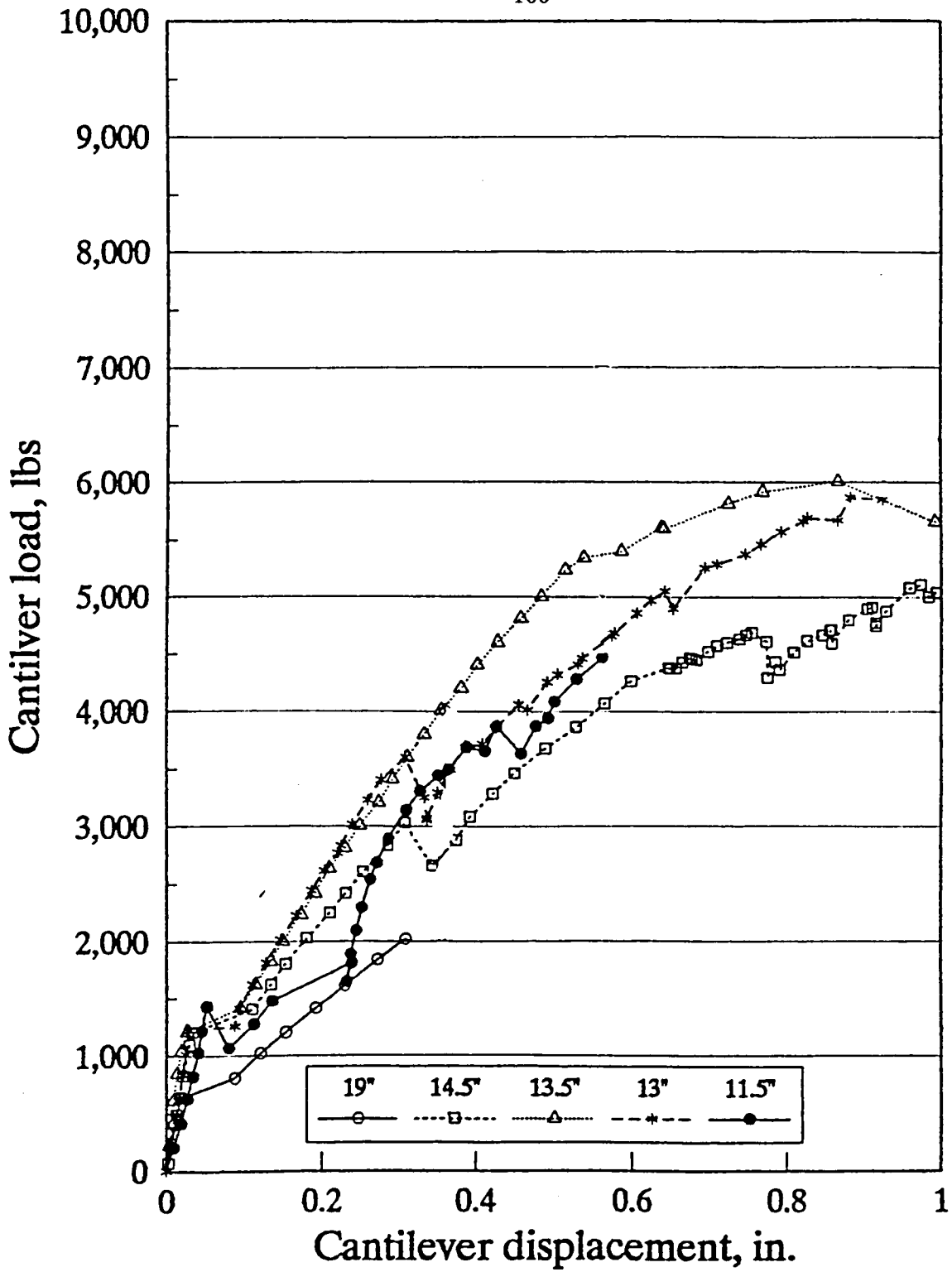


Figure 4.23: Load versus displacement for beam specimens tested in Group 3

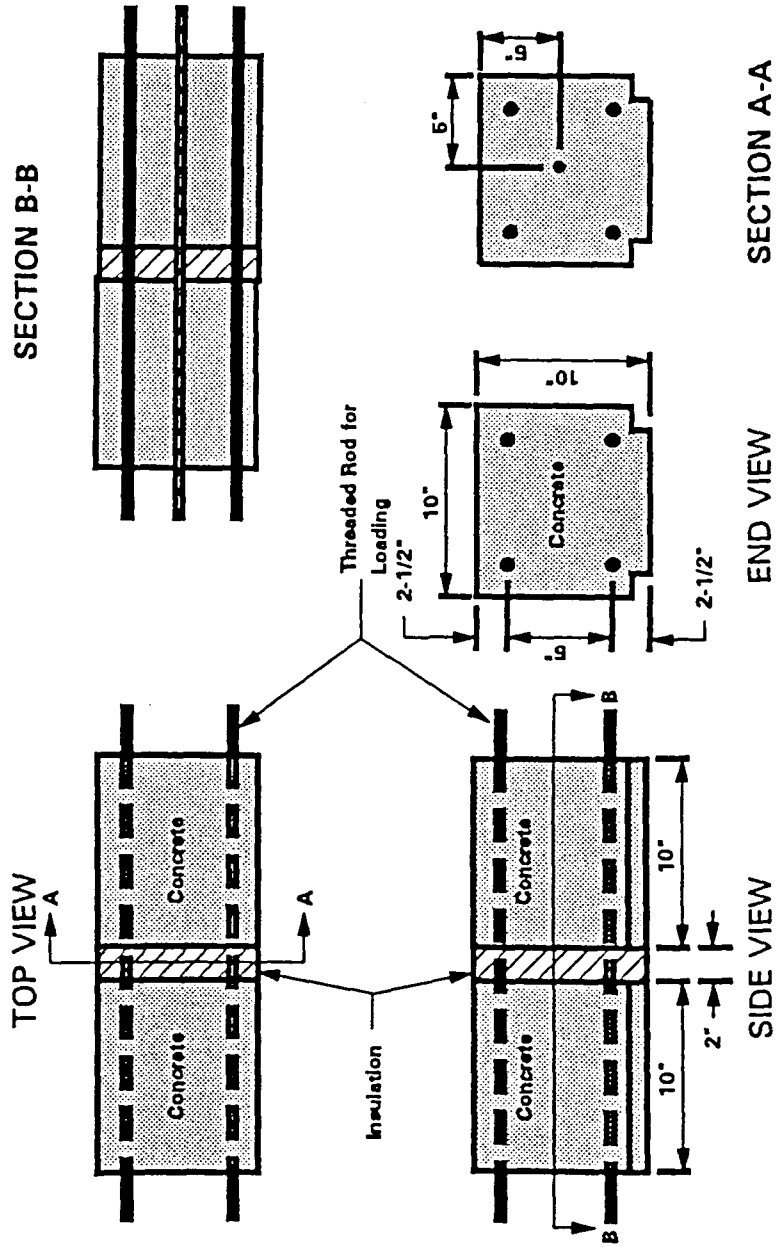


Figure 4.24: Pullout test specimen dimensions

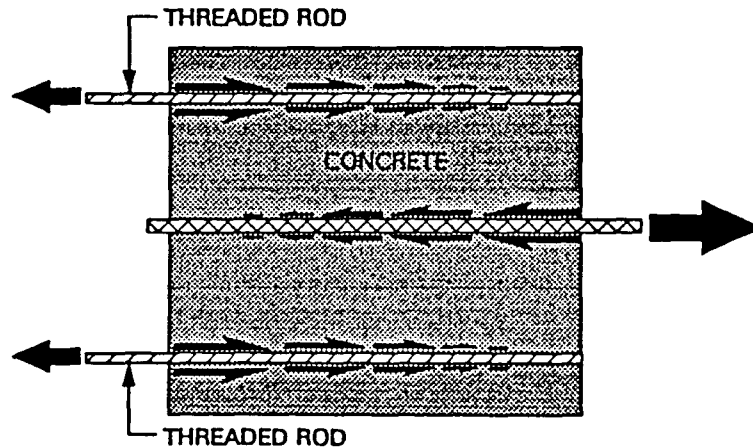


Figure 4.25: Pullout specimen force schematic

predamaging the specimen concrete interface. To avoid this pretest damage, the threaded rods were placed in the four corners of the concrete cubes. In addition to this, these rods were continuous across the insulation gap. The continuous steel rods served to absorb any twisting or bending forces present during lifting, thereby from the specimen. Furthermore, small recessed ledges were cast into the specimen as shown in Figure 4.24. These ledges allowed for lifting of the specimen without having to install lifting hooks into the concrete. The lifting apparatus was fabricated to provide support along the full length of the specimen. As a result of these precautions, any pretest damage to the specimen was minimized.

All pullout specimens were formed using steel formwork. The insulation and FC specimen were installed in the formwork and small pieces of Styrofoam were used to form the lifting ledges and also to secure the center insulation/specimen assembly in the formwork. The steel threaded rods were then installed in the four corners.

Concrete was delivered to the laboratory in a ready mix truck and the slump and air content were measured (standard C-4 mix). The concrete was transferred from the truck to a wheelbarrow and then to the individual specimens. Care was taken during the pour to ensure that both sides of the specimen were filled equally. This equal placement of the concrete prevented the insulation/specimen assembly from bowing or moving. All of the concrete was vibrated and finished. A specimen number was inscribed in the concrete, and all of the specimens were then covered with plastic and sprayed with water daily for one week, and then the specimens were allowed to cure for 28 days.

4.5.3 Pullout test procedure

The objective of the pullout test was to determine the required embedment length to attain zero end slip. This test was not designed to include shear and curvature effects since these effects are not a major component of the forces acting on the rods in the field. In order to reach this objective, a test procedure which minimized the confining effects of the loads and supports was designed.

In order to solve the aforementioned concerns, the pullout test frame was specially constructed. Load was applied to the specimens via threaded rods at the four corners of the specimens. These rods were located sufficiently far away from the specimen to remove the confining effects of the loads. The loading frame (refer to Figure 4.26) itself was constructed such that both ends of the framework were mounted on rollers. Rollers were located to guide the framework and keep the specimen aligned as shown in Figure 4.26. The roller assembly was then loaded through high strength threaded rods as shown in Figure 4.26. The East end of the frame served as a fixed

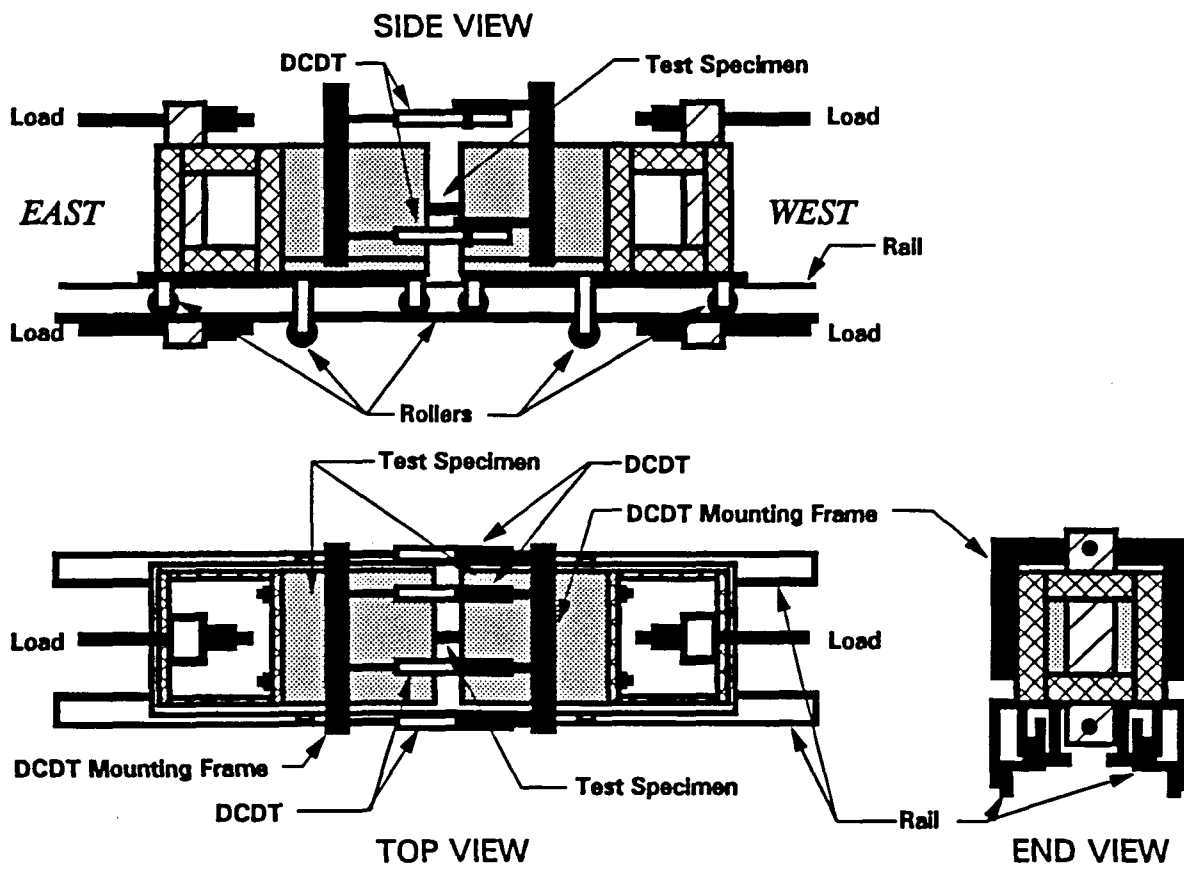


Figure 4.26: Pullout test frame

support for all of the specimens, while the West end of the frame accommodated the hydraulic ram and the loading apparatus.

At the conclusion of the curing period, the specimens were lifted into the testing frame. The East end of the specimen (fixed support) was attached to the frame. Following the attachment of the East end, the West end was fitted into the frame. The nuts which attached this end to the frame were only tightened to a snug condition. Any further tightening of these nuts could have led to eccentric forces induced into the specimen prior to the cutting of the threaded rod in the insulation gap. Following the attachment to the frame, the threaded rod in the insulation gap were cut. During this cutting, the FC specimen was protected by leather. The tracks for the rollers were then cleaned of all debris and the instrumentation was mounted to the specimen. Load was applied by the hydraulic ram on the West end of the frame and the data was collected at approximately 100-lb intervals. This data was composed of load and deflection values collected from the instruments discussed in the following section.

4.5.4 Pullout test instrumentation

The instrumentation used in the pullout tests included a load cell and DCDTs. These instruments were connected to a Hewlett Packard (HP) Data Acquisition System (DAS) which was controlled by a MS DOS PC. Data was collected from the instruments, stored, and printed at specified intervals. All of the instruments were calibrated prior to testing and the calibration numbers used were input into the data acquisition program.

DCDTs were placed on the specimen in order to detect any possible rotation of the specimen. Four DCDTs were placed at the corners of the insulation gap and one instrument monitored displacements inside the gap. The gap measurements were obtained by means of a scissors type device which transferred the specimen displacements from the inside of the gap to the outside of the specimen where an instrument could be installed. The data acquired from the four corner DCDTs were averaged to account for any rotational effects.

4.5.5 Results

A total of four specimens were cast with FC rod investigated in this research. The embedment lengths used for the specimens were 4, 6, 8, and 10 inches. The results from the pullout tests performed on these specimens were based upon the criterion of end slip. The failure of the specimen with 4-inch embedment length was essentially the pullout of the FC rebar. The specimen with 6-inch embedment length exhibited some pullout (bond failure) up until the peak load. This was followed by a partial pullout of the FC bar along with the tensile failure of the rebar. The 8-inch, and 10-inch embedment length specimens did not exhibit any end slip. The failure of these specimens was purely a tensile failure.

4.6 FC Rod Tensile Testing

4.6.1 Introduction

For a complete evaluation of a fiber composite rod for use as tie reinforcing in longitudinal joints of highway pavement slabs, the tensile strength of the rod must be determined. The function of tie reinforcing is to connect two adjacent lanes meeting

at a longitudinal joint together. The relative movement of the two slabs develops tension in the tie bar, requiring that the rod resist such tensile forces. Tensile testing was performed in conjunction with the bond development study for the FC rod material.

4.6.2 Materials and specimens

The FC rod consisted of E-glass fibers in a vinyl ester resin matrix as did the FC dowels tested. As a reinforcing rod, the resin and glass were formed into a helical wrapped rod, with a cross-section that was nearly oval-shaped. Because of the differing shape, no easy direct measurement could be used to determine the cross-sectional area. Therefore, a method of submerging sections of the rod in water while measuring the displaced water was applied. The quotient of the displaced volume and the length resulted in the average section area. Six sections of approximately 3 inches long were analyzed for determining cross-sectional area.

Specimens tested in tension were prepared to avoid damaging the FC rods during the tests. Because steel grips are used to pull the specimens in the testing machine, a copper tube and epoxy are used to protect the rod. The five-foot section of the rod had two 12-inch long pieces of the copper tube placed over each end of the rod, with epoxy filling around the FC. Each end of the specimen is placed into the test machine with the grips in contact with copper tubing as shown in Figure 4.27.

4.6.3 Test procedure

The test method developed at Iowa State University (Porter 1991) was used to determine the tensile capacity of the fiber composite rod investigated in this work.

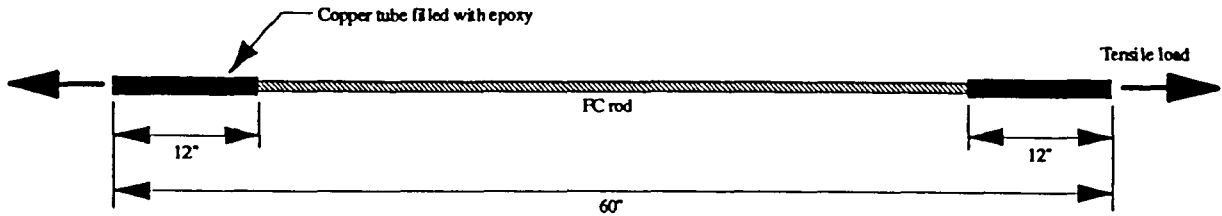


Figure 4.27: Dimensions and details of FC rod specimen used in tensile testing

The rod with prepared ends as shown in Figure 4.27, was placed in the grips of a hydraulic loading machine. The rod was then loaded in tension to failure at an approximate rate of 800 pounds per minute. The load frame control console recorded the peak load attained at failure.

4.6.4 Results

As mentioned before, the cross sectional area of the FC rod was found by determining the volume of the rod, and dividing the volume by the length of the rod. The average area of the rod used in this research was found to be 0.115 sq.in. as calculated in Table 4.3. The ultimate load and stress results from the tensile testing are presented in Table 4.4. The average tensile strength of the rod is reported to be 85.6 ksi.

Table 4.3: Determination of area of FC rod

Specimen No.	Length in.	Volume cm ³	Volume in ³	Area in ²
1	2.996	5.63	0.344	0.115
2	3.017	5.76	0.351	0.117
3	3.036	5.67	0.346	0.114
4	2.987	5.68	0.347	0.116
5	2.996	5.05	0.308	0.104
6	3.011	6.07	0.370	0.123

Table 4.4: Tensile Strength of FC rod

Specimen No.	Load at failure lbs	Tensile strength ksi
1	8260	72.0
2	11050	96.4
3	11380	99.2
4	8570	74.7

CHAPTER 5. ANALYTICAL INVESTIGATION

5.1 Introduction

One of the purposes of this investigation was to analyze the results of tests performed on full-scale slabs in order to present and compare the efficiencies of the dowel-concrete systems tested. As explained in Section 3.3, the efficiency of a doweled joint is defined by the relative deflection across the joint and the load transfer through the dowels acting as load transferring devices at that joint. Relative displacements were measured from the displacement instrumentation placed on the test slabs, and formed a major part of the direct results of experimentation. The presentation of relative displacements is done in Section 4.3.6.

The analytical investigation was focused mainly on determination of load transfer across the joints of individual test slabs. Three approaches were considered to analyze the results for establishing the load transfer. Data from supporting beam strain gages and dowel strain gages along with the relative displacements were used in the analyses presented in the following sections.

5.2 Load Transfer From Supporting Beam Data

The process of determination of load transfer from the strain gages placed on supporting beams is presented in Section 3.4.2. Whereas the placement of instru-

mentation on supporting beams is illustrated in Section 4.3.4.2, the testing involved in calibration of the beams to experimentally establish the load-strain relationships is explained in Section 4.3.5. The results of tests conducted on supporting beams are reported in Section 4.3.6 and depicted in Figure 4.14.

The calibrations of the supporting beams were done before the beginning of fatigue experimentation, and were assumed to remain unaltered throughout the experimental investigation. The strain gages placed on the supporting beams were read at periodic intervals along the course of fatigue testing. The strain gage readings of each beam were compared with the already established calibration curves (Figure 4.14) to determine the corresponding load carried by that beam. Out of the four supporting beams on which strain gages were placed, two were located beneath the slab on one side of the joint whereas the remainder were under the slab on the other side of the joint. Therefore, there were two beams on the loaded and unloaded side of the joint for each location of the load. After reading the calibration curves, the total load on each side of the joint was calculated by adding the individual loads carried by the beams on that side.

The sum of the loads on loaded and unloaded sides of the joint was approximately equal to the applied load, because the calculated sum of the beam loads the loads on the two outside beams which were not instrumented. However, the outside beams carried only a less significant load (less than 5% of the applied load) which was obtained by subtracting the sum of the loads carried by all of the instrumented beams from the applied load. Therefore, the quotient of the sum of beam loads on the unloaded side over that of all of the instrumented beams was assumed to be the same as that of the load transferred across the joint over the load applied.

The load transfer determined as explained so far, was plotted (Figure 5.1) against the number of load cycles for Slabs 2, 3, and 4. These results indicated that the FC dowels spaced at 8 inches provided a more efficient system initially, and a system that did not degrade as rapidly with repeated loads as did the steel dowels spaced at 12 inches, whereas the behavior of FC dowels spaced at 12 inches (Slab 4) was similar when compared to that of the steel dowels with the same spacing (Slab 3).

5.3 Load Transfer From Dowel Strain Gage Data

The portion of the total load that was transferred by each of the dowels must be known in order to design the dowel for critical stresses as explained in Section 3.3. The method of calculating load transfer by individual dowels involved development of relationships between the strains measured in both FC and steel dowels and the associated load transfer. Relationships between strain and load transfer were generated by applying the results of the elemental tests.

Previous work related to steel dowels at a spacing of 12 inches had approximated that only two to four of the dowels nearest to the point of a load are effective in transferring load at the joint of a pavement (Heinrichs 1989). If a joint is idealized as perfectly rigid, 50 percent of the load, or 4,500 pounds for a 9,000-pound loading, is transferred across the joint by all of the dowels. Therefore, by distributing the transfer of 4,500 pounds among effective dowels, an approximate minimum of 1,125 and an approximate maximum of 2,250 pounds would be transferred by each of four or two dowels, respectively. Because the joints tested in this research were assumed to be less than perfectly rigid, which the results confirmed, the load transferred by a single dowel was expected to be less than 2,250 pounds.

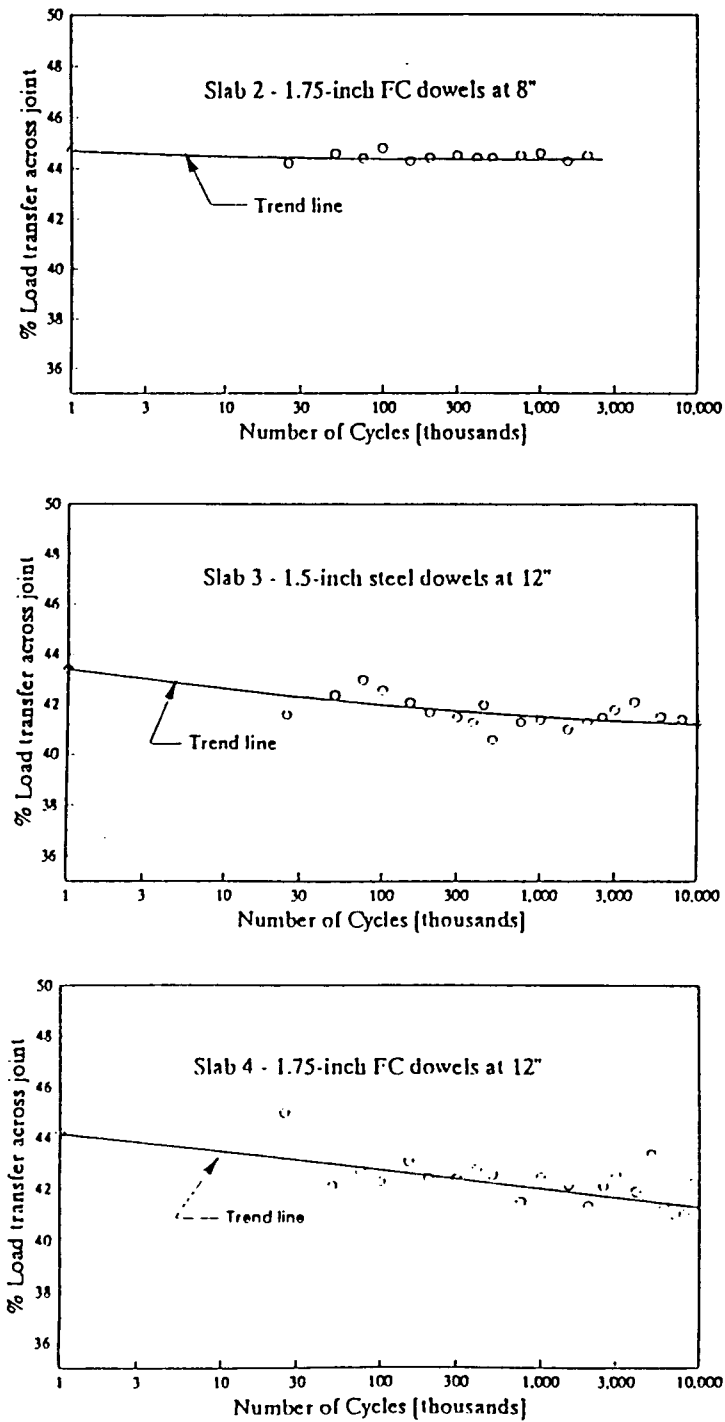


Figure 5.1: Percent of load transfer across the joint versus the number of applied load cycles for Slabs 2, 3, and 4.

Strain gage data from both elemental and full-scale slabs indicated a linear relationship between measured strains and loads. The data from elemental testing of 1.75-inch diameter FC dowels, as well as from elemental testing performed by Lorenz on 1.5-inch diameter steel dowels (Lorenz 1993), exhibited such a relationship. Linear regression of the data from the FC dowel elemental testing was discussed in Section 4.2.6 and a linear expression was given in Equation 4.1. A similar analysis procedure was applied to strain and load data from elemental testing of 1.5-inch diameter steel dowels performed by Lorenz (1993). The regression line equation for 1.5-inch diameter steel dowels was obtained as depicted by Equation 5.1.

$$P_s = 9.442 S_{1.5} \quad (5.1)$$

Because the FC dowels tested in the full-scale and elemental specimens were identical, calculation of moments from the dowel strains was not necessary in order to relate the results from the two tests. Therefore, measured strains from the elemental tests were used directly in the determination of the relationship with load transfer, as is shown in Equation 4.1.

The dowel strain data from the second full-scale slab was considered in order to determine the load transfer by Equation 4.1. In Slab 2, the three center dowels were instrumented with strain gages, and data was collected during the static load tests. Measured strains at the maximum load applied to the slab, which was 9,000 pounds, were substituted into Equation 4.1, with the resulting load transfer values as given in Table 5.1. Because during the static load tests, one side of the joint was loaded at a time, there were two sets of load transfer results; one set from when the North side of the joint was loaded, and the second when the South side was loaded.

Table 5.1: Load transfer across the joint by 1.75-inch diameter FC dowels in the second full-scale test slab

Dowel Name	Location	NORTH LOADED		SOUTH LOADED	
		Avg. Meas. Strain ($\mu\text{in./in.}$)	Load Transfer (lbs)	Avg. Meas. Strain ($\mu\text{in./in.}$)	Load Transfer (lbs)
1	8" East of CL	139	928	150	1001
2	Centerline	139	928	135	904
3	8" West of CL	143	958	125	837
		Total = 2814		Total = 2742	

The same procedure as described above for FC dowels was followed for the strain data collected from the dowels in the third and fourth full-scale slabs. Only the center two dowels of these slabs were mounted with strain gages. The strain values for the dowels in Slab 3 due to 9,000 pounds applied to each side were substituted into Equation 5.1, which was developed from elemental testing of 1.5-inch diameter steel dowels. Values for load transfer are listed in Table 5.2. Similar analysis was performed with the strains of the two center dowels of Slab 4 using Equation 4.1 for obtaining the load transfer. The details of calculation of the dowel load transfer are presented in Table 5.3.

The relation of elemental and full-scale test data indicated that the individual FC and steel dowels acted similarly in transferring load across the joints in the full-scale specimens studied in this research. Load transfer values calculated for both types of dowels demonstrated the behavior of the dowels with instrumentation in the full-scale specimens before cyclic loading was applied.

Table 5.2: Load transfer across the joint by 1.5-inch diameter steel dowels in the third full-scale test slab

Dowel Name	Location	<u>NORTH LOADED</u>		<u>SOUTH LOADED</u>	
		Avg. Meas. Strain ($\mu\text{in./in.}$)	Load Transfer (lbs)	Avg. Meas. Strain ($\mu\text{in./in.}$)	Load Transfer (lbs)
1	6" East of CL	97	916	114	1076
2	6" West of CL	98	925	105	991
			Total = 1841	Total = 2067	

Table 5.3: Load transfer across the joint by 1.75-inch diameter FC dowels in the fourth full-scale test slab

Dowel Name	Location	<u>NORTH LOADED</u>		<u>SOUTH LOADED</u>	
		Avg. Meas. Strain ($\mu\text{in./in.}$)	Load Transfer (lbs)	Avg. Meas. Strain ($\mu\text{in./in.}$)	Load Transfer (lbs)
1	6" East of CL	206	1380	190	1272
2	6" West of CL	188	1259	179	1199
			Total = 2639	Total = 2471	

In the full-scale specimen utilizing 1.75-inch diameter FC dowels spaced at eight inches, the calculated values of load transfer exhibited a rather uniform distribution of load to the center three dowels. The remaining six dowels were assumed to transfer the remaining load across the joint. Determination of the load transfer values for each of the dowels without strain gages would require speculation of their internal behavior, which was not attempted in this study. With regard to the previous work on the distribution of load transfer to the dowels nearest the load application (Heinrichs 1989), the FC dowels located 16 inches from the load point would most likely carry a large portion of the remaining amount of transferred load.

Results of the calculated load transfer amounts by the individual 1.5-inch diameter steel dowels at 12 inches were similar to those for the FC dowels. The load transfer was determined for only two of the steel dowels in the third slab. Because only four additional dowels were available to transfer load, significant loads were most likely transferred by all of the steel dowels in the full-scale specimen. As a result, the load transfer was distributed further away from the load point than for the specimen with FC dowels. Results from the static load testing of the second and third slab specimens indicated that the relative displacements at the steel dowels 18 inches from the load point were more significant than those at the FC dowels 16 inches from the load point.

The results from the fourth slab with 1.75 inch diameter FC dowels spaced at 12 inches indicated that the load transferred through the individual dowels located nearest the load point was higher than in previous slabs. However, since the total number of dowels near the load in Slab 4 was less than that in Slab 2, the total load transferred across the joint by the dowels was less. The difference between the load

transfers of Slabs 3 and 4 could also be attributed to the difference in dowel diameter.

The total load transferred by the dowels closest to the load point in Slabs 2, 3, and 4 was tabulated in Tables 5.1, 5.2, and 5.3. Slab 2 (1.75-inch diameter FC dowels spaced at 8 inches) transferred the largest amount of load due to the close spacing of the dowels and the larger diameter of the dowels. Slab 4 dowels (1.75-inch diameter FC dowels spaced at 12 inches) had the next highest loading. This loading follows the rational of Slab 2 since the dowels were of the same diameter as those of Slab 2 but were spaced further apart. The dowels in Slab 3 (1.5-inch diameter steel dowels spaced at 12 inches) exhibited the smallest dowel loading due to the smaller dowel diameter and larger spacing.

An additional consideration was made regarding the full-scale slab data. Because the elemental tests were conducted on a dowel specimen which had not been previously loaded, the relationships in Equations 4.1 and 5.1 should only be considered for the results of the initial static load tests. These tests were performed before fatigue loading of the slab had begun, and the same relationship would not apply during the course of fatigue experimentation.

5.4 Load Transfer From Dowel Analysis

The theoretical model developed for analysis of dowels as explained in Section 3.3. was applied to the FC dowels placed in the fourth slab in order to estimate the load transferred through the most highly stressed dowel. From the dowel strains and sectional and material properties of FC dowels, the bending moment in the dowel was determined at two locations. The locations investigated were at 1.5 and 4.0 inches away from the face of the joint where the strain gages were located.

The calculated moments in the dowel formed two out of the four boundary conditions necessary for the theoretical model. The other two boundary conditions required to solve the general differential equation for deflection (Equation 3.12) were obtained by equating the bending moment and the shear force at the end of the dowel to zero. The deflection equation was established by applying these boundary conditions to Equations 3.13 and 3.14.

By substituting different values of modulus of foundation, K in the equation for deflection, a relation between K and the relative deflection at the face of the joint was obtained. The experimental relative deflection was then used to read the particular value of modulus of foundation, which when substituted in the general differential equation for deflection, yielded the particular deflection equation of the dowel tested. The distribution of shear along the length of the dowel was obtained by differentiating the equation for deflection. The shear in the dowel at the face of the joint was taken as the load transferred through that dowel.

The dowel load determined as explained above, along with the corresponding calculated modulus of foundation is listed in Table 5.4. The fatigue effect on load transferred by the dowel can be observed from the degrading load transfer as the number of cycles of loading increases.

Table 5.4: Results of analysis of dowel

Cycles of fatigue	Input			Output	
	Dowel moment 4.0in (lb-in.)	Dowel moment 4.0in (lb-in.)	Relative deflection (in.)	Modulus of foundation (pci)	Dowel load transfer (lbs)
50000	558.61	183.05	0.00114	625000	1263.5
200000	587.02	195.67	0.00132	500000	1212.6
1000000	714.83	252.48	0.00153	425000	1103.1
6000000	751.13	252.80	0.00159	400000	1050.5

CHAPTER 6. COMPARISONS AND CONCLUSIONS

6.1 Introduction

Included in this study of non-metallic highway pavement dowels were several types of experimental and analytical investigations. Laboratory testing was conducted on full-scale concrete pavement and elemental dowel specimens, as well as full-size and reduced-size FC dowel flexure specimens. In addition, FC dowels were placed in transverse joints in an actual highway construction project, and the performance of the dowels was monitored and evaluated.

6.2 Comparisons

1. The 1.75-inch diameter FC dowels spaced at eight inches performed at least as well as 1.5-inch diameter steel dowels at 12 inches in transferring static loads across the joint in the full-scale pavement test specimens. The performance of the 1.75-inch diameter FC dowels spaced at 12 inches was similar to that of the 1.5-inch diameter steel dowels spaced at 12 inches with differences being attributed to dowel diameter.
2. Relative displacements measured at pavement joints with 1.75-inch diameter FC dowels spaced at eight inches were slightly smaller than those at joints with 1.5-

inch diameter steel dowels spaced at 12 inches. Both were subjected to similar load and support conditions during the testing. The relative displacements for Slabs 3 and 4 were similar.

3. Values of K for 1.75-inch diameter FC dowels were determined to be 358,300 and 247,000 pci for elemental specimens with concrete compressive strengths, f'_c , of 7,090 and 5,092 psi, respectively. These values compare to those determined by Lorenz (1993) of $K = 650,000$ pci for 1.5-inch diameter steel dowels in concrete with $f'_c = 7,090$ psi.
4. The modulus of foundation determined by applying the theoretical model developed in Section 3.3 to the full-scale slabs is listed in Table 5.4. The value corresponding to zero cycles (actually 50,000 cycles) was obtained as 625,000 pci which can be compared satisfactorily with that obtained from single dowel shear tests.
5. Load transfer through the critical dowel obtained from extrapolating the single dowel test results is presented in Table 5.3, from which the average individual dowel load can be obtained as 1277.5 lbs by dividing the sum of the two totals listed at the bottom of the table by 4. This load is very close to the value (1263.5 lbs) obtained from analyzing the dowel in the full-scale test slabs using the theoretical model developed.

6.3 Conclusions

1. The joints utilizing FC dowels studied in this research performed as well as joints utilizing standard steel dowels when both were subjected to conditions

which simulated actual highway pavement use, including cyclic loading.

2. The laboratory test methods for evaluation of highway pavement dowel bars, which were developed during this research, provided good behavioral results for highway pavement joint conditions.
3. The full-scale pavement testing procedures applied in this research provided a good method for monitoring and evaluating the behavior of dowels bars when placed in a concrete pavement joint and subjected to cyclic loading.
4. Load transfer by individual FC and steel dowels in a full-scale pavement joint can be determined by relating the measured dowel strains to the strains measured during elemental testing of the same types of dowels.
5. The use of steel beams as a simulated subgrade in place of a soil subgrade was effective for the study of pavement dowel performance under fatigue and static loading.
6. Finite element analysis of pavement slabs developed and used in this work was successfully verified by comparing the results of finite element analysis with experimental results.
7. The test procedure developed and applied in the full-scale pavement slab testing provided results which were valuable in performing an analysis of dowel behavior.

6.4 Recommendations

1. Idealization of a highway pavement slab for facilitating finite element analysis was attempted and successfully accomplished in this work. However, further development of finite element analysis of pavement slabs is strongly recommended. The future work should be focused on modeling the dowel-concrete interface.
2. The results obtained from testing the elemental shear specimens could be used to estimate the dowel load transfer in full-scale slabs. Similarly, investigation of the possibility of extrapolation of the results of cyclic tests conducted on single dowel specimens to envisage the fatigue behavior of the dowels of full-scale slabs can be considered for future work.
3. The procedure used, in this work, to establish the modulus of dowel support needs further verification. The recommended research in this regard would perform static as well as fatigue tests on specimens which encompass a variety of field conditions, and various concrete and dowel materials.
4. Additional tests on full-scale specimens are strongly recommended for supporting the results of this project. The future tests would consider extending the number of load cycles so that the laboratory specimen could be subjected to the magnitude and intensity of fatigue experienced by actual highway pavement over the service life of the pavement.

REFERENCES

- ✓ AASHTO Guide for Design of Pavement Structures. (1986). American Association of State Highway and Transportation Officials, Washington, D.C.
- Albertson, M.D., Porter, M.L. and Barnes, B.A. (1990). "Thermoset Concrete reinforcement: Progress Report for 1990." Iowa State University, Engineering Research Institute, Ames, IA.
- Annual Book of ASTM Standards, Volume 8.02, Plastics (II). (1991). American Society for Testing and Materials, Philadelphia, PA, pages 328-329.
- Auborg, P.F. and Wolf, W.W. (1986). "Glass Fibers." Advances in Ceramics, Vol. 18. Eds. D.C. Boyd and J.F. MacDowell. American Ceramic Society, Columbus, OH, pages 51-78.
- Bank, L.C. (1991). "Experimental Study of FRP Grating Reinforced Concrete Slabs." Advanced Composite Materials in Civil Engineering Structures, proceedings of the specialty conference, American Society of Civil Engineers, Las Vegas, NV.
- Barnes, B.A. (1990). Bond and Low Cycle Fatigue Behavior of Thermoset Composite Reinforcing for the Concrete Industry. M.S. Thesis. Iowa State University, Ames, IA.
- Beer, F.P., Johnston, Jr., E.R. (1981). Mechanics of Materials. McGraw-Hill Book Company, New York, NY.
- * Bradbury, R.D. (1933). "Design of Joints in Concrete Pavements." Proceedings of the 12th Annual Meeting of the Highway Research Board, Washington D.C., December 1-2, 1932, pages 105-136.

- Brown, G. (1988, November). "Fiber Glass Scores With Designers." Design News, pages 258-262.
- Cope, R.J. (1987). Concrete Bridge Engineering: Performance and Advances. Elsevier Applied Science, London.
- Corbo, V. (1990, January). "Advanced Materials Geared for the 90s." Design News, pages 69-70.
- DERAKANE Resins, Chemical Resistance and Engineering Guide. (1990). The Dow Chemical Company.
- * Fiber Reinforced Concrete. (1991). Portland Cement Association, Skokie, IL.
- Fish, K.E., Porter, M.L. and Barnes, B.A. (1992). "Fiber Composite Rods as Reinforcing for Concrete Structures: Thermoset and Thermoplastic Composite Reinforcement for the Concrete Industry." A report submitted to Center for Advanced Technology Development. Iowa State University, Ames, IA, pages 6-11.
- * Friberg, B.F. (1938). "Design of Dowels in Transverse Joints in Concrete Pavements." Proceedings, American Society of Civil Engineers, Vol. 64, Part 2, pages 1809-1828.
- Gibson, F.W. (1987). "Corrosion, Concrete and Chlorides - Steel Corrosion in Concrete: Causes and Restraints." American Concrete Institute, SP-102.
- * Heinrichs, K.W., Liu, M.J., Darter, M.I., et al. (1989, June). "Rigid Pavement Analysis and Design." Turner-Fairbank Highway Research Center, McLean, VA, Report No. FHWA-RD-88-068.
- Gangarao, H. (1991). "Bending Response of Beams Reinforced With FRP Rebars." Advanced Composite Materials in Civil Engineering Structures, proceedings of the specialty conference, American Society of Civil Engineers, Las Vegas, NV.
- Iyer, S. (1991). "Fiber Glass Pretensioned Piles for Marine Environment." Advanced Composite Materials in Civil Engineering Structures, proceedings of the specialty conference, American Society of Civil Engineers, Las Vegas, NV.
- Lorenz, E.A. (1993). Accelerated Aging of Fiber Composite Bars and Dowels. M.S. Thesis, Iowa State University, Ames, IA.

- McWaters, B. (1992-1993). Personal Interviews. Iowa Department of Transportation, Ames, IA.
- Medical Center Hospital, San Antonio, Texas. (1985). Reynolds-Schlatner-Chetter-Roll, Inc.
- Miessler, H.J. and Wolff, R. (1991). "Experience with Fiber Composite Materials and Monitoring with Optical Fiber Sensors." Advanced Composite Materials in Civil Engineering Structures, proceedings of the specialty conference, American Society of Civil Engineers, Las Vegas, NV.
- Pavement Design for Federal, State, and Local Engineers: a Training Course. 1993. Participant Notebook. Federal Highway Administration, National Highway Institute, Washington, D.C.
- Porter, M.L. and Barnes, B. A. (1991). "Tensile Testing of Glass Fiber Composite Rod." Advanced Composite Materials in Civil Engineering Structures, proceedings of the specialty conference, American Society of Civil Engineers, Las Vegas, NV.
- Porter, M.L., Lorenz, E.A., Viswanath, K.P., Barnes, B.A. and Albertson, M.D. (1992). "Thermoset Composite Concrete Reinforcement." Final Report, Part 1 for IHRB and IDOT. Iowa State University, Ames, IA.
- Potter, C.J. and Dirks, K.L. (1989, May). "Pavement Evaluation Using the Road RaterTM Deflection Dish." Final Report for MLR-89-2, Highway Division, Iowa Department of Transportation, Ames, IA.
- Richard R. D. (1991). "Use of GFRP Rebar in Concrete Structures." Advanced Composite Materials in Civil Engineering Structures, proceedings of the specialty conference, American Society of Civil Engineers, Las Vegas, NV.
- Rostasy, F.S. (1991). "FRP Tendons for the Post-tensioning of Concrete Structures." Advanced Composite Materials in Civil Engineering Structures, proceedings of the specialty conference, American Society of Civil Engineers, Las Vegas, NV.
- ✓ Teller, L.W. and Cashell, H.D. (1958). "Performance of Doweled Joints Under Repetitive Loading." Highway Research Board, Bulletin No. 217, pages 8-49.

- * Timoshenko, S. and Lessels, J.M. (1925). Applied Elasticity. Westinghouse Technical Night School Press, Pittsburgh, PA.
- * Timoshenko, S. (1976). Strength of Materials - Part II, 3rd edition. Robert E. Krieger Publishing, Huntington, NY.
- Tsai, S.W. and Hahn, H.T. (1980). Introduction to Composite Materials. Technomic Publishing Company, Inc., Lancaster, Pennsylvania.
- Wade, G.T., Porter, M.L. and Jacobs, D.R. (1988). "Glass Fiber Composite Connectors for Insulated Concrete Sandwich Walls." Civil and Construction Engineering Department Report. Engineering Research Institute, Iowa State University, Ames, IA.
- Walrath, D.E. and Adams, D.F. (1983, March). "The Iosipescu Shear Test as Applied to Composite Materials." Experimental Mechanics, pages 105-110.
- * Westergaard, H.M. (1928). "Spacing of Dowels." Proceedings, 8th Annual Meeting of the Highway Research Board, Washington, D. C., pages 154-158.
- * Westergaard, H.M. (1925). "Computation of Stresses in Concrete Roads." Proceedings of the 5th Annual Meeting of the Highway Research Board, Washington, D.C., December 3-4, pages 90-112.
- * Yoder, E.S. and Witczak, M.W. (1975). Principles of Pavement Design, second edition, John-Wiely & Sons, Inc.

ACKNOWLEDGEMENTS

The author would like to thank Dr. Max. L. Porter who acted as the principal investigator of the project (who is also the major professor of the author) for his continued support and guidance over the research work involved. Dr. Porter has been working in the area of fiber composite materials as applied to reinforced concrete construction and his arduous effort in forging these new materials into construction industry are to be welcomed as a healthy change. Without his passion towards FC materials, and his patient persuasion of solving trying problems and intelligent guidance, this project and the thesis would not have been possible.

The author would like to extend appreciation towards the help of Bruce A. Barnes (Research Associate) and Bradley W. Hughes (Graduate Student), the support of Douglas L. Wood (Structural Engineering Laboratory Supervisor) and the assistance of several undergraduate students. Without the invaluable and timely contributions of the above mentioned, the execution of the project would not have been successful.

Finally, the success of the research work depended on the coordination of Iowa DOT personnel namely, Brian McWaters and Vernon Marks, who extended support through their experience and knowledge of several pertinent areas.